

The influence of Snow Distribution in the Accumulation Area of Findelen Glacier on the Flow Dynamic and Geometry

**A modelling experiment with MATLAB based
on a case study of Findelen glacier**

Geo 511 Master Thesis

September 2015
Department of Geography
University of Zurich

Submitted by:
Ladina Glaus

10-720-126

Supervisor and Faculty Member:
Prof. Dr. Andreas Vieli



Cover photo: View from the glacier forefield of Findelen glacier in direction of Adlerhorn and Adler glacier (Photo: Ladina Glaus, September 2014)

Ladina Glaus
Heuelstrasse 4d
8800 Thalwil
l.glaus425@gmx.ch

Table of Contents

Table of Contents	I
List of Figures	II
List of Tables	III
1 Motivation	1
2 Introduction	5
2.1 Glacier definition.....	5
2.2 Glacier mass balance.....	6
2.3 Glacier flux.....	8
2.4 Velocity	11
2.5 Snow distribution.....	11
2.6 Climate change and its influence on glaciers	15
3 Investigation area	16
4 Methodology and strategy	20
4.1 Field measurement methods to determine mass balance.....	20
4.2 Glacier flow models	22
4.3 Glacier flow model applied for Findelen glacier.....	25
4.4 Introduction to the experiments.....	28
4.4.1 Reference case (F)	28
4.4.2 Left and right pattern (A and B)	28
4.4.3 Cut of accumulation (Experiment C)	30
4.4.4 Curvature (D).....	31
4.4.5 Wind model (E).....	33
4.4.6 Climate change.....	36
4.5 Parameter settings.....	36
4.5.1 Glacier bed (DEM):	37
4.5.2 Reference case.....	38
4.5.3 Experiment A and B: Snow shift to the left and the right side	39
4.5.4 Experiment C: Cut of increasing accumulation at 3350 m.a.s.l.....	39
4.5.5 Experiment D: Variability of snow on the base of the terrain.....	40
4.5.6 Experiment E: Snow distribution with wind and terrain.....	40
4.5.7 Climate change.....	40
5 Results	41
5.1 Extent of the reference case.....	41
5.2 Difference in geometry (A-D)	43
5.3 Change of velocity (A-D).....	47
5.4 Evolution of the glacier with time in the profile (A-D)	50
5.5 Wind (E).....	53
5.6 Climate change	57
6 Discussion	59
6.1 Snow pattern redistribution.....	59
6.2 Time aspect	63
6.3 Climate change	66
6.4 Experiment curvature and wind	67
6.5 Uncertainties	71
6.5.1 Findelen glacier bed vs. U-valley.....	71

6.5.2 Sun correction.....	71
6.5.3 Boundary between ice and glacier bed	73
6.5.4 Feedbacks.....	74
6.5.5 Constant meteorological conditions.....	74
7 Conclusion	75
8 Appendix.....	77
Acknowledgment	83
References.....	84
Personal Declaration	90

List of Figures

<i>Fig. 1: Work flow chart of the master thesis.</i>	3
<i>Fig. 2: Cryosphere diagram with ELA related to temperature and precipitation (Haeberli et al. 2002).</i>	6
<i>Fig. 3: Schematic representation of the altitudinal distribution of surface mass balance b, hypothetical elevation change and apparent mass balance over the glacier using linear elevation gradients (Huss & Farinotti 2012).</i>	8
<i>Fig. 4: Definition sketch illustrating the terms in the continuity equation (Benn & Evans 2010).</i>	9
<i>Fig. 5: Altitudinal distribution of surface net balance calculated for Grosser Aletsch glacier in 1977. The step function shows the mean net balance in elevation bands. Differences in the mass balance gradient and in the accumulation area are evident. Decreasing values in mass balance above 3500 m.a.s.l are due to effects of snowdrift and avalanches (Huss et al. 2009).</i>	13
<i>Fig. 6: Findelen Glacier in Zermatt (Geo.admin, 2015).</i>	16
<i>Fig. 7: Findelen glacier in Zermatt. Dots show manual snow probings', lines represent GPR profiles, the colour code shows measured snow depth in April 2010 (Sold et al. 2013).</i>	17
<i>Fig. 8: Raw LIDAR-derived elevation change from October 2009 to April 2010. The left figure (a) shows the mean mass balance, the right (b) figure the snow depth (Sold et al. 2013).</i>	18
<i>Fig. 9: Right (b): Measured snow depth with elevation from 403 probings' in April 2010. Left (a): vertical distribution of mean snow depth in 100m elevation bands derived from extrapolated snow probings', raw LIDAR-differencing and LIDAR-differencing corrected for emergence velocity, firn compaction and autumn melt (Sold et al. 2013).</i>	18
<i>Fig. 10: Identification of bare ice and snow covered area for separating accumulation and ablation zone (Huss et al. 2013).</i>	21
<i>Fig. 11: Schematic representation of a numerical flow model (Le Meur et al. 2004).</i>	24
<i>Fig. 12: Cut of glacier into two parts left and right. The black line indicates the elevation of the ELA. The colour bar shows the elevation of the glacier.</i>	29
<i>Fig. 13: Cut of increasing accumulation at a certain height. The bold line indicates the cut, the dotted one the initial assumption of an increase with elevation.</i>	30
<i>Fig. 14: Correlation of slope and curvature with snow depth (Farinotti et al. 2010).</i>	31
<i>Fig. 15: Curvature of Findelen glacier (performed by Matlab).</i>	33
<i>Fig. 16: Reduction of wind speed by aspect and inclination (slope) (Purves et al. 1998) .</i>	34
<i>Fig. 17: Profile lines for analysis of glacier evolution in ice thickness and length (Profile 1 and Profile 2).</i> ____	37
<i>Fig. 18: Glacier bed (DEM) of Findelen glacier from GPR measurement (3-D reconstruction performed with Matlab).</i>	38
<i>Fig. 19: The pink line shows the extent of the reference case with the two greatest snow-free spots below Adler glacier (Geo.admin, 2015).</i>	42

Fig. 20: Difference between output of ice thickness after snow redistribution and initial glacier geometry of reference case (steady state). A= shift to the left side, B= shift to the right side, C= cut of increasing accumulation at 3350m.a.sl, D= shift according to curvature, F= steady state (reference case) for comparison. _____	44
Fig. 21: Velocity of ice flow: A= experiment snow shifted to the left side, B= experiment snow shifted to the right side, C= cut of increasing accumulation at 3350 m.a.s.l, D= experiment of curvature, F= steady state (reference case). _____	47
Fig. 22: Change of thickness of the glacier along the profile (1 & 2) of the glacier. Lines represent run years. A= shift to the left side, B= shift to the right side, C= cut of increasing accumulation at 3350m.a.sl, D= shift according to curvature. Bluish lines are the first years of run, red the latter ones. _____	51
Fig. 23: South wind. E.1 = Difference in snow accumulation compared with the reference case (steady state), E.2 = wind direction and diversion, E.3 = Wind speed field. _____	54
Fig. 24: East wind. E.1 = Difference in snow accumulation compared with the reference case (steady state), E.2 = wind direction and diversion, E.3 = Wind speed field. _____	56
Fig. 25: Change in ice thickness at the glacier tongue. The first 150 years are run for the experiment A and B according to parameterization as explained in chapter 4.5.3, for the next 100 years the ELA was set at 3350 m.a.s.l. _____	57
Fig. 26: Mass balance gradient with elevation A= shift to the left side, B= shift to the right side, C= cut of increasing accumulation at 3350 m.a.sl, D= shift according to curvature, F= reference case. _____	61
Fig. 27: Change in thickness at the tongue: red line = experiment B (right), blue line = experiment A (left). _____	65
Fig. 28: The temperature anomaly in Greenland from 22 ka BP to present derived from ice core records (Brown et al. 2013). _____	67
Fig. 29: left: snow depth derived from LIDAR - DEMs; right: difference in snow accumulation depth between wind shift and reference case (steady state) (south wind). _____	68
Fig. 30: Snow depth measurements from winter mass balance April 2015 (Findel-Wiki 2015). _____	70
Fig. 31: Difference between reference case modelled with solar radiation (steady sun) and without solar radiation (steady no sun). Upper plot: difference in thickness; lower plot: difference in mass balance. _____	72
Fig. A1: View on Findelen glacier, September 2014 (Photo: Ladina Glaus) _____	77
Fig. A2: left: Adler horn and terminus of Adler glacier, right: Findelen glacier, September 2014 (Photo: Ladina Glaus) _____	77
Fig. A3: View towards the accumulation area of Findelen glacier, September 2014 (Photo: Ladina Glaus) _____	78
Fig. A4: left: snow pit, right: ablation stake, September 2014 (Photo: Ladina Glaus) _____	79
Fig. A5: Accumulation stake below Cima di Jazzi, September 2014 (Photo: Ladina Glaus) _____	79
Fig. A6: West-wind experiment. _____	80
Fig. A7: North-wind experiment. _____	81
Fig. A8: Glacier extent of experiment C after 150 years of run. Tongue retreated significantly. _____	82

List of Tables

Tab 1: Labelling of experiments and reference case. _____	36
Tab 2: Change in ice mass over time. _____	47

Abstract

Over the period 1880 to 2012, the global climate change has led to an increase in temperature of roughly 0.85°C (IPCC 2013). Consequently, almost all alpine glaciers are extensively retreating, only a few ones, located in maritime regions, show a slight advance due to an increased amount of precipitation (IPCC 2001). Glacier modelling thus has become an important research topic with the aim to understand the evolution and behaviour of individual glaciers as well as their future development (Le Meur et al. 2004; Linsbauer et al. 2012; Zemp & Haeberli 2007). A robust and reliable model for glacier model requires detailed knowledge of the interaction of the different key parameters and the understanding of the glacier dynamics. However, a model is always based on certain assumptions and simplifications (Solomatine & Wagner 2011). One of these is the impact of the distribution of snow in the accumulation area. In most cases accumulation is simply modelled assuming a homogeneous distribution using a linear relation between increase and elevation.

The aim of this thesis was to investigate whether this simplification is adequate or whether inhomogeneity has to be taken explicitly into account in the prediction of glacier dynamics and its geometry, consisting of glacier length, volume, flow velocity and glacier extent. For the analysis, five different snow accumulation redistribution scenarios ("experiments") were simulated based on the case study of Findelen glacier: (A & B) accumulating ten times more snow on the left than on the right side, and *vice versa*, (C) interrupting the increasing accumulation at the elevation of 3350 m.a.s.l, (D) shifting snow from convex to concave terrain and (E) snow redistribution with wind. The model was implemented with MATLAB®. The redistribution experiments resulted in an advance of the glacier in the first two experiments, whereby the glacier advanced only marginally in second experiment. In the third experiment the tongue retreated significantly. The different glacier behaviour is correlated to changes in ice fluxes and the influence of the glacier bed und surface slope of the ice. In the case of the curvature experiment hardly any changes in the glacier's geometry were observable. Unfortunately no conclusions could be drawn for the wind scenario owing to inadequacies of the model.

Additionally, the impact of increasing temperature resulting in upshifting the equilibrium line altitude (ELA) was examined in the first two experiments. After running the model for both experiments until the glacier reached almost a new steady state, the increase of the temperature resulted in the same relative loss of mass in both experiments.

It can be concluded from the various experiments that snow accumulation patterns have a significant influence on glacier dynamics. The discussion of the results leads to the hypothesis

that at least parts of the observed changes have a generic character. They can be observed independently of the local morphological and meteorological conditions. This conclusion has been corroborated by the demonstration that the relative mass changes were independent of the elevation of the ELA.

1 Motivation

Since the 19th century, the global climate change has led to an increase in temperature of roughly 0.85°C (IPCC 2013). The warming is stronger in the Northern Hemisphere. As a result, almost all alpine glaciers are extensively retreating, only a few ones, located in maritime regions, show a slight advance due to an increased amount of precipitation (IPCC, 2001). The retreat of glaciers results in hazards such as glacier lake outbursts, thawing of permafrost, destabilization of rock walls and consequently rock falls. Further changes are found in the water cycle of the discharge from glacier melt (Fischer et al. 2006). Thus, research is focusing increasingly on the understanding of natural hazards and the evolution of concepts to prevent disasters and to save lives (Carey et al. 2012). However, understanding the reaction of glaciers to global warming is not a simple task since glaciers react very diversely due to variations in geometry or location in varying climatic regimes (Kuhn 1985 in; Oerlemans et al. 1998). Several models have been developed to investigate the evolution and behaviour of individual glaciers and their reaction to climate change (see for example: Le Meur et al. 2004; Linsbauer et al. 2012; Zemp & Haeberli 2007; Huss et al. 2013). A robust and reliable model requires knowledge about the glacier and its flow dynamics. However, one must keep in mind what is meant by “model”. Modelling a glacier is the reproduction of the reality based on the most important characteristics and processes of the system, including a set of variables and equations. It aims to simplify the reality which in turn causes several uncertainties (Solomatine & Wagner 2011). This thesis will analyse one of those simplifications and its impact on the modelling of glacier fluxes.

Most discussions in literature focusing on glacier flow modelling refer to mass balance considerations of snow (Huss et al. 2007, Sold et al. 2013). Frequently overlooked is the investigation of how the distribution of snow accumulation and the evolution of the glacier with time are connected (Benn and Evans 2010). For long term modelling, accumulation is often extrapolated from precipitation measurements to keep this process as simple as possible (Sold et al. 2013). This results in a linear increase of snow accumulation with elevation but neglects the lateral variation. For the snowline, an elevation gradient is used as well as a threshold defining whether precipitation falls as snow or rain (Benn & Lehmkuhl 2000).

Moisture carried by the wind needs to overcome the mountains and because of the uplift the air cools down. The resulting rain increases with altitude and explains the increase in snow accumulation with higher elevation (Grünewald et al. 2014). However, this rule does not always apply. In the case of some mountains, for example in the region of Columbia Glacier, the snowfall even decreases with increasing elevation (Benn & Evans 2010). Calculating the snow

accumulation just from temperature and precipitation is over-simplified. Wind, for example, leads to the shifting of snow and to enhanced variability in snow depth. Furthermore, there are inputs from outside of the glacier system like e.g. avalanches (Sold et al. 2013). More refined models which try to improve the simplification of the linear increase additionally include redistribution processes (Purves et al. 1998).

The aim of the present thesis is to analyse, whether the simplifying assumption of the increasing snow accumulation with elevation is sufficient for glacier flow modelling or if the redistribution of the snow has an influence on the glacier dynamics and its geometry. In the former case, the spatial accumulation pattern can be neglected in glacier dynamic modelling.

Whether this simplification is sufficient or not will be tested with help of a case study on Findelen glacier. It is then the question to what degree the results can be generalised to other glaciers in different locations or under different climatic conditions. The parameter settings as well as the choice of the patterns in this thesis were chosen in a way that a maximum potential for generalisation could result. Owing to the limited scope of this work, the results could not be verified with field data.

This thesis is based on the following research questions:

- Do changes in the pattern of snow accumulation induce changes in glacier dynamics compared to the reference case in terms of extent, length, volume, ice thickness and flow velocity?
- If the glacier responds to the redistribution of snow accumulation, how long does it take until it reaches a new equilibrium state and does the accumulation pattern influence the response time?
- How does wind drift and topography control the accumulation? In a simple wind drift model, what effect does the wind-driven redistribution of snow accumulation have on the flow dynamics?
- How does the glaciers react to sudden climate change? Does the glaciers adaptation on the new circumstances depend on the accumulation pattern?

For the investigation of the impact of a non-linear approach of the snow accumulation distribution five different experiments with new accumulation distribution were undertaken. The models in this thesis were generated using the commercially available simulation tool Matlab®. The various snow distribution patterns used in the experiments are the starting conditions for the glacier flow model. The flow model was provided by A. Vieli (Geographic Institute University of Zurich) (Brown et al. 2013). The results of the experiments are compared with the base scenario in which a homogeneous snow distribution was assumed using a linear increase of snow with elevation. The chosen procedures are graphically summarised in Fig. 1.

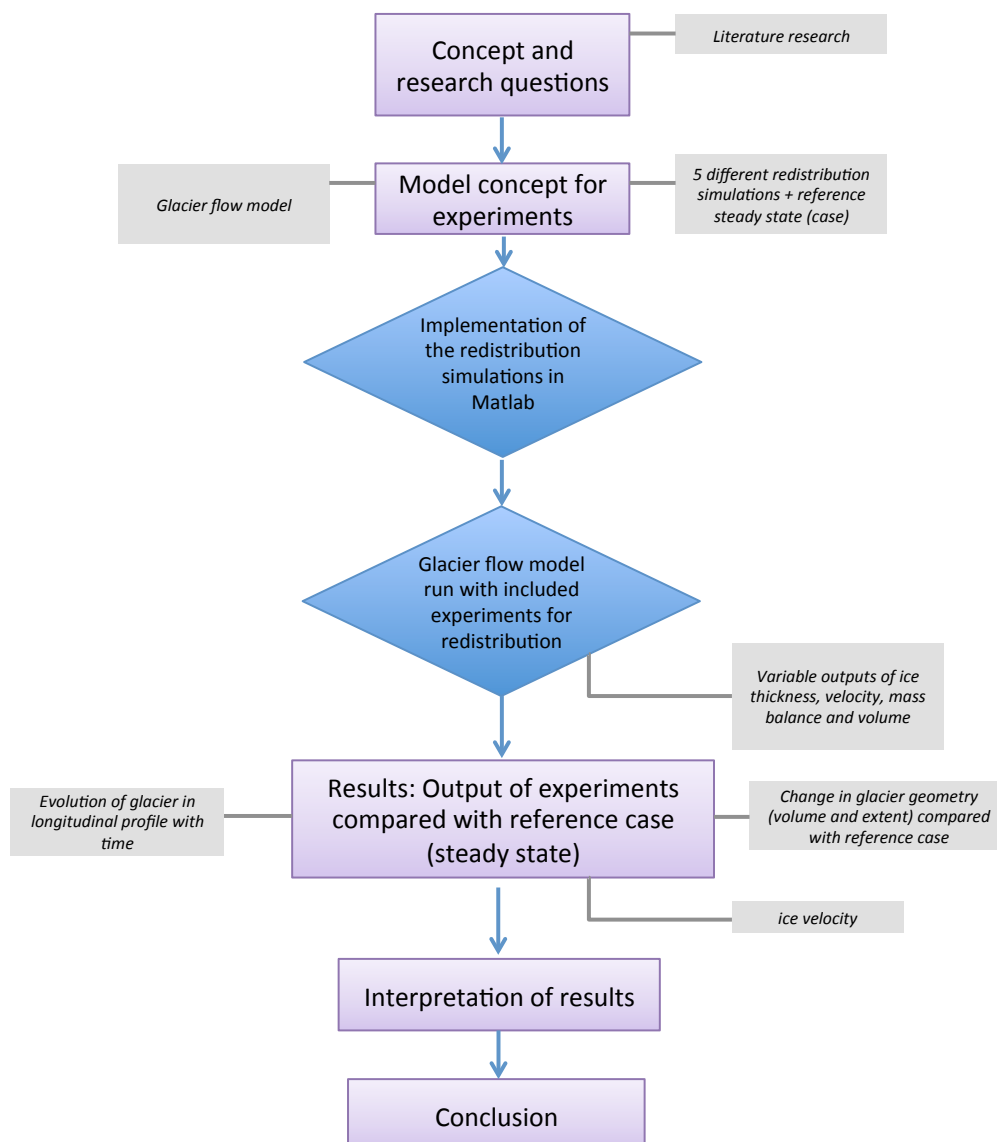


Fig. 1: Work flow chart of the master thesis.

The thesis is structured as follows: The first chapter 2 includes background information about the basic understanding of glacier dynamics, its components and most important parameters. Chapter 3 is concerned with the investigation area. Chapter 4 deals with the methodology and introduces the flow model as well as the five different experiments for snow redistribution in the accumulation area: Division of snow once to the left and once to the right side, interruption of the increase of snow accumulation with elevation, shifting snow from convex into concave curvature and relocation of snow based on wind distribution. A further experiment is the impact of climate change after the redistribution. In chapter 5 the results are represented. Chapter 6 discusses the achieved results and possible uncertainties of the model and provides an outlook, which questions have been answered and what might need to be further examined and discussed.

2 Introduction

In this chapter the key parameters of the glacier will be explained for a thorough understanding of its dynamic. This is an important basis for the subsequent description of the impact of accumulation variation on the glacier. It shall further be discussed how they can be calculated and modelled in general.

2.1 Glacier definition

By the definition of the “Glossary of Glacier Mass Balance and Related Terms by Gogley et al.” (2011) *glacier* is a “perennial mass of ice, and possibly firn and snow, originating from the land surface by the recrystallization of snow or other forms of solid precipitation and showing evidence of past or present flow” (Terminology, 2011, p.45). The glacier itself is divided into two parts: (1) the *accumulation area*, where the input snow constitutes accumulation and is transformed into ice, and (2) the *ablation area*, where mass is lost by discharge due to melt (Terminology 2011). The *equilibrium line altitude* (ELA) separates the two parts. This line defines the elevation of zero mass balance, which means that there is neither loss nor gain of glacier mass. The elevation of the ELA depends strongly on the climatic zone of the glacier (Fig. 2). Humid-maritime climates have “temperate glaciers” with relatively fast ice flow and high mass turnover, meaning fast renewal of the ice mass. The ice in these regions is at the melting temperature and thus the ELA at low altitude. ELA’s at high elevation are found in dry continental areas such as Alaska, Arctic Canada, and parts of Russia. The firn ice is cold with temperature below the melting temperature. Thus, glaciers in continental areas show low mass turnover (Zemp & Haeberli 2007).

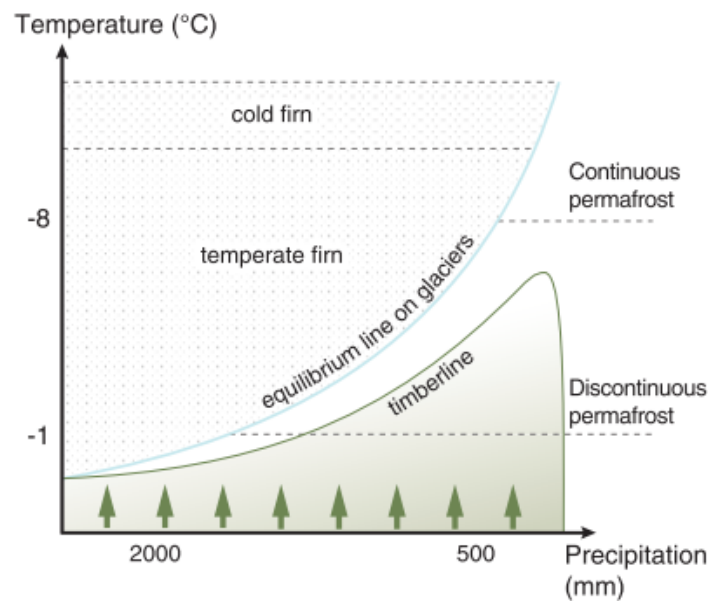


Fig. 2: Cryosphere diagram with ELA related to temperature and precipitation (Haeberli et al. 2002).

The processes of accumulation and ablation determine the flux of the glacier ice and whether retreat or advance occurs (Cuffey & Paterson 2010). The downhill flow of ice from the accumulation zone towards the terminus is induced by gravity but additionally influenced by internal stress and friction as well as basal sliding. The efficiency of the glacier flow is influenced by hydrology, drainage system, sediment particle size, as well as the slope of the bed topography (Benn & Evans 2010). Thus, the glacier flow and its dynamic is a complex process consisting of an interaction between different variables. Cause and effect cannot always be strictly separated strictly.

2.2 Glacier mass balance

The change in mass over the whole glacier during a defined time period can be defined as the *mass balance* (Benn & Evens 2010), expressed as water equivalent depth (SWE) (Benn & Evans 2010; Hubbard & Glasser 2005). If the mass balance is determined over a certain dimension, as the entire glacier, it is called the *specific mass balance* (Terminology 2011). A positive annual mass balance indicates a gain and negative values a loss of ice mass over the year (Terminology 2011). The balance itself is not just the mass exchange at a certain location but further depends on the transfer of mass through flow. It is very important to notice that the mass exchange between accumulation and ablation area varies with elevation but the glacier surface adjusts to the flow of the ice (Cuffey & Paterson 2010).

In the mid and high latitudes the annual minimum of the glaciers mass balance occurs in the end of summer and the beginning of fall while the maximum is reached in the end of winter (Benn & Evans 2010).

The study of mass balance as well as the ELA are important since they are significant indicators for global warming and show the health of the glacier. With increasing temperature the ELA rises as well (Hubbard & Glasser 2005).

The *mass balance gradient* defines the rate of change of mass balance [m] with elevation [m]. A linear mass balance gradient indicates a constant increase of the mass balance (Terminology 2011).

The mass balance gradient depends on climatic regions and is related to the ELA, which likewise depends on climatic conditions, particularly the share of solid precipitation and air temperature. Local effects have a strong influence on the mass balance gradient such as snow redistribution due to avalanches or wind shift (Benn & Lehmkuhl 2000). Generally, the accumulation and ablation area do not have the same gradient. The ratio between the two gradients is called the *balance ratio (BR)* and is calculated from the ablation gradient (db_{nb}) and the one from the accumulation area (db_{nc}).

$$BR = \frac{db_{nb}}{dz} / \frac{db_{nc}}{dz} \quad (1)$$

In the simple case where the temperature decreases with altitude and the mass balance is linear the gradient for the accumulation is less steep than the one for the ablation area (Fig. 3) (Benn & Lehmkuhl 2000). The thermal lapse rate decreases normally with increasing altitude. The average lapse rate is about 6.5°C/km with a variation of 4°-9°C/km (Benn & Evans 2010). However, variation in cloudiness and humidity lead to a non-linear ablation gradient. Glaciers in tropical areas and the alpine areas usually have smaller ablation areas with the ELA closer to the glacier terminus and hence typical values of 0.0028-0.0027m/m. This means that snow accumulation increases with 0.0028-0.0027 meter per meter elevation. For glaciers in dry climate areas the values are between 0.002-0.004 m/m (Leysinger Vieli & Gudmundsson 2004). In case of a steep increase of snow accumulation with elevation, the balancing processes, such as the ice flux, increase as well and convey the ice mass to the tongue.

With increasing mass balance gradient the glacier becomes larger. For example, if the gradient increases from 0.005 up to 0.01 m/m, the glacier flux increases by 50%, in order to conserve mass balance (Oerlemans 2001). In the following chapters the definition “accumulation

feedback” will emerge several times. It is used to explain the effect of an increase of the snow accumulation on the ice flux based on the mass balance gradient.

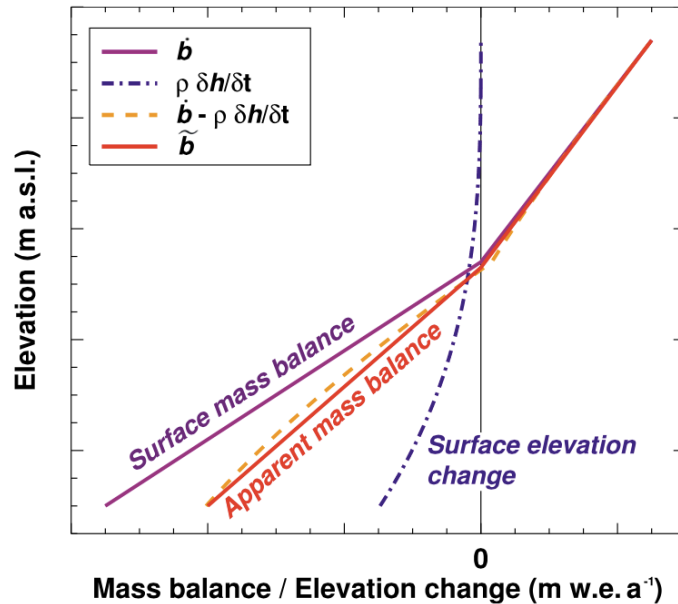


Fig. 3: Schematic representation of the altitudinal distribution of surface mass balance b , hypothetical elevation change and apparent mass balance over the glacier using linear elevation gradients (Huss & Farinotti 2012).

2.3 Glacier flux

According to the glossary of Cogley et al. (2011) the *glacier mass flux* is defined as the horizontal flow rate of mass through a plane normal to the direction of the horizontal velocity vector (Terminology 2011). The main flux processes can be grouped in sliding, deformation of the ice and the glacier bed (Benn & Evans 2010). The flux is controlled by the input of snow, which determines the ice thickness and the geometry of the outlet. Gravitational forces lead to glacier flow as soon as enough ice has accumulated. The movement of ice along the glacier bed and marginal areas, however, generates forces of resistances, which in turn depend on the properties of the ice and the geometry of the glacier bed, including its slope. The glacier ice only moves if gravity overtops the resisting forces (Cuffey & Paterson 2010).

The whole process of flow gets more complex if water is present at the interface between the ice and the glacier bed. The water can either originate from surface melt being discharged subglacially or it can be formed owing to melting of the ice due to high pressures of the overlaying glacier. Under these conditions the ice body starts to slide, which is called basal

sliding (Van der Veen 2013). Equally important are the mechanisms, which operate at the boundary between the glacier and the atmosphere.

Atmospheric processes generate sources and sinks. Snowfall in the accumulation area leads to thicker ice, which must be transported to the area, where it melts or calves due to climatic conditions to keep up the mass balance. Therefore, the flux is also the redistribution factor of ice mass. In the case of a steady or equilibrium state, the system is balanced by the same amount of gain and loss (Cuffey & Paterson 2010).

Dynamic processes such as the glacier flux have an influence on the glacier thickness and its change over a certain period of time (Benn & Evans 2010). Let's imagine a random cross section of the glacier (Fig. 4). Q is the ice discharge and b_s and b_b are the balance rates at the upper surface and the bed. The annual flux of ice through this cross-section must transport the total snow input from the accumulation area down to the tongue. However, the budget of the glacier varies within one year. In winter, accumulation exceeds ablation, while the situation is vice versa in summer. The net change over the annual cycle shows whether a glacier has gained or lost mass over one year (Cuffey & Paterson 2010). A positive or negative sum for the terminus reflects advance or retreat of the glacier (Benn & Evans 2010). This means that if fluxes are too slow to transport the accumulated snow, the glacier gains in mass (Cuffey & Paterson 2010).

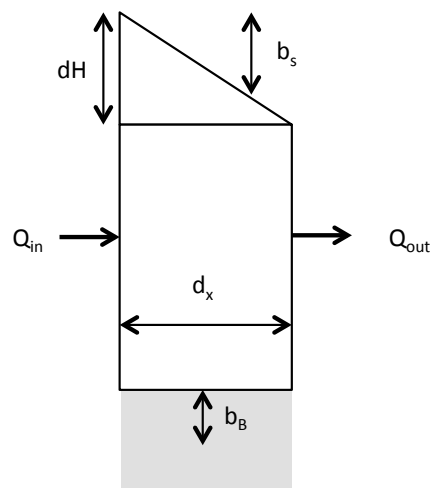


Fig. 4: Definition sketch illustrating the terms in the continuity equation (Benn & Evans 2010).

Elevation can influence the mass exchange, yet the glacier surface adjusts to the flow. If, for example, a glacier increases the speed of the flow more mass is conveyed to the ablation zone. In a first phase, the tongue will advance. Consequently, ice gets transported to lower and warmer areas, which in turn reinforces ablation. This leads to increased loss in mass. Thus, mass

exchange also influences the amount of discharge, which leaves the glacier (Cuffey & Paterson 2010).

For the calculation of the ice discharge a commonly used method is the Glen's flow law (Benn & Evans 2010). This law describes ice flow as the internal deformation and the basal motion. The former can be determined by the driving stress given by the surface slope of the ice. The latter on the other side is defined by pressure-dependent "sliding laws".

$$Q = u * H * W = \frac{2A(\rho g)^n}{n+2} H^{n+2} \left(\frac{\Delta s}{\Delta x}\right)^n W \quad (2)$$

Q (kg m^{-2}) is the conveyed ice through a vertical profile of thickness H (m). The density of the ice is described with ρ in kg/m^3 , g is the gravitation (m/s^2) and s the surface elevation at a certain location x . The vertical average flow speed u (m/s) and the rate factor A need to be determined as well. The flow exponent n mostly is chosen as 3. This means that the ice flux behaves proportional to the surface slope of the power of 3 and to the ice thickness of the power of 5 ($n+2$). W is the valley width, assumed to be a parabolic profile. Glen's flow law takes into account the internal deformation from the movement between ice crystals of the ice into account with the assumption of now basal sliding or longitudinal stresses (Benn & Evans 2010).

Ice thickness can be calculated from topography, since thick ice is found in flat or narrow areas and thin ice in steep slopes (Huss & Farinotti 2012; Linsbauer et al. 2012). The *continuity equation* eq. (4) explains the factors that influence the change in glacier thickness change with time:

$$\frac{\Delta H}{\Delta t} = -H \frac{\Delta u}{\Delta x} + \frac{\Delta Q}{\Delta x} + b_s + b_B \quad (3)$$

$\Delta H/\Delta t$ is the change in ice thickness with time. $\Delta Q/\Delta x$ is the gradient of the ice. $\Delta U/\Delta x$ is the velocity gradient, measuring rates of downglacier stretching of the ice. Stretching occurs due to locally higher velocities. This results in thinning of the ice and is calculated by multiplying velocity with ice thickness. To ensure that the equilibrium state remains and the ice mass is not changing, all the terms on the right side must sum to zero (Benn & Evans 2010).

2.4 Velocity

The flow velocity of the ice (u_x) eq. (5) can be expressed as a function of how much ice is transported through a certain cross section area (mass flux), which is determined by the characteristics of the glacier bed (Fig. 4).

$$u_x = \frac{Q_x}{A_x} \quad (4)$$

A_x is the cross-section area, u_x (m/s) the average velocity and Q_x (kg m^{-2}) the ice discharge. The movement of the glacier ice is controlled by bed deformation and basal mechanism such as sliding and deformation along the glacier bed (Fischer & Clarke 2001). High velocities are found in small cross-sections as well as steeper areas, where ice is thinner than in flat areas. Further, a steep mass balance indicates higher flow velocities, since greater rates of flow are required to keep up an equilibrium state. Furthermore, thick ice increases the flow velocity by lowering the pressure melting point and enhancing the sliding of the glacier (Fischer & Clarke 2001).

The velocity of the ice is restricted by resistive forces, which act as opposite reactions to the driving stresses forcing the glacier flow. Driving stresses are mainly controlled by gravity. Shear stresses or driving stresses are determined by the surface slope of the glacier and are expressed as the force per unit area of the glacier. The shear stress forces ice always to flow in direction of the maximum surface slope. It is further calculated from ice thickness, surface slope and ice density. Resistive forces on the other hand, also called resistive stresses, act as friction between the ice and the glacier bed or lateral margins against the shear stress (Van der Veen, 2013; Cuffey & Paterson 2010). Increase of water pressure leads to reduced resistance forces and consequently to faster glacier flows. Next to the water component, material properties of the glacier bed and the ice further influence the resistive force (Cuffey & Paterson 2010). If gravity and the resulting driving stress overcome resistive forces, the glacier starts to flow. However, determining the velocity of the glacier flow is not easy due to the nonlinearity of the flow law. Using very simple models, where only one or more of the resistances are considered, an analytically derived calculation is possible (Van der Veen 2013).

2.5 Snow distribution

Snow distribution is strongly heterogeneous due to the complex interactions of wind, radiation, canopy cover as well as accumulation differences produced by topographic features such as hills and depressions. Further impacts are due to climatic factors like solar radiation, which influences the melt rates. The resulting heterogeneity in snow depth can vary from one meter to

more than 100 meters. This heterogeneity reflects the fact that earth/atmosphere energy and mass fluxes, mountain hydrology and the alpine ecological system are linked to each other (Winstral & Marks 2014). Even on a regional scale, the snow distribution affects climate, vegetation and topography (Liston 2004). Wind distribution is among the key factors that need to be understood regarding the accumulation pattern (Dadic et al. 2010).

Lehning et al. (Lehning et al. 2008) demonstrated that precipitation contributes to the heterogeneous accumulation of snow. Snowfall also has preferential deposition associated with wind and terrain characteristics.

Wind driven processes can multiply snow accumulation by a large factor and can exceed melt rates from solar radiation (Dadic et al. 2010). Local wind turbulences further affect energy exchange and thereby can create snow and ice melt, which in turn influences the mass balance (Dadic et al. 2010). There is a strong correlation between the juxtaposition of topography and wind, which influences the snow distribution patterns and maximum snow depths (Winstral & Marks 2014). Wind has such a strong effect that accumulation patterns created by wind may control the amount of ablation rather than melting rates (Winstral & Marks 2014 in; 2012; Grünewald et al. 2010; Lehning et al. 2008)

The main process induced by wind is snowdrift. At the windward side of a hill, where wind speed increases, snow gets eroded and deposition is reduced. On the lee side, the speed declines and deposition of snow occurs (Dadic et al. 2010). Measurements have shown that twice as much snow can be accumulated on a lee slope of mean angle than in the adjacent wind ward slope (Fohn & Meister 1983). Snow transportation further depends on a threshold of wind speed. Determining this wind speed threshold is rather challenging, since it is not only linked to physical conditions of snow but also to other parameters such as meteorological conditions (Li & Pomeroy 1997). The threshold friction velocities mainly depend on snow properties such as density, dendricity, sphericity and particle size (Gallee et al. 2001). Particularly the snow metamorphosis can change this threshold (Li & Pomeroy 1997). Snow crystals from fresh snow, for example, indicate small cohesion in the snow pack, which allows high mobility of snow. Older grains are already larger since they lost their original shape due to sublimation and other mechanisms. They have larger cohesion, which decreases the potential for snow erosion.

Wind distribution can be observed on different scales. Saltation and turbulence exchanges of snow particles occur on a small scale and have hardly any influence on the wind distribution. Snow shift from ridges is more dominant and happens on a larger scale (Lehning et al. 2008).

Wind, however, does not only contribute to the redistribution of snow on the glacier, it also contributes to the activity of avalanches, which also shift snow on the glacier. Avalanches bring snow input from outside of the glacier and thus contribute to the heterogeneous accumulation distribution of snow in marginal zones (Fig. 5) (Huss et al., 2009). The more a glacier is surrounded by steep slopes, the more it benefits from input by avalanches, since a critical slope is required for triggering avalanches (Bloschl et al., 1991). Studies have shown that snow deposited by avalanches along the sides and the head of the glacier produces unusually large accumulation relative to altitude (Cuffey & Paterson 2010).

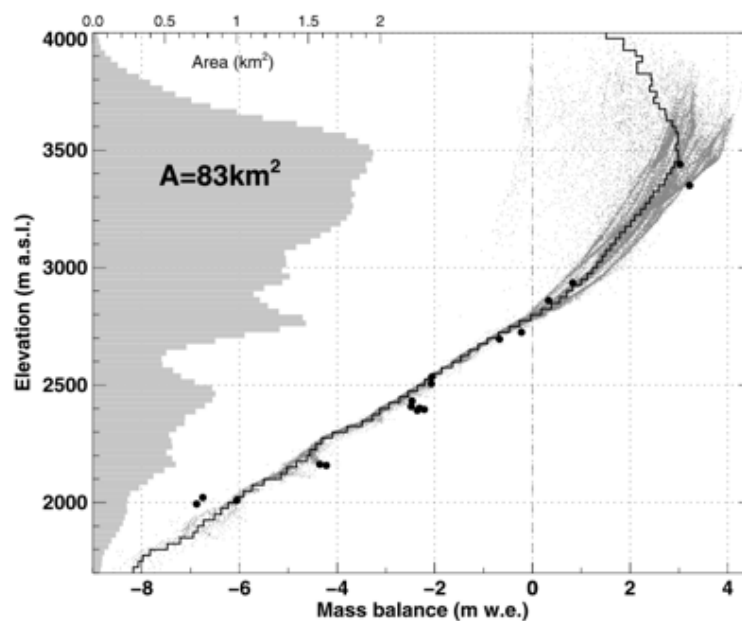


Fig. 5: Altitudinal distribution of surface net balance calculated for Grosser Aletsch glacier in 1977. The step function shows the mean net balance in elevation bands. Differences in the mass balance gradient and in the accumulation area are evident. Decreasing values in mass balance above 3500 m.a.s.l are due to effects of snowdrift and avalanches (Huss et al. 2009).

For the calculation of snow distribution, the so-called “apparent mass balance \tilde{b} ” (m/y) needs to be determined (eq. 5). This variable is derived from the surface mass balance \dot{b} (m/y), balanced by ice flux divergence and the change in surface elevation of the glacier over time ($\Delta h/\Delta t$) and the snow density ρ (kg m^{-3}).

$$\tilde{b} = \dot{b} - \rho * \Delta h/\Delta t \quad (5)$$

From the calculation of \tilde{b} (m/y), it is possible to estimate the snow distribution. Additionally, balance ice volume flux can be calculated even if the glacier is not in a steady state.

2.6 Climate change and its influence on glaciers

Climate change has a strong impact on glaciers. Therefore, glaciers are key indicators for changes in meteorological conditions. An increase in temperature by one tenth over ten years can lead to a retreat of the glacier terminus by more than 100 meters (Haeberli et al. 2000 in: BAFU, 2013). It is estimated that between 1850 and 1975 the glaciers in Europe have lost almost 50% of their volume and another 25% by the year 2000 (Haeberli et al. 2007). Recently, glaciers lose 0.5-1.5 m water equivalent per year. In very warm summers, such as in 2003, this number rose to 2.5 m (BAFU, 2013). The total glacier volume in 1850 is estimated at 200 km³, today just one-third is left (Zemp et al. 2006). Further shrinking is expected in the future. An increase in summer air temperature of about 3°C could lead to a reduction of the European glacier cover of around 80%, especially on ice masses located lower than 3000 m.a.s.l. In the case of 5°C, the glaciers would probably disappear completely (Zemp et al. 2006). Observations of glacier sensitivity and reaction to climate change can be done by analysing changes in the equilibrium line altitude (ELA). This is especially appropriate since it is the lowest boundary of climatic glaciation. As stated above, it defines the boundary between the annual accumulation and ablation area. Future scenarios assume that a temperature increase of 1°C would raise the ELA by approximately 100 m. The same increase could also be achieved by a reduction of precipitation by 20% (Zemp et al. 2007).

Changes in climate and glacial cover have consequences for landscape appearance, slope stability, water cycle, natural hazards and sediment budgets (Barnett et al. 2005).

3 Investigation area

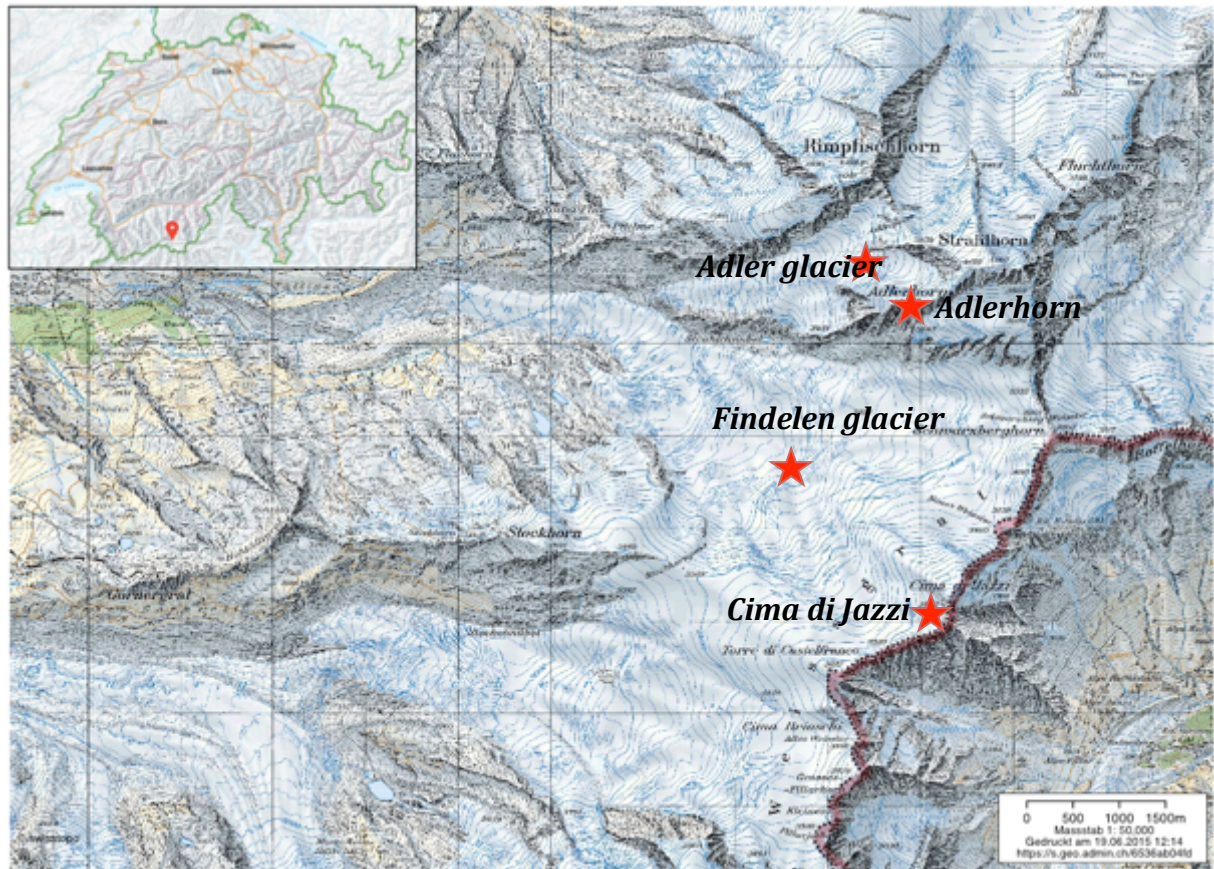


Fig. 6: Findelen Glacier in Zermatt (Geo.admin, 2015).

This study focuses on Findelen Glacier, which is located in the Swiss Alps above Zermatt (46°N, 7°52'E) (Fig. A1 & A2). It is a temperate valley glacier with a length of 6.7 km and an area of 13 km² according to the year 2010. Since the end of the Little Ice Age around 1850, when the glacier reached its maximum extent, it has lost approximately 3.7km of length and 6.96km² area of ice (Maisch 2000). This is about a 30% loss (Joerg et al., 2012). The elevation range is from 2600 to 3900 m.a.s.l with exposition to the northwest and west. The accumulation area of Findelen glacier strongly benefits from south and south-easterly wind, which brings precipitation (Sold et al. 2013).

Adler glacier (2 km²) is a former tributary of Findelen glacier, which lost contact in the 1990s. Today they are separate and independent ice bodies (Joerg et al., 2012; Report 2014). Findelen Glacier has been chosen due to the large amount of information, which is available of this glacier. The ice surface is almost debris free and the glacier is quite flat with a fairly constant slope. It can be accessed from the side and is suitable for almost all kind of

measurement techniques and practically the entire glacier surface allows in-situ measurements. Furthermore, Findelen glacier is more protected from increased temperature since it is located at high altitudes, thus it will probably sustain stronger melt for another few decades (Farinotti et al. 2011 in: Joerg et al. 2012). Nonetheless, Findelen glacier lost in the period of 2005-2010 about -2.7 meters w.e (Joerg et al., 2012).

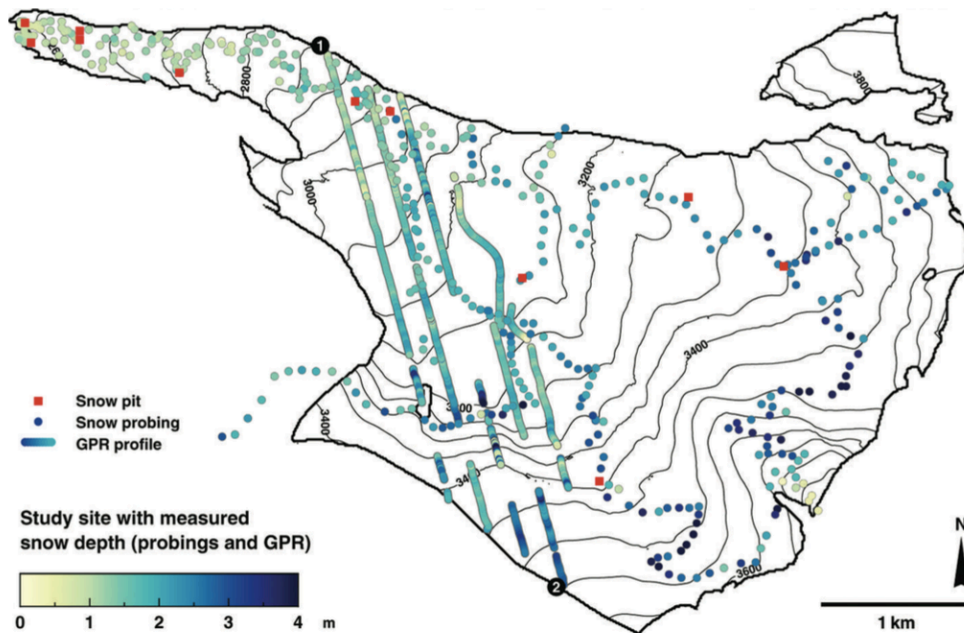


Fig. 7: Findelen glacier in Zermatt. Dots show manual snow probings', lines represent GPR profiles, the colour code shows measured snow depth in April 2010 (Sold et al. 2013).

The University of Fribourg and Zurich have been leading an investigation program of mass balance measurements and glacier monitoring on Findelen glacier since 2004 (Huss et al. 2013). (Fig. 7) The research project conducts the monitoring of two accumulation stakes in the accumulation area of the glacier at an elevation of 3300-3500 m.a.s.l and twelve ablation stakes in the ablation area (2574-3300 m.a.s.l). Additionally, four stakes are set on the Adler glacier (Sold et al. 2013). Winter and summer mass balances are recorded every year. Attending to the stake measurements, the outline of the two glaciers are further observed with airborne LIDAR (Report 2014). In 2005 and 2010 the accumulation distribution was measured with helicopter-borne ground-penetrating radar (Fig. 8) (Huss et al. 2013).

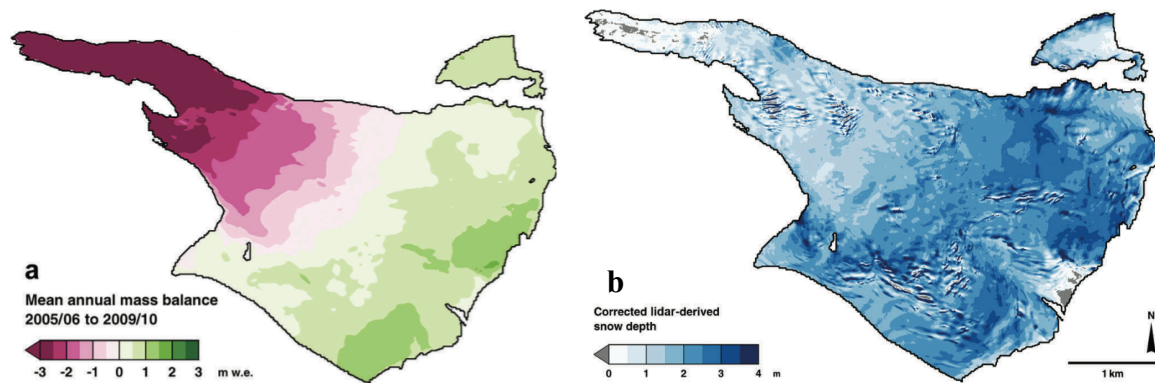


Fig. 8: Raw LIDAR-derived elevation change from October 2009 to April 2010. The left figure (a) shows the mean mass balance, the right (b) figure the snow depth (Sold et al. 2013).

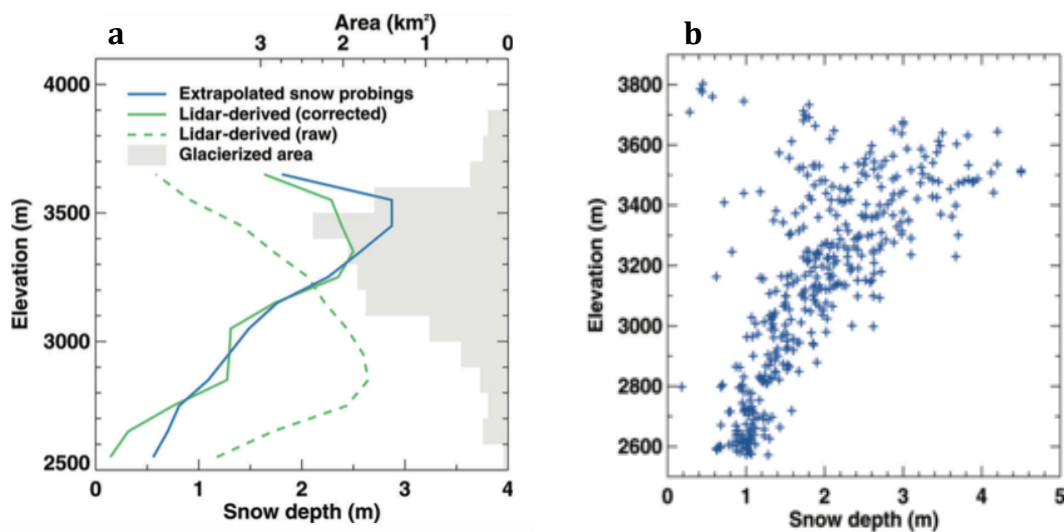


Fig. 9: Right (b): Measured snow depth with elevation from 403 probings' in April 2010. Left (a): vertical distribution of mean snow depth in 100m elevation bands derived from extrapolated snow probings', raw LIDAR-differencing and LIDAR-differencing corrected for emergence velocity, firn compaction and autumn melt (Sold et al. 2013).

In April 2010, the mean snow depth was 1.86 m. The results have shown that the snow depth is elevation dependent. Investigation of bulk density produced values from 223 to 294 kg m⁻³ and in the tongue to 407 kg m⁻³. These values indicate the evolution of the annual snow pack and the effect of local wind distribution, erosion and deposition of snow and also the input from avalanches. Steep slopes of >40° show a decrease of snow depth. Fig. 9b shows the linear

increase of the snow depth with elevation from snow probing records. Below 3300 m.a.s.l the linearity is well recognizable. In the upper area, however, higher complexity and more heterogeneity in snow depth can be seen. The values vary between 2 and 3 meters on the same elevation level. This observation gets even more obvious considering the snow depth with elevation in Fig. 9a. The blue line represents the interpolated snow probing measurements, the green one the LIDAR-driven corrections. Until an elevation of 3400 m.a.s.l the snow depth increases almost linearly with elevation, in higher areas it declines again. The reduction in snow depth, which values mainly refer to Adler glacier, disproves the simplified assumption of the linear increase (Sold et al. 2013). The reason why Adler glacier indicates less snow accumulation than Findelen glacier was not found in literature. According to personal communication, Adler glacier lies in the lee of the south wind, which brings the snowfall. The high rock walls from Adlerhorn shield the glacier from precipitation input. Further values which influence the curve in Fig. 9b come from Cima di Jazzi (3803 m.a.s.l) where lower snow depth was measured. This hill is exposed to wind erosion (Fig 8b).

4 Methodology and strategy

The first section 4.1 provides an overview of how mass balance is measured by using in-situ ground survey and remote sensing. Section 4.2 introduces glacier flow modelling. The third section 4.3 is dedicated to the flow model being used in this thesis. The model itself was written in Matlab. Section 4.4 gives overview of the implementation of the reference case and the five experiments as well as the input parameters. Section 4.5 refers to the parameter setting of the experiments.

4.1 Field measurement methods to determine mass balance

Mass balance can be determined by field measurements, monitoring or by computer modelling. Commonly, collecting data in the field is carried out by taking point measurements with stakes. With this approach, the accumulation over a few years can be recorded. Ablation and accumulation stakes (Fig. A4.b, A5) are being drilled into the ice or firn in the beginning of the accumulation season before snowfall starts. In order to measure the ablation, on one side, one has to look at the stakes, which melt out of the surface during summer. The difference in stake length above the ice surface between the two time steps (typically the period of one year) shows the respective ablation at this point. The recording of the snow accumulation, on the other hand, is done in spring before the melt season starts. Similar to the ablation measurements, accumulation stakes help to record the increase of snow during winter. In the following fall, an additional series of measurements record the ice mass lost during summer (Hubbard & Glasser 2005). Loss or gain is not expressed by difference in thickness. Instead, the term “snow water equivalent” (SWE) is used, i.e. the water content in the snow cover. Thus, snow density needs to be measured as well (Huang & Cressie 1996). By combining the winter and summer records the annual mass balance can be determined.

A different approach to the stake method is the use of an avalanche probe. The probe is stuck into the snow until it comes to rest on the underlying ice or firn of the previous year (Hubbard & Glasser 2005). In spring, the boundary between ice/firn and snow on Findelen glacier is found on average at a depth of 1.86m (Sold et al. 2013). In order to identify the multi-year accumulation layers, snow pits need to be dug (Fig. A4.a) (Hubbard & Glasser 2005). However, as a consequence of using point measurement, data an interpolation over the investigation area is needed. Hence, microscale effects disappear (Machguth et al. 2006). Furthermore, general

field studies are often hampered since not all areas are accessible for the researchers, mainly due to crevasses, avalanches, rock- or ice falls (Huss et al. 2013).

Another method of monitoring glacier mass balance is the usage of photogrammetric method. Aerial photography is a useful approach for calculating the mass balance of the glacier. The snowline and the accumulation-area ratio (AAR) are determined from recorded photos. Compared with the stake method, time-laps photography allows monitoring the snow-cover patterns and its changes over the whole year. For drawing the snowline, bare and debris-covered ice need to be identified (Fig. 10), which might provide a challenge. The separation is done manually or by using an algorithm, which automatically determines the snow line during the ablation season. However, this method is constrained by good weather conditions with no clouds. The classification between ice and old snow is not always easy and requires some knowledge and experience (Huss et al. 2013).

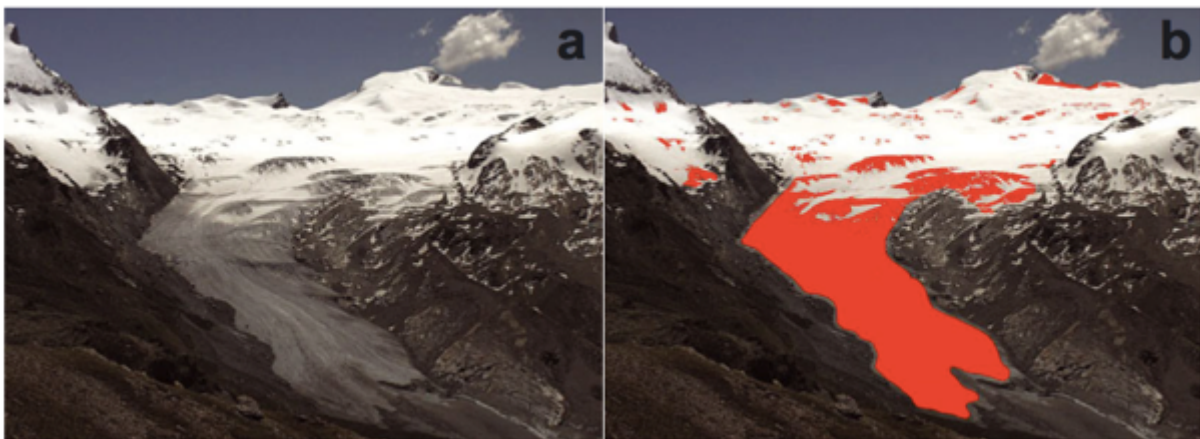


Fig. 10: Identification of bare ice and snow covered area for separating accumulation and ablation zone (Huss et al. 2013).

A further method for collecting surface data is laser sources such as airborne light detection and ranging (LIDAR) with the aim to calculate the surface elevation to a digital elevation model (DEM). Different time-laps DEM's, can be compared to obtain elevation changes. However, the two mentioned methods often do not apply sufficient contrasts and are bound on good weather conditions for the recordings.

Monitoring methods based on radar are not dependent on good weather conditions, meaning they can measure surface elevation under any circumstances (Haug et al. 2009). This allows observing the evolution of the mass balance over longer time with an improved temporal resolution. Additionally, larger areas can be monitored (Huss et al. 2013). One option is ground

penetration radar (GPR) in form of an airborne application or a ground survey measurement. In case of the former, the measuring instruments are fixed to an aircraft. GPR is a useful method for measuring ice thickness and snow depth due to deep penetration of the seismic signal in ice and snow and its reflection. Boundary layers can be detected due to the contrast in dielectric permittivity. Furthermore, the properties of the material are identifiable. This is ideal to distinguish ice from the glacier bed (Sold et al. 2013; Joerg et al. 2012). Volumetric changes are observed from geodetic methods such as repeated topographic survey and subsequently the comparison of the different DEM's to determine changing thickness and differences in extent (Hubbard & Glasser 2005).

4.2 Glacier flow models

Chapter 1 indicated how important modelling of glaciers and the understanding of glacier behaviour is to predict the reaction of the ice body on global warming. Considerable interests are aroused by the impact of changing climate conditions and the glaciers' reaction, especially regarding water cycle or natural hazards. However, for achieving valid and consistent forecasts, the choice of an appropriate model type is crucial. There are different types of models and not all of them are suitable, depending on the input variables and the intention for the results. In this section, two model types will be examined, one based mainly on meteorological input data and the other on numerical laws.

If enough knowledge about the mass balance and sufficient climate data exist, calibrated mass balance models as (positive-) degree-day (DDM) or energy balance considerations are appropriate. Otherwise, other more schematic attempts need to be taken. Numerical models for example are more often based on calculations from physical laws and boundary conditions (Oerlemans et al. 1998). Those two model types are explained in more detail in the following section.

Degree-day models are very useful for calculating snow melt and thus changes in glacier thickness from near-surface air temperature. This approach is particularly suitable if the ablation area of the glacier has to be investigated and modelled (Gardner & Sharp 2009). DDM's depend on the input of temperature data from meteorological stations, preferably close to the study area. The meteorological station collects data in intervals of hours, days or months. One crucial advantage of the DDM is the consideration of local climatic conditions related to the topography. With this method, direct monitoring of the temporal variation of the sun radiation due to day and night as well as seasonal variability and topographical effects is possible (Hock

2003). DDM's further include the diminishing of incoming radiation through cloud coverage in the sky (Mölg et al. 2009). Most other models, which use meteorological data with a larger resolution, have to downscale them to the scale of the investigated area, blurring the local variability. A good example for such a downscaling is in the case of precipitation data. Further, simplified assumptions as, for example, linear changes in temperature with elevation (6-7°C/km) do not fully reflect reality. The temperature gradient over ice, for example, was determined to be less steep than the free air values (Greuell & Böhm, 1998 in: Gardner & Sharp, 2009).

There are two kinds of degree-day models. On the one hand, there are index models, which are based on the sum of positive degree-days just from temperature measurements. By fitting a glacier-specific factor, the glacier melt can be determined (Paul et al. 2007).

Energy-balance models on the other hand, use energy fluxes at the glacier surface and from physically based calculations. Therefore, directly measured data from meteorological variables such as radiation balance and turbulent fluxes are necessary (Pellicciotti et al. 2005). Melt is calculated from the positive energy balance equation (Paul et al. 2007).

Studies have shown that the albedo and the high temporal variation of the incoming radiation are some of the most important parameters to determine snow melt, especially in the Alps with rough topography.

Degree-day models are based on point measurements from a local meteorological station. This kind of data collection requires subsequent interpolation. This often requires to include additional stations, which probably are located further away. Consequentially a mixture of microclimate on the glacier and data from conditions far away from the study site is created. Another disadvantage of this method is the high amount of data required. The model is appropriate for individual glaciers and is less often applied to larger regions (Paul et al. 2007).

The development of numerical models, which are mostly independent from field data began in the early 1980s. In this time the Columbia Glacier started to retreat very rapidly. For better understanding of such processes and prediction of the future, first numerical models were developed. Rasmussen and Meier (Rasmussen & Meier 1982) created a simple one-dimensional (1D) model for the tidewater glacier, which was based on mass conservation. Models for ice-sheet flow were also developed for dating ice cores or investigating the coupling of the glacier ice with the climate system. High interest also lies in the understanding of the mountain glacier, since they, as already discussed in chapter 2.6, react very sensitively on climate changes in their geometry and dynamics. Le Meur (2004) declares that the use of numerical models was the only good way to investigate and model the complexity of glaciers and ice-sheets and how they

interact with climate and changes in their environment (Fig. 11) (Le Meur et al. 2004). Simple one-dimensional models are based on analytical solutions. For two dimensional-models, a numerical approach is required. In case of the latter, geometry properties are better included and the outputs are easier to interpret and compare to topographical maps. One-dimensional models provide only results along the flow line, glacier extent is not considered (Le Meur & Vincent 2003). A two-dimensional model responds to numerous processes and the expression of basic physical principles to simulate the dynamic of the glacier. A third dimension can be added by including the elevation. The glaciers reaction to climate forcing is non-linear and very complex. With the help of numerical models, resulting time lags can be represented and long-term predictions can be made for the response of glacier to climate scenarios (Le Meur & Vincent 2003).

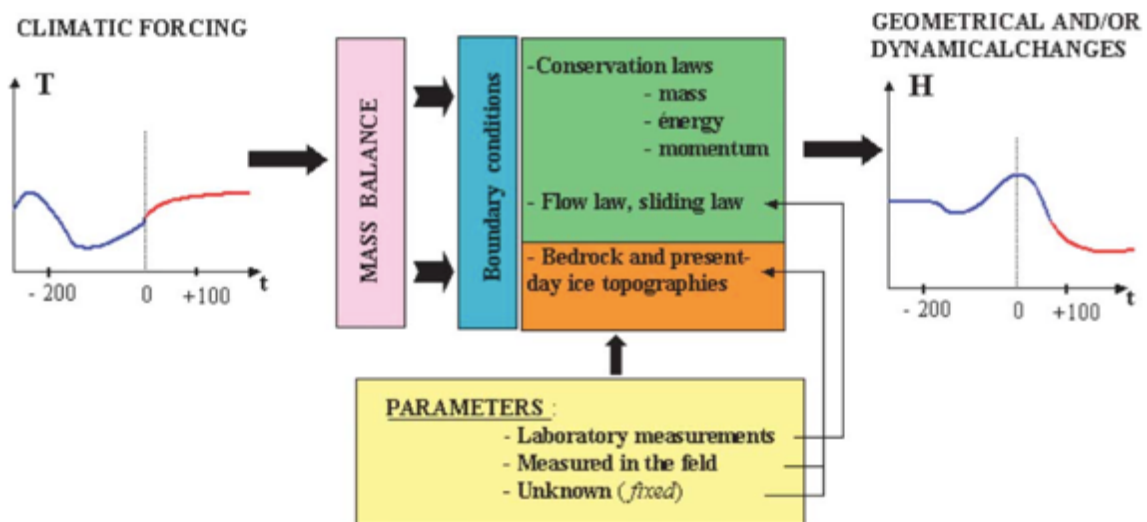


Fig. 11: Schematic representation of a numerical flow model (Le Meur et al. 2004).

The numerical flow model itself is physically based since it makes use of laws of conservation of mass (mass, momentum, energy). The model is very useful since it needs hardly any input data and most variables are derived from physical equations. Fieldwork and measurements are not necessarily needed. For a spatial and time discretization, physically based models often use grids, triangular irregular networks or other responding units. A further advantage of this model type, aside from the input parameters, is that the analysis can be done on any scale while point measurements from fieldwork often just cover a small area. However, the scale of the model can be influenced by the grid resolution. This type of model is well suited for sensitivity analysis (Solomatine & Wagner 2011).

Nevertheless, few key parameters and boundary conditions are to be set up (Solomatine & Wagner 2011). Those conditions include energy exchanges between the ice and atmosphere interface and parameters, describing the interaction of the glacier with the glacier bed. This also includes the prescription of limitation of the domain. For the simplification of the model, assumptions are made for some parameters as, for example, the perfect plastic rheology of the ice or the omission of basal sliding. With such simplification the model is easier to handle but this can also lead to some uncertainties (Le Meur et al. 2004).

4.3 Glacier flow model applied for Findelen glacier

The glacier flow model used for the experimental research of this thesis was initially created for the investigation of a glacier in the Antarctica but has been further adapted for valley glaciers (Brown et al. 2013). The concept is a mass conserving numerical flux model. Glacier flux itself is determined as mentioned with “Glen’s flow law” eq. (3) and the “continuity equation” eq. (4). The parameters set up in advance are the ELA, the ratio between accumulation and ablation area (mass balance ratio), the mass balance gradient, the grid resolution and the time step of how many calculations are done. The only parameter based on field measurements is the DEM of the glacier bed. In the end, the new ice volume is calculated with further information about ice flow velocity, ice thickness and the mass balance.

In order to achieve the glacier reconstruction, first of all the mass balance needs to be calculated. Since no field data is used in the modelling, equation parameters are derived from the DEM and the underlying processes. In case of a linear approach of the accumulation, the net mass balance \dot{b} (m/y) can be calculated from the slope of the glacier bed as follows:

$$\dot{b}(x) = gs * (s(x) - ELA) \quad (4)$$

ELA is the equilibrium line altitude, gs the gradient of the mass balance curve. The amount of accumulation and ablation ice results from the term gs , corresponding to the balance ration, which is further to set up (Brown et al. 2013). The increases of the factor \dot{b} is responsible for the feedback from the accumulation area (Benn & Evans 2010). The thicker the glacier gets, the larger is the share of the glacier that reaches up to higher elevation, thus more mass is attained by the convey system (Oerlemans 2001). Theoretically, it is possible to start the model with zero ice and let the glacier grow from the base of the DEM surface. With every year of run, the model

more and more approaches a robust state where the equilibrium of the glacier flux is hold by the balance ratio. Since a start from zero ice thickness takes many years of running, which is very time consuming, a fictive ice thickness was chosen as an initial input for the implementation of the reference case.

One of the crucial impacts on the mass balance is solar radiation since it determines a considerable part of the melt and thus mass loss. Instead of including the incoming short wave radiation and thus snow melt, the ELA can be corrected with a factor k , which lowers or shifts up the equilibrium line depending on the aspect of the terrain

$$\dot{b}(x) = g_s * (s(x) - (ELA * k)) \quad (6)$$

The sun correction factor k is determined by a function including solar radiation, aspect orientation, mass balance gradient and elevation. In south facing areas the ELA is shifted upwards, on north-facing slopes it is lowered down (Farinotti et al. 2010). Since this effect complicates the modelling of the following patterns for the snow distribution, it was decided not to include the solar correction. Snow melt due to sun is thus neglected and just determined by the condition of mass conservation, which regulates the ice loss depending on the amount of snow input in the accumulation area. Consequently, the ice volume is overestimated which is not further to interfere since the thesis focuses on the sensitivity of the glacier reaction and not the net volume change.

With the determined mass balance, the ice thickness and its change over time at each location are further to be calculated. This step is needed before the glacier flux can be determined. For the calculation of the ice thickness, the mentioned continuity equations (eq. 4) can be applied. Since this equation (4) complies with a 2D model, a third dimension needs to be added. The x- and the y-axis describe the horizontal ice flux ($Q_{x/y}$) in two directions and the third dimension is described by the thickness.

$$\frac{\Delta H}{\Delta t} = \dot{b} - \frac{\Delta Q_x}{\Delta x} - \frac{\Delta Q_y}{\Delta y} \quad (7)$$

H (m) is the ice change in thickness over time Δt . If the glacier gets thicker and thus reaches a higher altitude, the mass balance is forced to adapt the alteration due to the linear increase with elevation. Therefore, those two parameters are strongly related to each other (Benn & Evans 2010).

For the calculation of the flux Q (kg/m^3), Glen's flow law is used (eq. 3). In our specific case of flow the two directions are defined by the x- and y-axis and glacier thickness in z-direction.

$$Q_x = \bar{u}_x * H = \frac{2A}{n+2} * H^2 \tau^n \quad (8)$$

$$Q_y = \bar{u}_y * H = \frac{2A}{n+2} * H^2 \tau^n \quad (9)$$

$$\tau = \rho g H * \frac{\Delta s}{\Delta x} \quad (10)$$

The basal shear stress is expressed with τ . The variable $\bar{u}_{x/y}$ is the velocity of a column ice in horizontal direction. Vertical velocity changes are not included in the model, the values are assumed to be constant with ice depth.

Velocity is indirectly calculated from a diffusivity equation which explains the mass flux change per time and length unit (Oerlemans 2001). The horizontal velocity of the glacier ice is calculated out of two velocity vectors, one in x (u_x) and one in y (u_y) direction (Hooke 2005).

$$\bar{u}_{x/y} = \sqrt{(u_x^2 + u_y^2)} \quad (11)$$

A is the flow law parameter and n the exponent ($n=3$). A flow exponent of 3 means that the ice flux behaves proportional to the surface slope of power of 3 and of the power of 5 ($n+2$) to the ice thickness. Glen's Flow law just takes into account the internal deformation of the ice. The basal sliding is not explicitly included in the calculation. The rate factor A is a measure of the deformation ability of ice. The higher this number, the faster the glacier flows. An influencing factor on A is the ice temperature ($0^\circ\text{C} \approx 0.8 \times 10^{-16} \text{Pa}^{-3} \text{y}^{-1}$). With this factor the basal sliding can be compensated since the ice temperature is a key factor for the amount of water at the glacier bed. Of course, the melting point also depends on ice thickness. The gravitational driving stress is composed of the ice density, the gravitation ($9.81 \text{ m}/\text{s}^2$) and the ice thickness H as well as the ice density ($910 \text{ kg}/\text{m}^3$) and the glacier flow diffusion $\frac{\Delta s}{\Delta x}$. The latter parameter is the substitute gravitational driving stress expression into the flux equation. It reacts very sensitively to slope and ice thickness (Benn & Evans 2010; Paterson & Bud 1982).

The time step for the calculations depends on the grid resolution and the ice diffusivity. The latter is not a constant value. For a grid of 100 m a time step of 0.01 to 0.05 is suitable to ensure stability. Otherwise the glacier flows too fast and the geometry can not adapt to the changes (Oerlemans 2001).

4.4 Introduction to the experiments

With the help of the flow model, five different experiments were performed, which will be explained in the following section. The first section 4.4.1 contains the description of the reference case of the glacier, which serves as the reference basis for all of the following experiments. In sections 4.4.2-4.4.5 the initiation of the experiments is described. For each of them, a script was written in Matlab with the aim to generate a new accumulation distribution. The whole thesis is based on the assumption of a summer situation where snow is found in the accumulation area and the ablation zone indicates only ice. Thus, all the experiments only concern the accumulation area with positive mass balance values for the redistribution. Section 4.4.6 introduces a further experiment where climate conditions change. The parameter setting for the experiments is explained in section 4.5.

4.4.1 Reference case (F)

Running the glacier model until a steady state is reached, called the reference case, generates the starting position for the experiments. This means that the glacier is in a stable and robust situation where the same amount of snow is added in the accumulation area as lost in the ablation area. For achieving the initial steady state of the glacier, the model was run until the glacier's length and volume do not change anymore. Without the steady state as the initial situation, feedbacks due to changes in the accumulation zone would falsify the results of the redistribution experiments. They influenced the results and the reaction of the glacier could not exclusively be assigned to the varying accumulation pattern. The reference case serves for all of the following experiments as the input geometry.

4.4.2 Left and right pattern (A and B)

These two experiments are the examination of what would happen if almost the whole snow was accumulated only on one side of the glacier. This experiment indicates a very extreme form of snow redistribution, which would not occur in reality as such. The idea of this extraordinary form of snow shift is to get an impression of the sensitivity of the glacier to the impact of the distribution and its relevance. Therefore, the glacier is cut into two parts of different area sizes. By shifting most of the snow to the left side, the ice thickness of this pattern will be thicker than by shifting it to the right side, which is larger in size.

The cutline for the separation follows a ridge on the glacier down from Cima di Jazzi (3803 m.a.s.l.). Fig. 12 shows the two parts, orographically divided into left and right. It must be noted that the redistribution of snow is just done in the accumulation area.

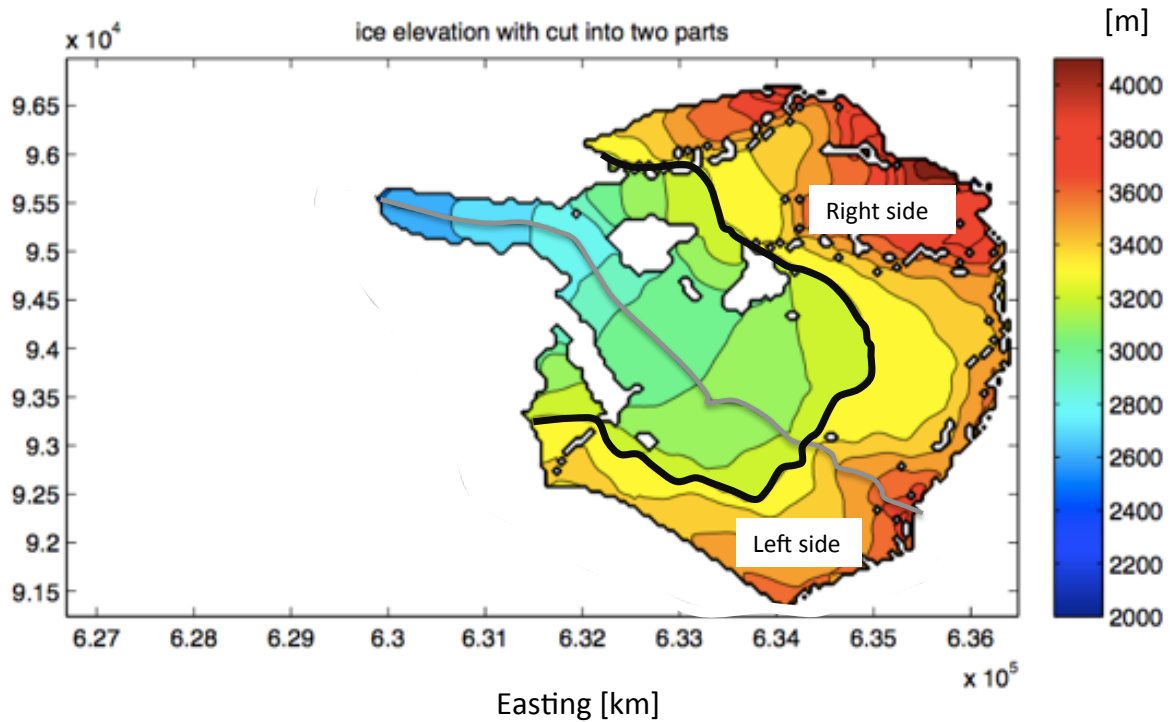


Fig. 12: Cut of glacier into two parts left and right. The black line indicates the elevation of the ELA. The colour bar shows the elevation of the glacier.

The redistribution of the snow in a first step is done by distributing the whole snow accumulation from the initial input of the reference case between the two sides in a certain ratio. For ensuring that the effect is clearly revealed, an extreme ratio of 1:10 between the two sides was deliberately chosen. The following calculation was made to conserve the accumulation mass:

$$MB = \frac{mb}{vol_p} * vol_{tot} * w \quad (12)$$

The units are all in meters. The whole snow accumulation is summed up to get the total volume vol_{tot} . Additionally, the volume of each pattern vol_p is determined as well. For the calculation of the new accumulation MB, the initial accumulation mb , which corresponds to the mass balance values, is at each grid cell divided by the volume of the pattern vol_p , multiplied with the total accumulation area multiplied with a weight w . This is the ratio between the two sides. This

calculation ensures that all the grid cells are weighted against each other. A certain location with higher amount of accumulation than neighbouring cells should still be higher weighted after the redistribution. During the following runs, the accumulated snow resulting from the previous run is again distributed between the two patterns in the same ratio. For the verification of mass conservation the sum of the new accumulation $\sum MB$ has to be the same as the sum of the initial accumulation $\sum mb$ in the end.

4.4.3 Cut of accumulation (Experiment C)

The next analysis was done by investigating the consequences of an interruption of the increasing snow accumulation with elevation, which generates substantially less snow input (Fig 13). The accumulation measurements of Sold et al. (2013) exhibited the heterogeneous snow distribution in the accumulation area of Findelen glacier. Fig.9a showed that the extrapolated snow depth from the probing increases until an approximate elevation of 3400 m.a.s.l but then starts to decrease.

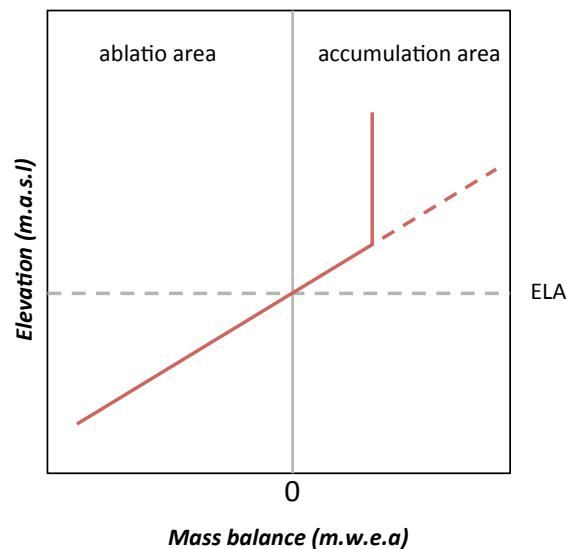


Fig. 13: Cut of increasing accumulation at a certain height. The bold line indicates the cut, the dotted one the initial assumption of an increase with elevation.

In Matlab a function was written which defines the cutting elevation where the increase stops. All the grid cells, which lie above this cutting line, receive the same accumulation value. Mass conservation is no longer sustained and the overall amount of snow accumulation will be far less.

Instead of this abrupt cut, other approaches would have been possible, too. For example an exponential decline of the accumulation in a certain way as the observation of Sold et al. (2013) have shown. The criteria for the cutting elevation will be explained in chapter 4.5.4.

4.4.4 Curvature (D)

A further experiment is a redistribution depending on curvature, where snow is shifted from ridges into depressions. The variable curvature is often used since terrain strongly influences distribution and depth of snow. Curvature, aspect and elevation are supposed to be the most important terrain variables (Marchand & Killington, 2005). However, there is some debate in the literature over the strength of the correlation between snow distribution and terrain. Snow pattern analysis by Farinotti et al. (2010) pointed out a weak correlation between curvature and snow depth in general. High snow depth values are found where curvature is very flat, neither on convex nor on concave terrain. However, these authors emphasize that this does not automatically mean that snow depth is not influenced by curvature (Fig. 14). A possible explanation for the impression of no correlation might be an interaction of the curvature with other variables.

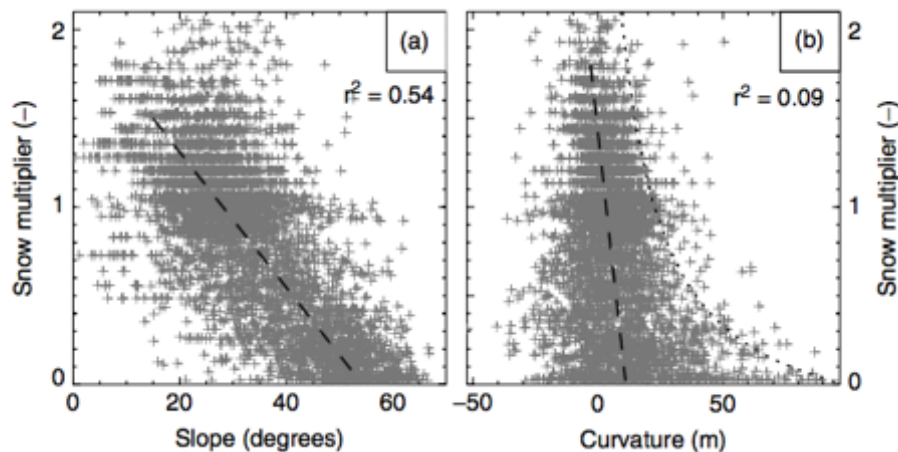


Fig. 14: Correlation of slope and curvature with snow depth (Farinotti et al. 2010).

Marchand & Killington (2005) on the other hand emphasise a significant correlation of slope and curvature with the variation in snow depth: “Concerning the hypothesis of the redistribution of snow by wind, these findings would make sense since the redistribution is influenced by terrain variables like slope, curvataure and aspect [...]” (Marchand & Killington, 2005, p.368). Steep

terrain, which exceeds hill slopes of 40°-55° are mostly snow free due to gravity-driven mechanism as avalanches or slush-flow and other processes such as wind drift and erosion (Farinotti et al. 2010).

This experiment shall investigate whether shifting of snow from hills into hollows over 150 years changes the geometry of the glacier. Compared to the distribution pattern with shifting snow to the left and right side, this attempt implements a snow shift on a much smaller scale. Again, the whole mass, which gets eroded, needs to be deposited in order to conserve mass.

The curvature of the glacier surface is calculated according to the method of Zevenbergen & Thorne (1987). With help of a 3x3 matrix, each elevation pixel is weighted against its eight neighbours. There are two different approaches, the “profile” and the “plan curvature”. The former refers to the rate of change of slope while the latter is the curvature of land surface across the slope direction. For this case, the former method was chosen, as it affects the flow of aggradation and degradation which fits in with the experiment of snow erosion and deposition in the terrain (Zevenbergen & Thorne 1987).

$$G = \frac{\frac{z4+z6}{2}-z5}{L^2} \quad (13)$$

$$E = \frac{\frac{z2+z8}{2}-z5}{L^2} \quad (14)$$

$$F = \frac{-z1+z3+z7-z9}{4L^2} \quad (15)$$

$$G = \frac{-z4+z6}{2L} \quad (16)$$

$$H = \frac{z2-z8}{2L} \quad (17)$$

$$\text{Profile Curvature} = \frac{-2DG^2+EH^2+FGH}{G^2+H^2} \quad (18)$$

To ensure mass conservation, again the sum of the initial accumulated mass $\sum mb$ must be the same as the one of the new accumulation mass after redistribution ($\sum mb_{\text{new}}$):

$$\sum mb = \sum mb_{\text{new}} \quad (19)$$

Whether snow gets eroded and deposited depends on the terrain. Negative values of the calculated curvature refer to concave (hollows) and positive values to convex terrain (hills) (Fig. 15). One assumption is that the higher a ridge is the more snow is supposed to be eroded. For depressions the reverse will hold. This effect is regulated with the smoothing factor f , which has a range of 0-1. A very small value for f achieves a stronger smoothing and thus higher

erosion and deposition. If the value is 1, no smoothing occurs. The influence of the curvature cur is weighted proportional according to the divergence of each grid cell to the zero point of no curvature (cur/cur_{max}). At the choice of the maximum curvature it must be ensured that outlier data points are eliminated. The correction value n ensures the mass conservation.

$$mb_{new} = nmsb - f * \frac{cur}{cur_{max}} * mb * n \quad (20)$$

$$n = \frac{\sum mb}{\sum mb * (1 - f * cur)} \quad (21)$$

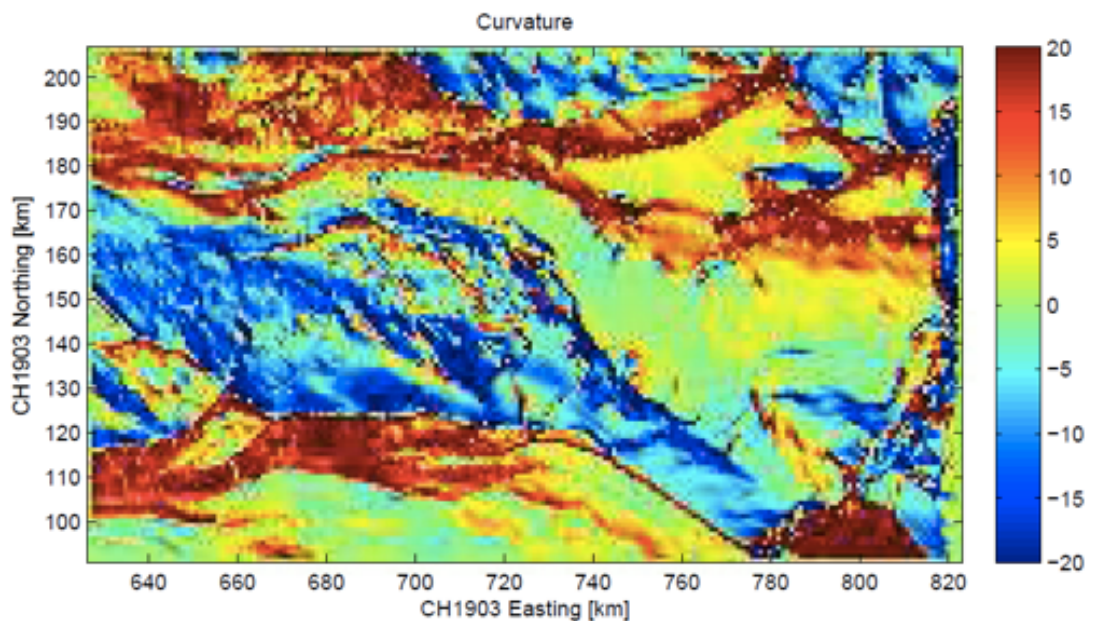


Fig. 15: Curvature of Findelen glacier (performed by Matlab).

4.4.5 Wind model (E)

Since the curvature experiment occurs on a very small scale, the experiment can be enhanced with including wind drift and thus transport of snow over larger areas. In chapter 2.5 the importance of wind on the redistribution of snow has been mentioned.

The implementation of the wind model for the thesis and consequent snow shift is based on a model created by Purves et al. (1998). Initially, this model was built for use in a GIS. Since all thesis experiments are run in Matlab, the wind model was transferred into this software. From

an initial wind direction and speed, the model generates a new wind field depending on the terrain of the glacier. The initial conditions can be roughly determined from meteo data. If the wind speed is high enough, snow is eroded and transported until the wind speed falls below the threshold.

The first step was to model the wind direction field, applied to the topography of Findelen glacier. Needed input parameters are an initial constant wind speed and direction as well as the glacier surface. The “shelter-index strategy” affects the wind deflection as well as the alteration of the wind speed depending on slope and aspect. For the deflection of the wind, the following equation by Ryan (Ryan 1977) was used:

$$Fd = \theta - 0.255sd * \sin(2(A - \theta)) \quad (22)$$

Fd is the wind diversion (degree), sd the inclination (%), A the aspect (deg) and θ the initial wind direction. The deflection is done for every single grid cell. For the adaption of the wind speed the following procedure was performed. The wind speed is weakened if a cell is located within a mean aspect of 45° of the leeward slope. Further, the inclination needs to be greater than 5° . Those cells receive an index between 0 and 1. Highest speed occurs in the direction of the lee and thus receives the index 1. Consequently, cells lying in the swath of 45° get an index of 0 for the most distinct decrease of speed (Fig. 16). Great deflection cause greater weakening of the wind (Purves et al. 1998).

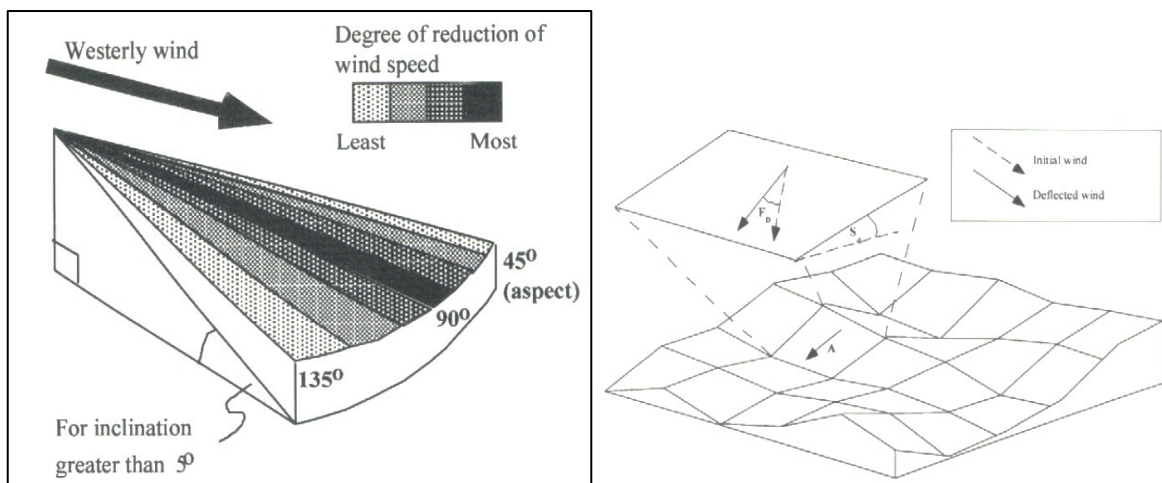


Fig. 16: Reduction of wind speed by aspect and inclination (slope) (Purves et al. 1998).

After the determination of the new wind field with new wind direction and speed it has to be examined whether snow can be transported or not. Wind must exceed a threshold velocity. Following a study of Mellor (1965) a wind speed of 3-8 m/s dislodges loose, unbound snow. If the speed exceeds values higher than 30 m/s, even bonded particles due to freeze-thaw processes can be shifted. The wind speeds are measured at a height of 10 m (Mellor 1965). It should be taken into account that the wind speed threshold is derived from complex physical factors since the deposition of snow depends on temperature, humidity, time and size of particles in initiate saltation. A melt-freeze cycle with absence of fresh snowfall for example raises the threshold very high for potential erosion. Transport is not possible during a melt phase since the snow cover is too wet. Thus, to enhance the model, a look-up table could be included with the occurrence of melt and freeze cycles. For this thesis any metamorphism of snow, as in case of freeze-melt cycles will be neglected. The available snow for the distribution is the entire accumulation area.

The flux of snow is considered to be a linear function of velocity. First the flux term needs to be determined, which decides where mass is shifted and where deposition occurs

$$\text{Fluxterm}(i, j) = \left(\frac{\Delta t}{2\Delta}\right) * ((\text{rightMass} * \text{rightVel}) - (\text{upMass} * \text{upVel}) + (\text{downMass} * \text{downVel}) - (\text{leftMass} * \text{leftVel})) \quad (23)$$

The term $\left(\frac{\Delta t}{2\Delta}\right)$ is the time constant, which depends on wind speed and grid resolution and ensures the model to remain stable (Press et al. 1993). Finally, the new snow mass Q is determined as follow:

$$Q = 1/4 * (\text{leftMass} + \text{rightMass} + \text{upMass} + \text{downMass}) - \text{Fluxterm} \quad (24)$$

The whole modelling is an iterative process and is determined for a specified time period (Purves et al. 1998).

The initial intention, to include the new snow pattern from the wind model into the flow model, turned out to be inoperative. Wind direction, wind speed and diversion functioned adequately and erosion and snow deposition occurred. However, combined with the wind model, the criteria from the flow model that walls steeper than 40° are snow-free turned out to be problematic. Accumulation pixels within this threshold value are zero and the wind model thus

assumes no wind and therefore deposition in those areas. Consequently, almost the whole snow accumulation was deposited in the rock walls. Due to technical circumstances it was not possible to find a way that the model deposits the snow in front of the rock walls.

The mentioned complications were corrected calculating the initial input snow in the accumulation area simply with the assumption of a linear increase with elevation and neglecting the rock walls criteria of 40°. However, with this approach, not all of the boundary conditions are fulfilled anymore. Rock walls are not snow-free anymore. The used wind model would work for very flat areas, but for the complex terrain on the right side around Adler glacier the model is not adequate for this thesis.

4.4.6 Climate change

An additional experiment next to the accumulation redistribution is the analysis of the impact of a sudden climate change. This is the first time where the climatic conditions get relevant while they were kept constant in the previous experiments. After running the two experiments of snow shift toward the left and the right side until they nearly or entirely reached a new steady state, the ELA was raised 50 m up to 3350 m.a.s.l to simulate increasing temperature. Both experiments of the left and right pattern are to be run another 100 years with the new ELA, the remaining variables stay the same. The aim of this trial is to examine how the two patterns react in volume, length and thickness change and whether they differ from each other or not.

4.5 Parameter settings

The following section provides an overview of the parameter settings for the experiments as well as an introduction how the results will be analysed. Each experiment is labelled with a letter A-F (Tab. 1).

Tab 1: Labelling of experiments and reference case.

Letter	Experiment
A	Snow shifted to the left side (cut left)
B	Snow shifted to the right side (cut right)
C	Cut of increasing accumulation at 3350 m.a.s.l (cut 3350)
D	Curvature
E	Snow shifted by wind
F	Geometry of reference case

The analysis of the glacier evolution (chapter 5.4) over time is evaluated by analysing the change in ice thickness along a two profiles. Profile 1 follows the left side of the glacier and profile 2 the right side (Fig. 21).

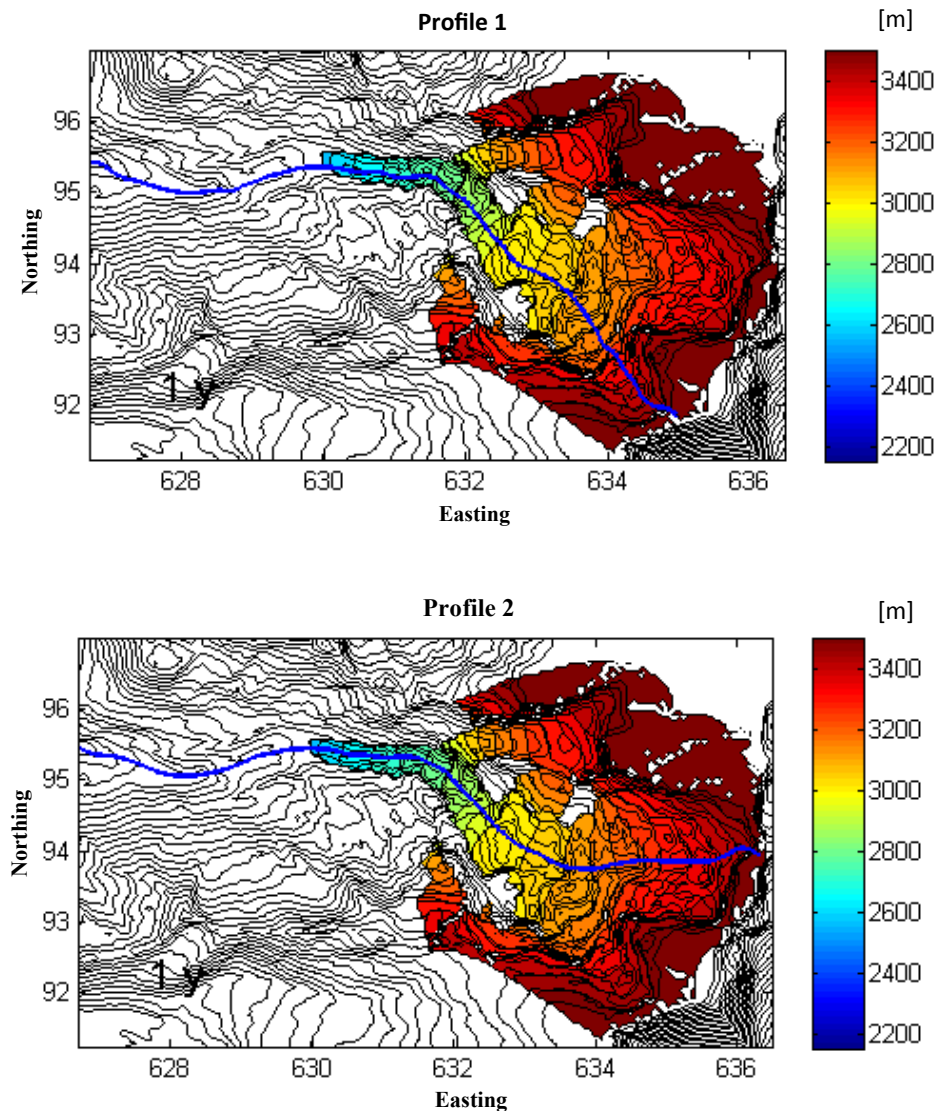


Fig. 17: Profile lines for analysis of glacier evolution in ice thickness and length (Profile 1 and Profile 2).

4.5.1 Glacier bed (DEM):

The morphological input parameter needed for the flow model is a digital elevation model (DEM) of the glacier bed with a resolution of 50 m (Fig. 18). The DEM was obtained from ground penetration radar (GPR) and provided by the Geographical Institute of Zurich (A. Vieli). The DEM indicates some inaccuracy in the accumulation area which might be explained with the water content of the snow and thus dimmed penetration of the reflection signal of the radar. For

the first runs of the model, these deficiencies in data of the glacier bed affect the glacier surface but after several runs of the flow model this error disappeared. Generally, the effect of the bed topography is of minor importance since the thesis is a “sensitivity analysis” and the glacier surface does not necessarily need to perfectly reflect the reality.

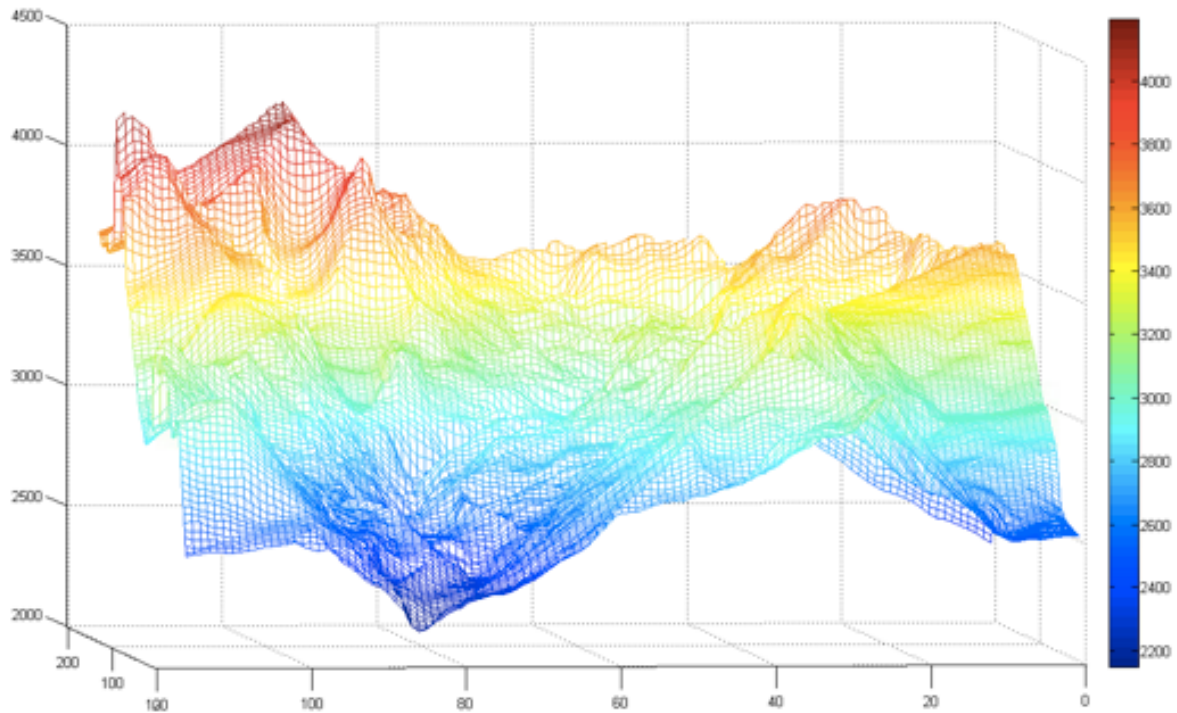


Fig. 18: Glacier bed (DEM) of Findelen glacier from GPR measurement (3-D reconstruction performed with Matlab).

.4.5.2 Reference case

The constants, which need to be determined before running the model, are first of all the elevation of the ELA, which is set at 3300 m.a.s.l. This parameter will only be changed for the experiment of the climate change influences. The chosen elevation corresponds approximately to the ELA height measured in the year 2007/08 (Bauder et al., 2014). The ice temperature is kept constant and set to 0°C (Brown et al., 2013). Further, the ratio between the accumulation and the ablation area (balance ratio) is defined as 1.6. This means that the accumulation area has a little bit more than twice as much area as the ablation zone (Brown et al., 2013). This is a common value. A rough approach to estimate the ratio between the area of the accumulation and ablation area is a 2:1 ratio (Maisch 2000).

The mass balance gradient and thus the mass turnover, which is the renewal of the ice mass (Terminology 2011), is set at 0.0066 m/m. This value is in good agreement with typical values for wet climates of the mid-altitude area conditions and high mass turnovers (Leysinger Vieli & Gudmundsson 2004; Benn & Evans 2010). The time resolution is set at 0.02 y⁻¹, which means that 50 calculations are implemented per year. The narrow time resolution is needed to ensure the stability of the forward scheme since a large number would lead to more gaps and data errors. The glacier would grow too fast (Oerlemans 2001). Solar radiation is excluded, snow melt occurs only due to conservation of mass.

All these constants will not be changed for the following distribution experiments unless specified otherwise as for the case of the climate change.

4.5.3 Experiment A and B: Snow shift to the left and the right side

For the first two experiments the snow was shifted once towards the left (A) and once to the right side (B). The ratio of the distribution was 1:10. This means that in case of shifting to the left side, this area pattern gets 10 times more snow accumulation than the right side. The available snow for the shift is the amount of accumulated snow of the reference case. The large ratio has been chosen to obtain unambiguous patterns. Each experiment is run for 150 years to ensure that the glacier almost or entirely achieves a steady state. Each year, the total accumulation mass is calculated from scratch and distributed again with the same ratio. Mass conservation is guaranteed for the annual redistribution. The total volume may thus change between years during which the glacier grows or retreats in consequence of the new input snow distribution.

4.5.4 Experiment C: Cut of increasing accumulation at 3350 m.a.s.l

For the experiment C, the increase of accumulation with elevation was cut at a height of 3350 m.a.s.l. According to Fig. 9b, this is the elevation where the decreasing snow accumulation was measured with LIDAR (Sold et al. 2013). Each grid cell, which lies at higher altitudes, receives the determined value of the cutting height. Therefore, this experiment is not mass conserving.

4.5.5 Experiment D: Variability of snow on the base of the terrain

This experiment addresses the curvature of the terrain, where snow is shifted from convex to concave surface. For the maximal curvature, a value of 50 m has been chosen. The model reacts very sensitive to this value. If it is chosen too high, hardly any snow gets shifted. The constant f is 0.5. This value influences the smoothening of the redistribution. On the other hand if the value is set too low, less snow shift occurs. The sensitivity of those two parameters will shortly be discussed in chapter 6.4. For this experiment the mass conservation is maintained as well. The input volume gain is used from the reference case.

Snow shift just happens between neighbouring pixels, which means that this experiment is settled for a very small scale.

4.5.6 Experiment E: Snow distribution with wind and terrain

For the last experiment addressing the effects of wind, the parameter settings are somewhat more sophisticated. The variable for the snow, which is prone to erosion, is the positive mass balance. The wind direction was selected on the base of meteorological data measured at the weather station of Gornergrat (626900°N/92512°E). The meteorological station is located south of Findelen glacier on an elevation 3129 m.a.s.l. The mean annual velocities measured are 2.7-3.4 m/s during the years 1994-2014 (IDAWEB 2015). Since this value is a little too small for a clear effect of snow drift, a speed of 4 m/s was chosen.

The main wind direction of the Findelen area is south and south-east (Sold et al. 2013). Thus, the experiment was run once for a northwest wind of 350° and a south east wind of 177°.

According to the research of Li et al. (1996), the threshold wind above which snow is transported was determined to be 3 m/s.

4.5.7 Climate change

For the climate change the ELA was shifted up 50 meters and is now set at 3350 m.a.s.l. This experiment is performed once for the pattern experiment A and once for the pattern experiment B. The only parameter which changes is the ELA, all the others remain as defined in chapter 4.5.3.

5 Results

This section describes the results obtained from the different experiments of snow redistribution. The scenarios are labelled with letters A-F (Tab. 1). Section 5.1 provides the reference case. Sections 5.2, 5.3 and 5.4 describe the changes in geometry of the scenarios, regarding differences in thickness, mass balance and the modified velocity for experiment A-D (Tab. 1). Section 5.5 shows the results from the wind experiment. In this case only the new snow pattern was implemented without including it into the flow model. The last part concerns the results from the climate experiment.

5.1 Extent of the reference case

The model result of the reference case (pink line) is in good agreement with the state of the glacier these days (Geo.admin, 2015) (Fig. 19). The cartographic status is from 2007, where the terminus reached further down compared with the year 2015. Differences between the modelled and the cartographic state (2007) include that in the case of the first, Adler glacier and Findelen glacier are still connected by two tributary flowing down to the left and right side of Strahlchnubel (3215 m.a.s.l). The rock walls are increased covered with glacier ice. The two pink polygons indicate ice-free areas.

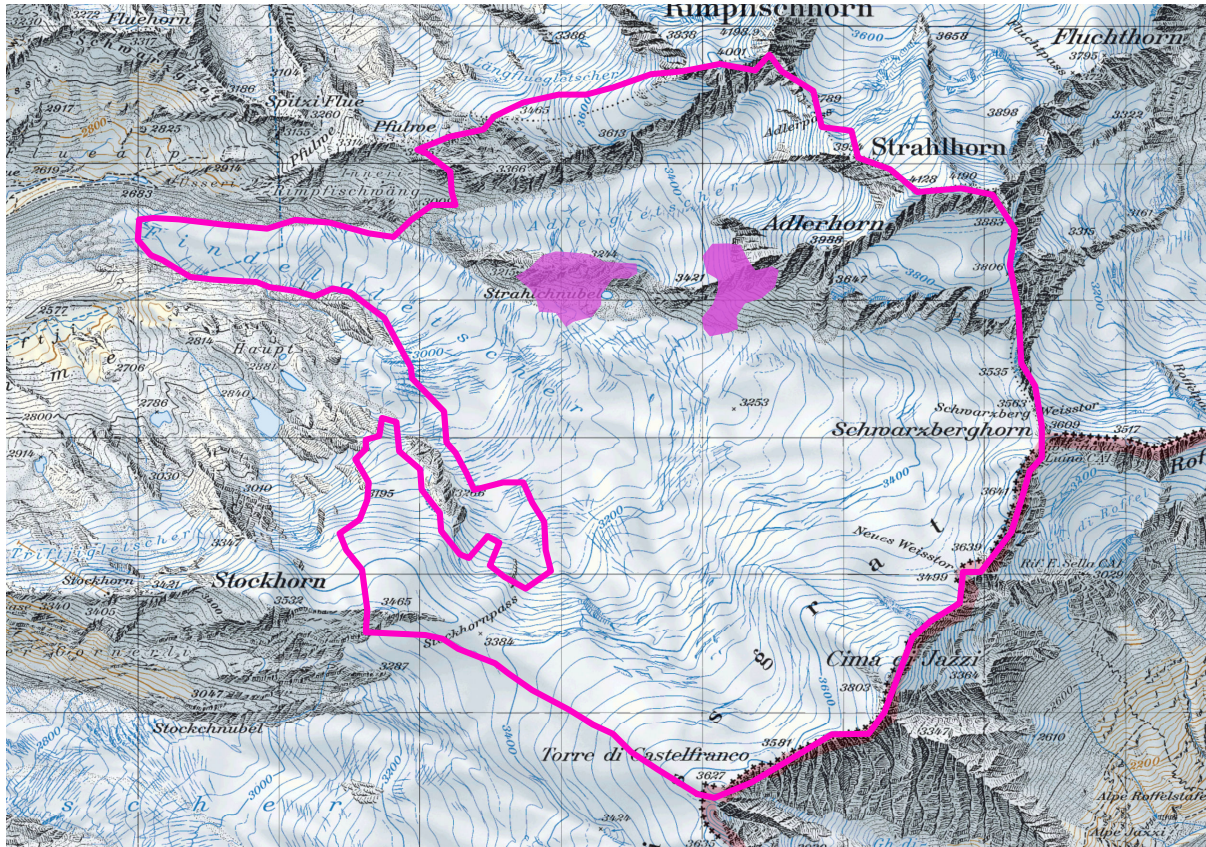
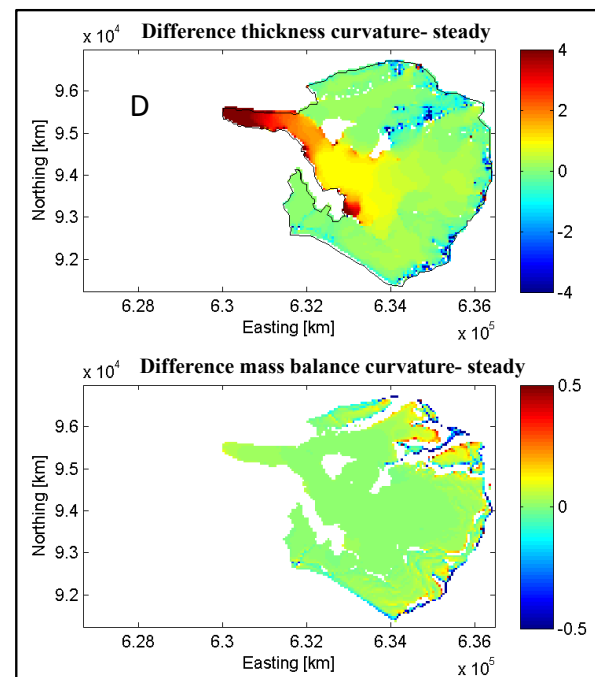
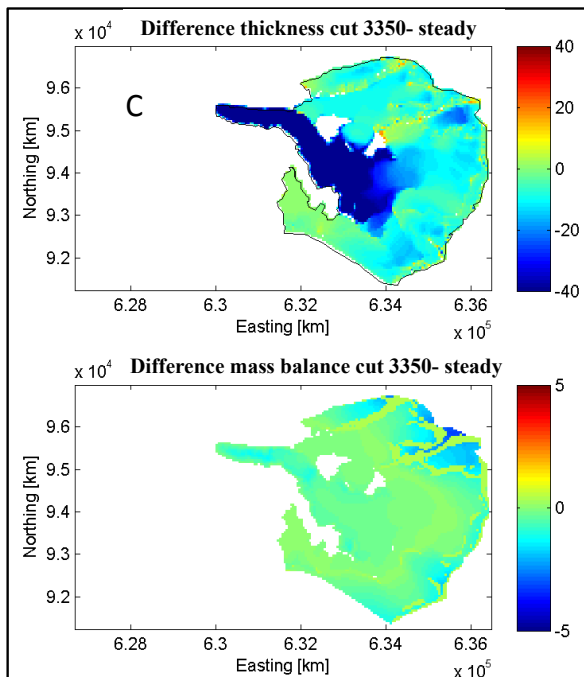
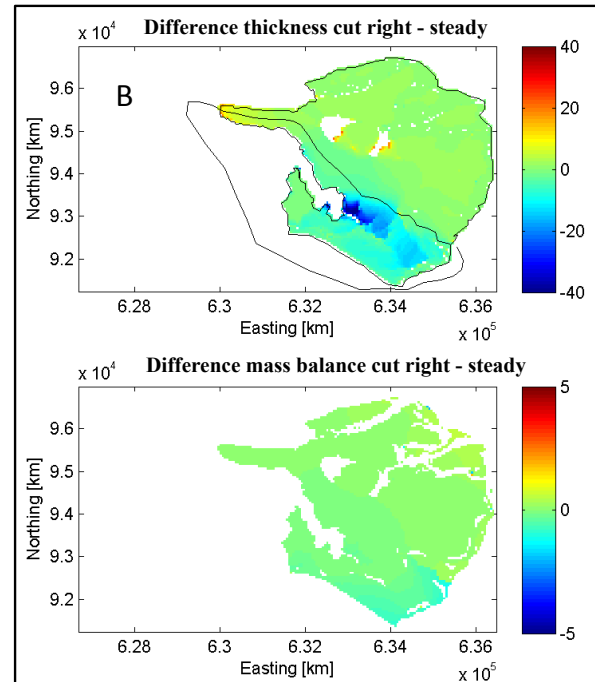
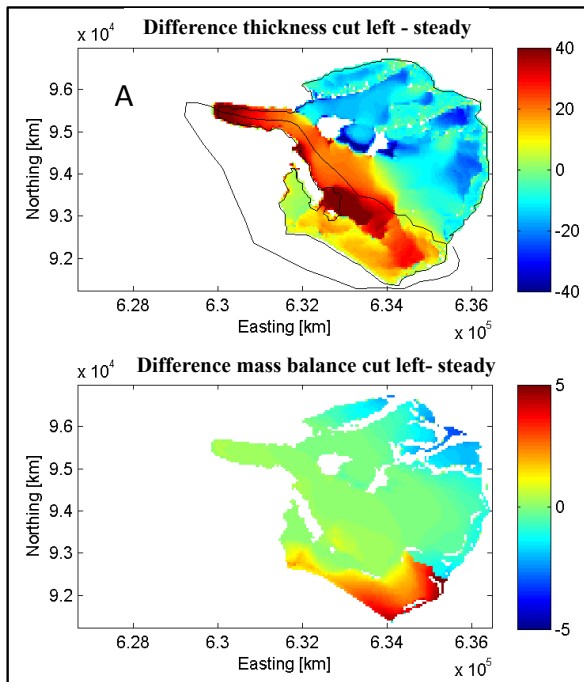


Fig. 19: The pink line shows the extent of the reference case with the two greatest snow-free spots below Adler glacier (Geo.admin, 2015).

5.2 Difference in geometry (A-D)



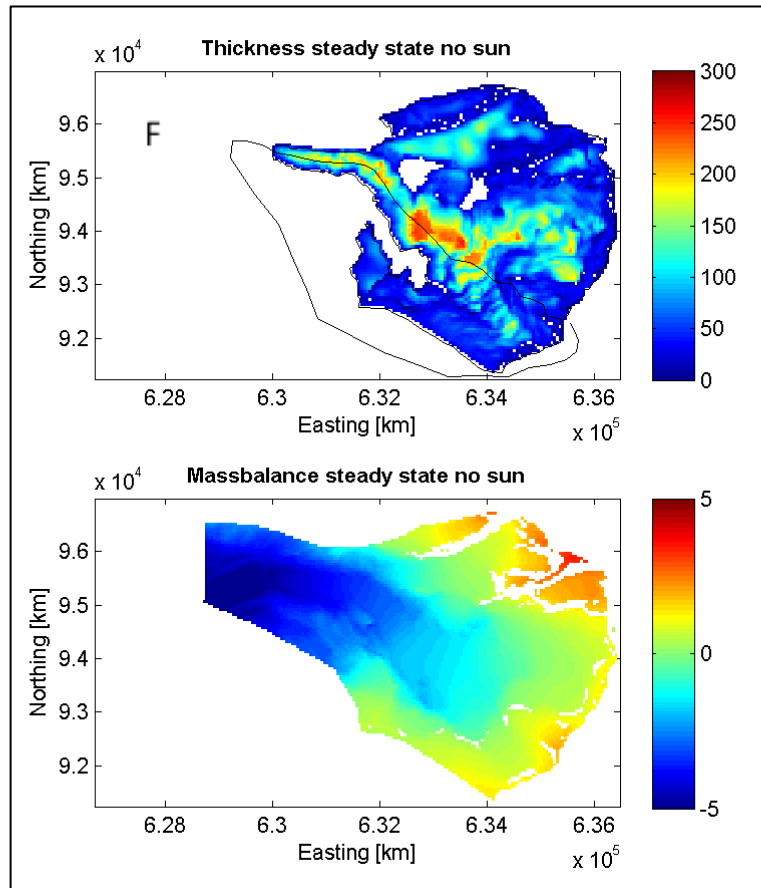


Fig. 20: Difference between output of ice thickness after snow redistribution and initial glacier geometry of reference case (steady state). A= shift to the left side, B= shift to the right side, C= cut of increasing accumulation at 3350m.a.sl, D= shift according to curvature, F= steady state (reference case) for comparison.

The reference case shows a maximum ice thickness of 250 m in the centre of the glacier as well as in the two depression areas to the left and the right of Cima di Jazzi. The thickness of the tongue is approximately 200 m. The ice is very thin at the location where Adler glacier and Findelen glacier confluence (Fig. 20 F). The lower plot of Fig. 20 F shows the mass balance which indicates a homogeneous snow accumulation distribution due to the linear increase. Maximum values are approximately 5 m.

The results A-E in Fig. 20 show the difference in thickness between the output geometry after the redistribution of snow in the accumulation area and the initial geometry of the reference case. In this experiment the model ran for 150 years. The black line around the glacier represents the glacier outline of the reference case. The cases A and B also include a line, indicating the cut between the left and the right side of the glacier. This line was drawn as a polygon, which might appear confusing but was easier to implement for computational reasons. The line follows along a ridge. The x- and y-axes refer to the easting and northing [km] of the

Swiss coordinate system. The legend shows the range of the differences in thickness. Reddish colours represent a mass gain, bluish imply a mass loss. The results of each of experiments A-E are summarised in two plots. The upper one shows the differences in ice thickness as well as the modification of the outline of the glacier, thus indicating the retreat of the glacier to an extent. The lower plot illustrates the difference of the mass balance, showing the distribution of the accumulated snow and additionally the division of the accumulation and ablation area in the experiments A and B.

The result of experiment A (Fig. 20 A) shows a mass gain on the left side of the glacier while the surface on the entire right side is sinking by losing mass. This change in thickness is apparent in the accumulation area as well as in the tongue even. In volume terms, the glacier gained around 40 m ice mass on the tongue and in the accumulation area. The mass loss is around 30 m on the right. The mass gains surpass the loss since the glacier tongue has advanced a few meters. Furthermore, an overflow of the initial outlines can be seen at the left side where one side branch gets separated from the main glacier. The glacier bed is very flat at this section.

In the central part of the glacier, the mass gain on the left side extends also to the right side. Considering changes in the snow accumulation the linearity of an increasing accumulation with elevation within the two patterns is still visible. The largest gains and losses happen in the highest altitudes. Especially the area of the Adler glacier and the small glacier to the right side of Adlerhorn show a reduction of snow accumulation up to 5 m. In contrary, the left side gained at most parts 1 -5 m of snow accumulation. The ratio of 1:10 is clearly visible, whilst looking at the two patterns. In summary it can be said that the redistribution impacts are visible over the whole right pattern from the accumulation area down to the tongue.

For experiment B, the snow mass was shifted to the right side, again at a ratio of 10:1. The glacier gained mass on the right side and experienced a slight depression in terms of surface on the left side (Fig. 20 B). In the first 50 years, the tongue gained 20m of mass, the accumulation area on the left side lost about 10-15 m of ice. However, for the following 100 years, the advance of the slowly diminishes and even starts to retreat slightly. This reduction of ice flow to the tongue is evident since the amount of the mass gain after 150 years is only 10-15 m. On the right side of the accumulation area hardly any changes can be observed, mostly the ice thickness differences are roughly 1-5 meters. This gain refers to the flat areas of the glacier topography.

Looking at the change in the mass-balance (Fig. 20 B), a similar pattern is recognizable. The accumulation area on the right side shows little increase in the mass-balance. On the left side the main loss in snow accumulation appears where the terrain is steeper. In this case, the ratio of

10:1 is less evident in the difference in mass balance compared to the previous experiment. The linear approach of increasing accumulation with elevation is less apparent than in the case A. This can simply be explained with the distribution on a larger area. Compared with experiment A, the impacts are only visible in the tongue, while in the accumulation zone remains mainly constant.

In case of experiment C, the increasing accumulation was cut at the elevation of 3350 m.a.s.l (Fig. 20 C). The absent input snow shows a significant impact in the tongue where the glacier distinctly lost mass of approximately 30 m. Considering the glacier extent, the terminus retreated significantly (Fig. A8), which is not observable in Fig. 20 C since only the differences in ice thickness are illustrated. The scattering mass gains at the left boundary side are most probably due to modelling errors or outliers and can be neglected until further note. The main loss of snow accumulation in the upper area of the glacier occurs where the terrain is steep. The cut at 3350 m.a.s.l is visible in the lower plot in Fig. 20C by the difference of the snow accumulation. It mainly follows the transition between the green and the blue values in the accumulation area. Adler glacier and its surrounding area are the most affected by the reduced accumulation input.

The curvature experiment D (Fig. 20 D) shows the influences of snow accumulation variability on a different scale compared to the previous experiments. Considering the units of the thickness change, we see that gain and mass loss range from -1 to +1m, whereas most values are situated around 0. The lower plot with the accumulation change indicates that shifting mainly happened in the boundary regions. The pixels at the edges of the glacier are probably again errors due to boundary effects since snow cannot leave the glacier in the calculations.

The plot showing the difference in thickness indicates hardly any changes in the upper area of the glacier. The convex terrain of Cima di Jazzi (3808 m.a.s.l) lost some snow while the concave surface to its left and right side was slightly filled with snow. In the centre of the glacier a slight increase in mass is observable of approximately 1 m. The tongue shows a clear gain in ice mass of 4 m. However, referring to the extent of the glacier, no real changes are visible compared to the reference case outline.

The mentioned changes in geometry are also visible considering the variation of the total ice volume (Tab. 2).

The initial mass in the reference case amounted to 1.307 km³ ice. In case of the shift of snow to the left side and the curvature experiment the glacier gained ice mass by 0.0675 km³. The shift of

snow to the right side resulted in an initial mass gain in the first 50 years but after 100 years the glacier starts slight to loss ice mass. Thus the glacier lost 0.033 km^3 . The most significant ice loss of 0.348 km^3 occurred in experiment C with the cut accumulation in the elevation of 3350 m.a.s.l.

Tab 2: Change in ice mass over time.

Experiment/Years	50y	100y	150y	250y and ELA 3350
Steady state		1.307		
shift left	1.3488	1.3703	1.3744	1.114
shift right	1.2951	1.2811	1.2731	1.011
cut 3350m.a.s.l	1.1183	1.0031	0.9588	
curvature	1.2107	1.3129	1.3137	

5.3 Change of velocity (A-D)

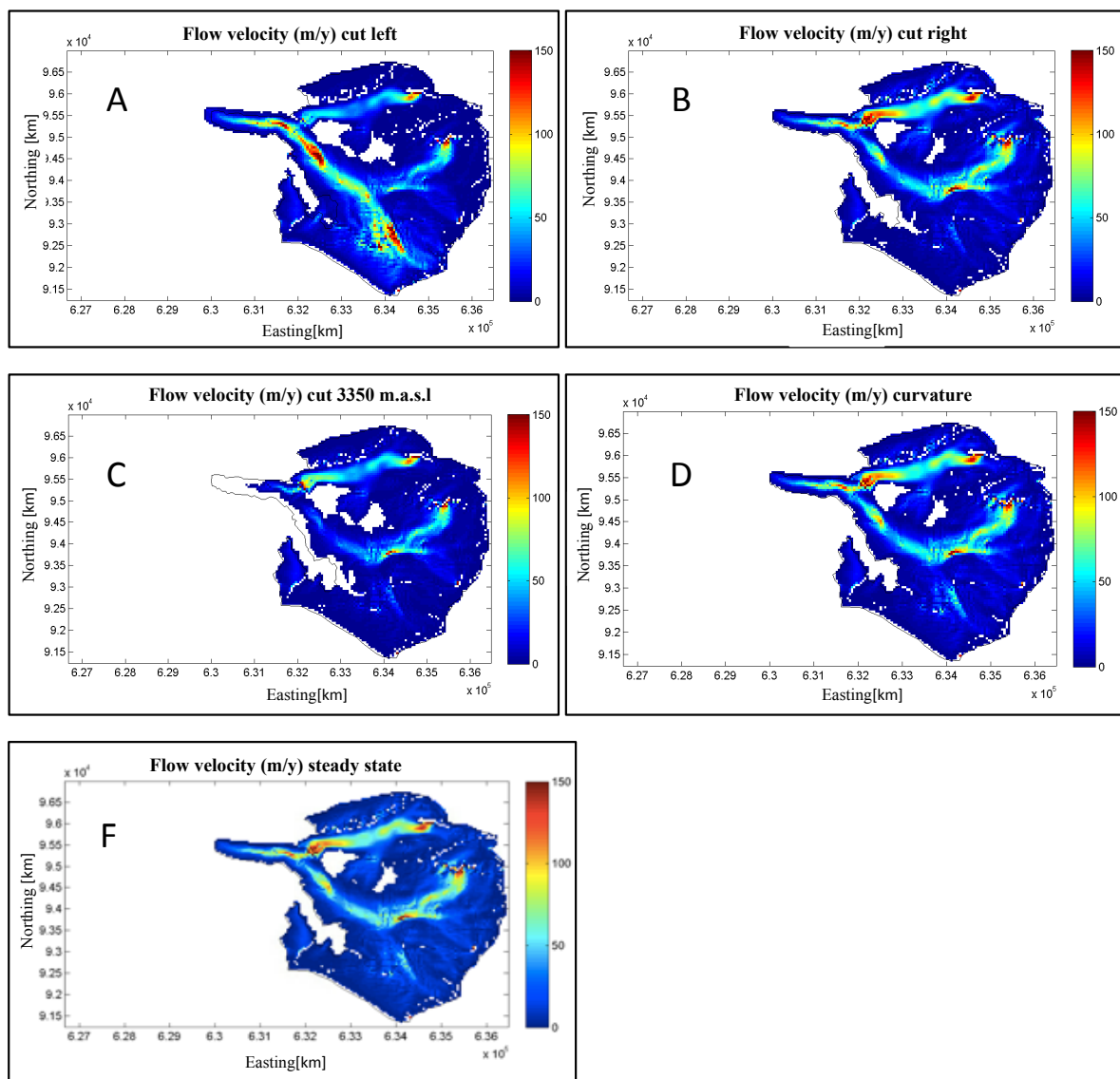


Fig. 21: Velocity of ice flow: A= experiment snow shifted to the left side, B= experiment snow shifted to the right side, C= cut of increasing accumulation at 3350 m.a.s.l, D= experiment of curvature, F= steady state (reference case).

The flow velocity plots show the main flow streams and how fast the ice moves. The x- and y-axis indicate again the Swiss coordinate system [km], the colour bar shows the velocity in meter per year. The plotted values are the state of the glacier calculated after 150 years. All dark blue pixels indicate no or very little movement of the ice.

In the reference case (Fig. 21 F), two main flow streams are observable, one coming down from the right accumulation area, flowing through the centre to the tongue. A second one is coming down from Adler glacier. Maximum values are in the range of 150 m/y, the mean values approximately 90 - 100 m/y. The stream flowing from the left side is very weak.

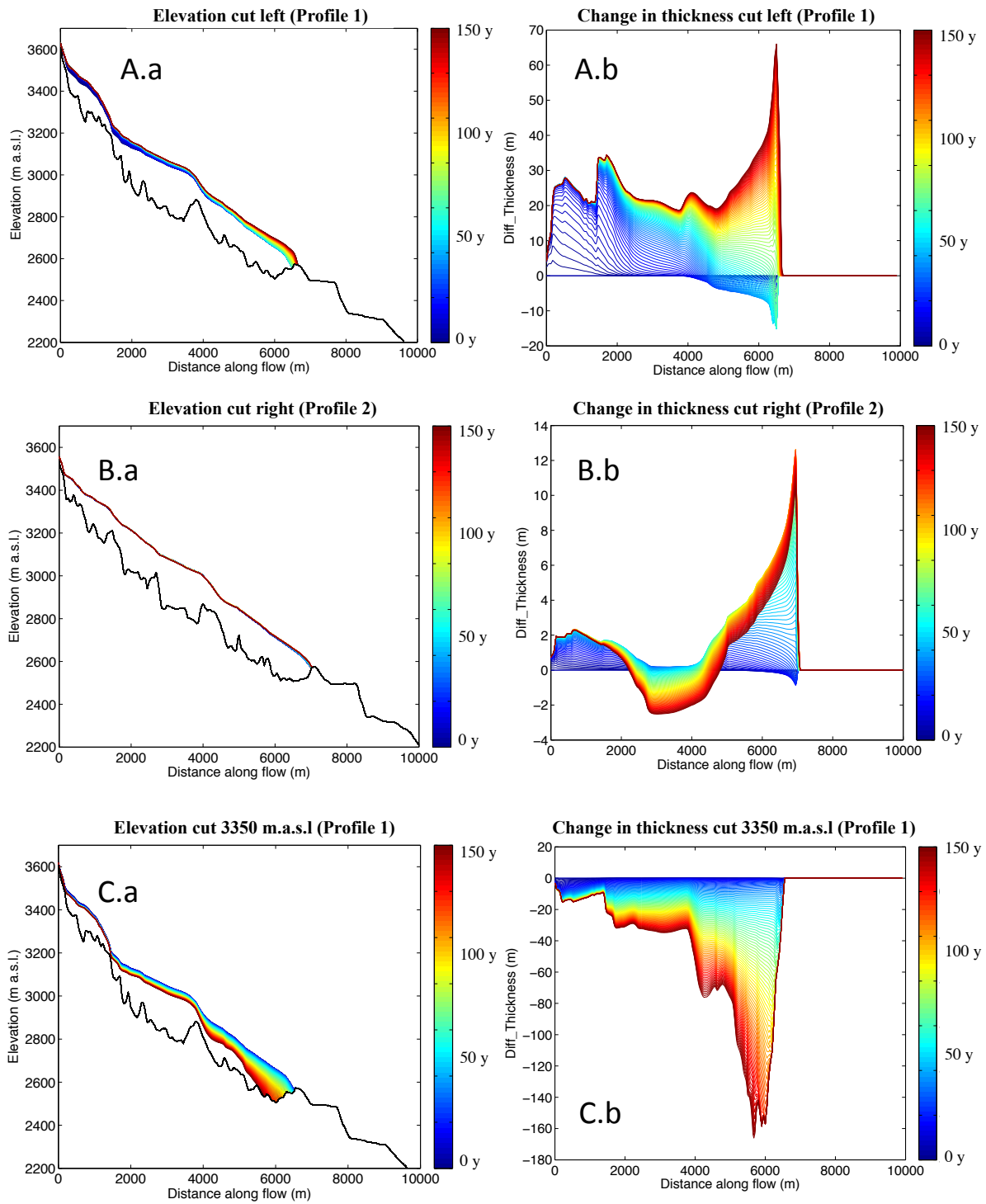
In experiment A, the main flow stream changed to the left side compared to the reference case. Highest values now occur on the left side, while in case of the reference case, those were found in the right basis in the accumulation area and the Adler glacier (Fig. 21 A). The maximum flow value is in the range of 150 m/y. Not surprisingly, the maximal speed is found where the terrain is steep. The two main hot spots are found in the accumulation area and at the tongue. In the centre part of the glacier, the ice is dammed up on the left side (Fig. 20 A). At this location the glacier flow is slower. This is also the location where the two main flow streams contribute from the left and right side. Even if the area of Adler glacier lost snow input, there is still ice flowing down. This flow stream has not yet lost the connection. The same applies for the stream coming from the right side. Yet, the input from the right side greatly subsided. The tributal on the very left side seems not to be fed from the accumulation area since there is no movement visible towards this direction.

The main flow streams of experiment B (Fig. 20 B) do not differ significantly from the ones of reference case. They continue to flow from the centre of the glacier as well as from the left side down of Adler glacier. Looking into details it can be seen, that after the snow shift, the left side has no influence anymore while the results of the reference case indicate some ice flowing into the main flow stream (Fig. 21 F). Highest values are approximately 104 m/y.

Similar to experiment B, the cut of the accumulation at 3350 m.a.s.l. (C) does not influence too much the flow behaviour of the glacier with regard to its main flow streams. Those streams continuously run from the right side. However, the glacier flow slowed down. Maximum flow speeds are in the range of 100 m/y, the mean flow speeds of approximately 80-100m/y. Also in the tongue area, less movement of the glacier is noticeable (Fig. 21 C).

The flow patterns of experiment D do not differ from the reference case. Neither the flow directions changed, nor the values of the flow velocity (Fig. 21 D). Mean flow speeds are in the range of 100 m/y, maximum values of 150 m/y.

5.4 Evolution of the glacier with time in the profile (A-D)



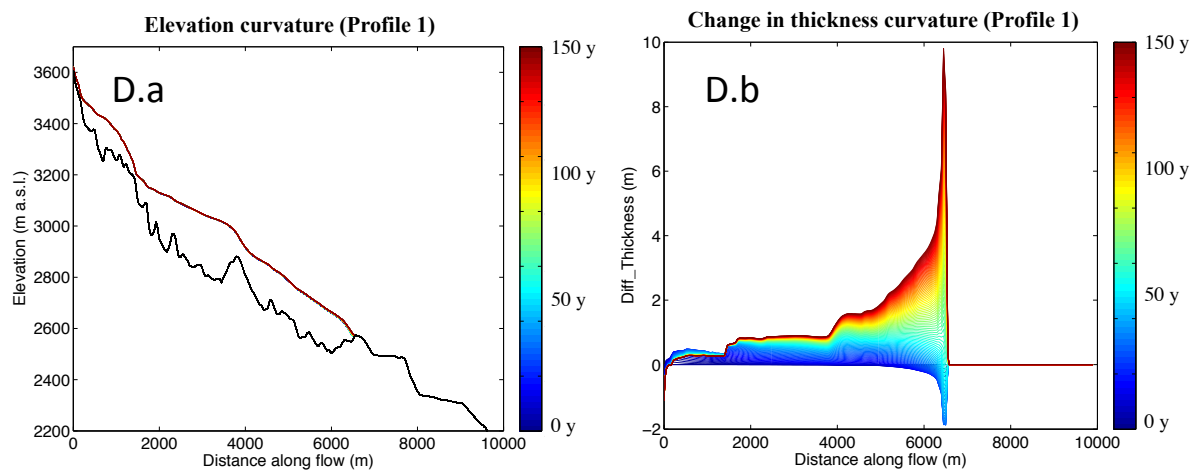


Fig. 22: Change of thickness of the glacier along the profile (1 & 2) of the glacier. Lines represent run years. A= shift to the left side, B= shift to the right side, C= cut of increasing accumulation at 3350m.a.sl, D= shift according to curvature. Bluish lines are the first years of run, red the latter ones.

The results for the evolution of the glacier with time are summarised in two plots for each experiment. The plot on the left side shows the whole profile of the glacier with the length of the glacier on the x-axis. The zero point is on the top. The coloured lines show the surface of the glacier after each year. Bluish are the lines in the early stage, while the change towards red occurs with every further year. The black line indicates the topography of the glacier bed. The y-axis represents the elevation in meters. The right-hand plots illustrate the modification of the thickness [m] compared to reference case along the chosen profile. On the x-axis the length of the glacier [m] is plotted, on the y-axis the difference of ice thickness [m]. The colours represent the years of run. The colours change with every year from blue to red.

As we already have seen in the previous results, the experiment A shows the strongest impacts. Fig. 22 A.a provides the thickness along profile 1, which follows the left side. We see that the first alterations of the glacier after a few years occurred in the upper area of the glacier (blue lines). While the upper parts of the glacier gained mass of 25-30 m in the first years, a loss of about 5 m can be seen in the tongue area (Fig. 22 A.a). This number does not match perfectly with the one from Fig. 20 A. The reason is that the profile line leaves the glacier not exactly at the end of the tongue. The real thickness difference over time can be seen in Fig. 22 A.b.

With time, the increased mass in the accumulation area was transported through the middle part of the glacier into the ablation area and reaches the tongue in the end. The accumulation area shows no further alterations anymore (Fig. 22 A.a). The slight advance of the tongue is indicated with the red line. In the entire topography, changes in thickness are more evident at locations where the glacier bed is flatter. For example, after a length of 2000 m.a.sl the glacier

bet terrain levels off and the ice thickness increases significantly. Before a length of 4000 m, the glacier needed to overcome an obstacle. At this location, the thickness reaches its maximum thickness due to damming by this hill before becoming thinner again.

To enhance comparability, the right plot shows the dynamics more precisely (Fig. 22 A.b). The blue lines again indicate the earliest changes, first an increase of thickness in the accumulation area and the early retreat of the tongue. In the end (red), the tongue advances obviously. Based on the illustrated spacing of the lines the advance of the glacier is characterised by fast changes, which stagnate in time. Probably, the glacier almost has reached a new steady state since the red lines (after 150 years) are very narrow.

For the second experiment B where snow was shifted to the right side, the profile analysis was done with the help of the third profile (Fig. 17), which follows the main flow stream along the right basin. The increase in mass is much less due to the distribution over a relatively large area in the accumulation zone (Fig. 22 B.a). Therefore, the reaction of the glacier is clearly less distinct than for experiment A. Changes in thickness occurred mainly in the lower of the glacier (Fig. 22 B.a & b). The accumulation area gained merely a few meters of ice thickness, approximately 2 m. The tongue on the other side lost simultaneously some mass, which is still less compared to the shift to the left side. The middle part of the glacier lost primarily mass but stagnated towards the end of the run.

After the early retreat, the tongue advanced again after 20 years. Compared to the experiment A, this advance reached its maximum extent after 100 years and then started to lose its mass. However, this decline in mass does not yet constitute a retreat of the tongue (Fig. 22 B.b). Viewed over the whole glacier, the development of the ice is more regular since the spaces between the lines are smaller. The narrow lines after 150 years again indicated that the glacier is not far or has already reached a new equilibrium.

For the experiment of the cut accumulation at 3350m.a.s.l (Fig. 22 C), the whole glacier constantly has lost mass, a gain is never apparent. The evolution with time seems to be quite constant over the whole area (Fig. 22 C.a). Lower and upper areas of the glacier react similarly with regard to gain or loss of ice mass. The tongue lost ice thickness of more than 150 m, the accumulation area lowered by approximately 15 m. According to the spaces between the lines in Fig. 22 C.b, it took a few years until the glacier started to react on the missing input. After 150 years of run the lines are less narrow than in the previous cases. Thus, the glacier is still in a phase of retreat.

Since the accumulation redistribution in the experiment D assessing the curvature (Fig. 22 D) is preceded on a much smaller scale, the impact on the glacier evolution also falls shorter. The accumulation area gained approximately 1 m of mass in the first years. The tongue reacted on the snow distribution similarly as in experiments A and B. In the early stage of the model run, it lost some mass but recovered and started to grow again (Fig. 22 D.b). In this case the tongue advanced correspondingly also just a few meters. However, the tongue still gained almost 10 m in thickness. The spaces between the year lines are very small indicating the reaction to be very slow and soon to start stagnating. In the end the lines are so close that the glacier probably almost or soon reached the new steady state.

5.5 Wind (E)

As already mentioned in chapter 4.4.5 it was not possible to include the wind model into the flow model for experiment E. Therefore, the output shows only the snow redistribution induced by wind. Ten time steps were necessary to obtain a smooth surface while it was quite pixelated with just one or two steps. The redistribution occurred just in the accumulation area but this time snow could leave the glacier towards the sides. Consequently snow mass was not conserved. The first output (E.1) shows the difference between the initial snow accumulation and the new distribution. The second plot (E.3) indicates the generated wind field with arrows for wind direction. In the third plot (E.2) the wind speeds are represented. X- and y-axis show the Swiss coordinate system.

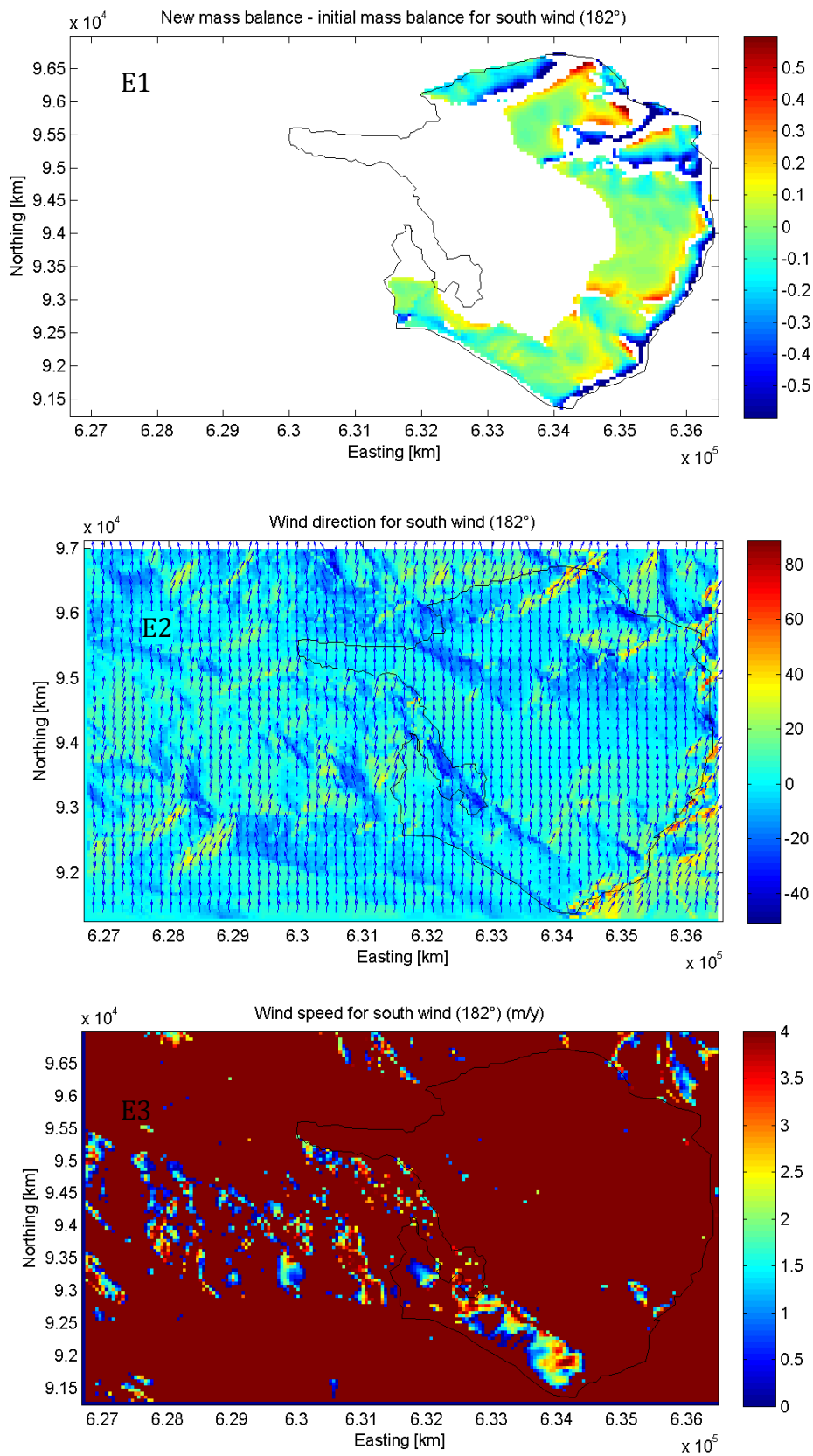


Fig. 23: South wind. E.1 = Difference in snow accumulation compared with the reference case (steady state), E.2 = wind direction and diversion, E.3 = Wind speed field.

In the first case (Fig. 23), wind comes from the south side. According to theory, deposition is supposed to happen if wind speed gets slower than the threshold speed for erosion or in front of convex terrain where the wind is diverted along the hill or wall. On the top of hills and ridges on the other side we assume erosion. Thus, concave terrain is filled with snow while convex surface is shaped by erosion. In Fig. 23E.1 it can be seen clearly that around Cima di Jazzi snow is deposited along the hill where the terrain flattens while on the top erosion occurs. Further, most of the snow is eroded along the east edge where the glacier ends and the terrain falls down into "Monterosa East-wall". Here wind blows over the border away. In the North area of the glacier, the terrain is characterised by steep walls, coming down from Adler glacier. Here, on Findelen glacier itself snow is deposited in front of the walls since wind is diverted. On Adler glacier, erosion occurs on the south side and again deposition in the northern areas.

Since field studies further indicate multiplied eastern wind circumstances, Fig. 24 shows the redistribution with wind coming from this direction. The plot of the difference between the new accumulation and the initial one shows a similar pattern as obtained with south wind. Again, hollows accumulate more snow. Along ridges and very steep terrain snow is eroded on the other hand. In comparison to Fig. 23 more snow is accumulated along the foot of rock walls, especially on the ridge side below Adler glacier (Fig. 24 E.1). Further the snow is more regularly distributed over the whole accumulation area. Deposition is more characterised by speed due to steeper slopes than diversion since no barriers as rock walls remain in place (Fig. 24 b, c).

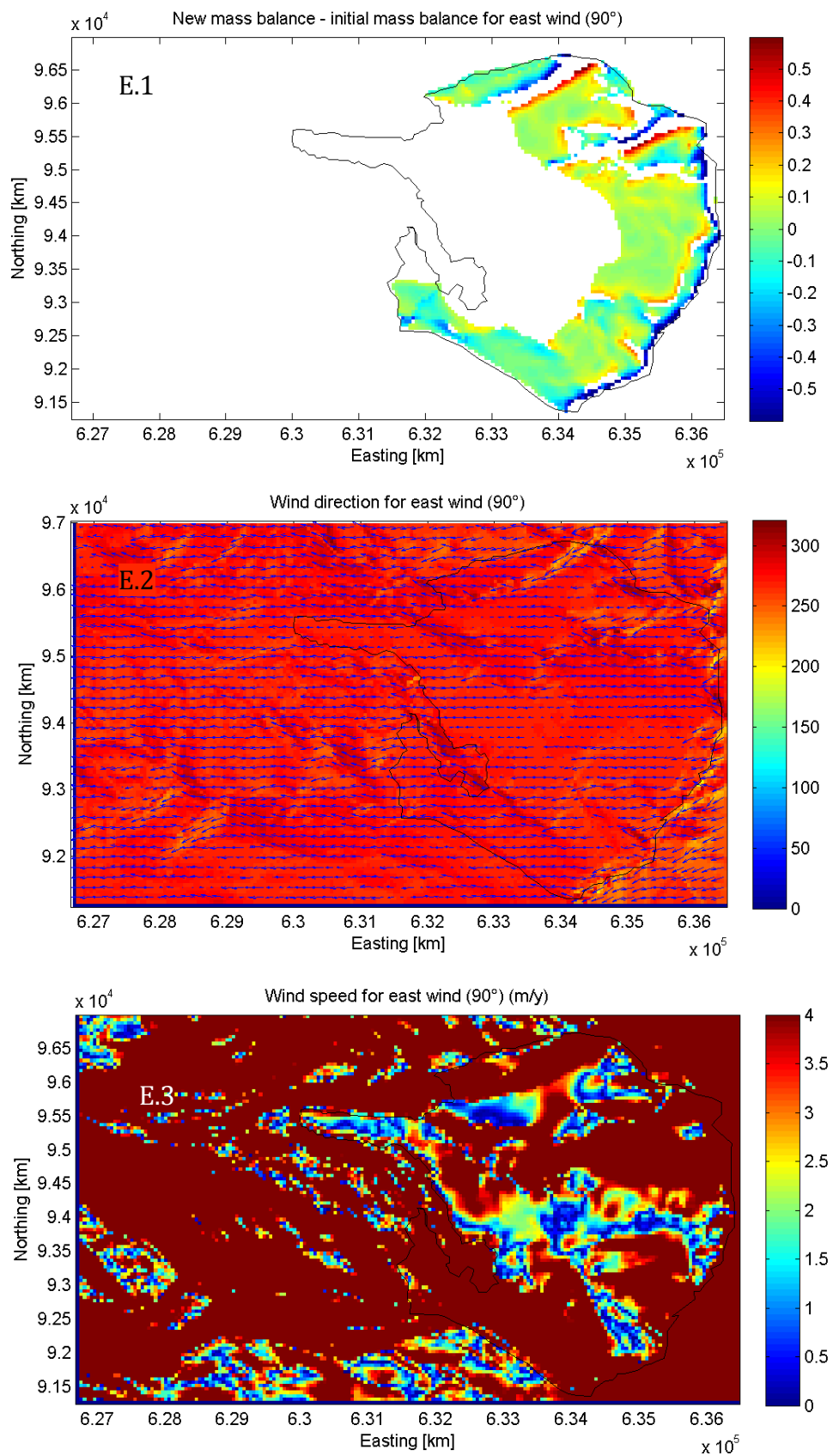


Fig. 24: East wind. E.1 = Difference in snow accumulation compared with the reference case (steady state), E.2 = wind direction and diversion, E.3 = Wind speed field.

5.6 Climate change

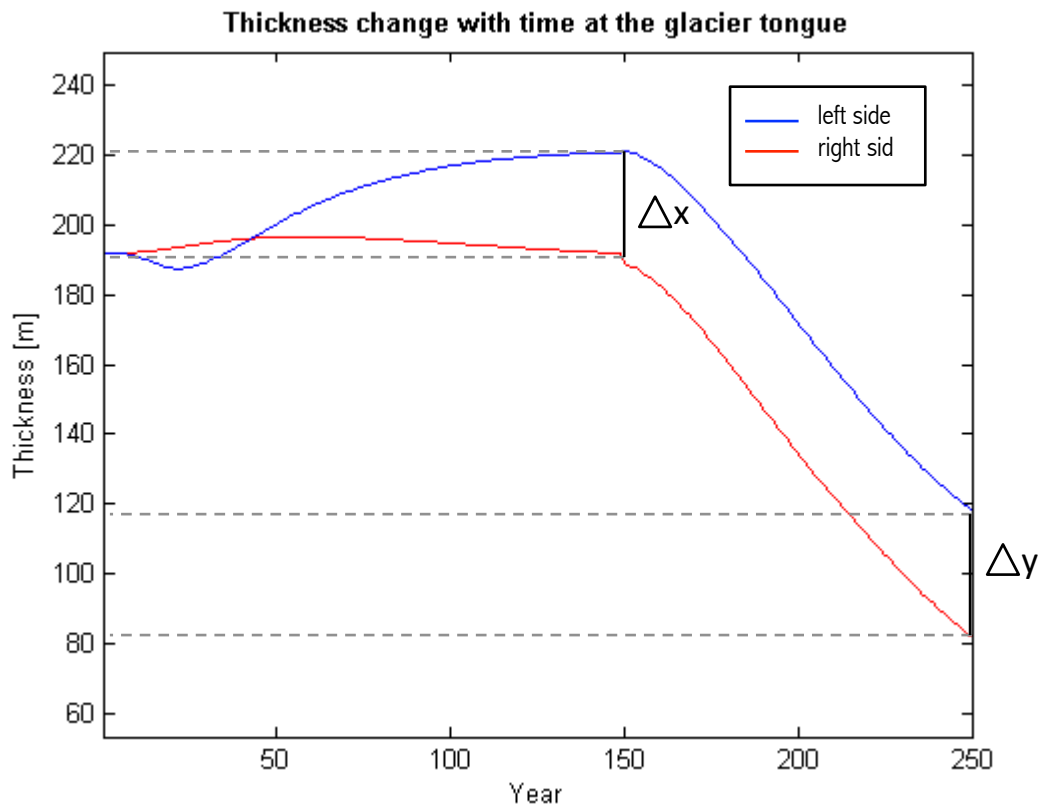


Fig. 25: Change in ice thickness at the glacier tongue. The first 150 years are run for the experiment A and B according to parameterization as explained in chapter 4.5.3, for the next 100 years the ELA was set at 3350 m.a.s.l.

This experiment analysed the impact of climate change on the two experiments A and B, after they have almost reached the steady state. The analysing is done by observing the change in thickness of the glacier at the tongue (630000°N/95400° in Fig. 12). The new equilibrium state is reached as soon as now changes in thickness occur anymore.

For the first 150 years the conditions are set as in chapter 4.5.3 for experiment A, which is represented with the blue line and for experiment B, indicated with the red line. For the last 100 years, the ELA was raised up by 50 m to an altitude of 3350 m.a.s.l, what indicates the increased temperature. The x-axis represents run time, the y-axis the thickness of the ice. The changes are determined at one grid point on the tongue.

In case of experiment A, the tongue loses in the early stage some ice mass. As soon as the accumulated ice is transported fully down, it gains mass which results in an increase of ice

thickness. Towards 150 years, the curve starts to stagnate since it has almost reached its steady state. The red line on the other side of experiment B increases in the beginning slightly and then starts to fall slowly but steady. Not enough ice is conveyed towards the tongue to prevent a mass loss.

Both curves immediately react to the change in temperature after 150 years and drop steeply. What is striking about this fall is that even if the two curves were at very different stages of glacier extent, both fall with the same slope. Before and after increasing temperature, the ratio of thickness remained the same. Similarly can be stated for the ratio of glacier volumes before and after increasing temperature (Tab. 2). The ratio of the volume change in both cases was 1.2.

6 Discussion

The results show that the redistribution of the snow accumulation does have an impact on the glacier flow dynamics and its geometry. The behaviour of the glacier was different in each experiment depending on the various starting situations in the accumulation distribution. Thus, the question arises whether those changes are associated in principle with the properties of the different accumulation patterns themselves e.g. amount of snow or pattern size, or if other local factors play a major role. Chapter 2 indicated that the glacier's mass flux is not only determined by the mass balance. The evolution of the glacier is an interaction of different parameters such as surface and bed topography, volume, thickness, and flow velocity of the entire glacier. The role of these parameters will be discussed below.

In section 6.1 the three pattern experiments of shifting snow to the left and the right side and the cut of increasing accumulation with elevation are discussed first since their results are on the same scale.

The knowledge gained by the experiments is discussed in section 6.2 to shed light on how the modified flow dynamics of the different experiments affect the evolution of the glacier over time and how long it takes until a new equilibrium state is achieved.

Section 6.3 discusses whether the different accumulation patterns influence the behaviour of the glacier under increased temperature. The last section covers the uncertainties of the flow model and the experimental approaches of the redistribution.

The curvature and wind experiments are discussed separately in section 6.4 since the curvature has to be interpreted on a smaller scale and the wind experiments were not performed with the flow model.

6.1 Snow pattern redistribution

The change in snow distribution resulted in a glacier advance for experiment A (left) whereas the glacier advanced to a much lesser degree, in experiment B (right), and the mass even starts to decrease after a run-time of 100 years. The largest loss occurred in experiment C (cut at 3350 m.a.s.l). The cause for the three different behaviours is explained by the unequal snow fluxes resulting from the different accumulation input situations. The left accumulation pattern area was defined to be smaller than the right one. Thus, experiment A received significantly more snow than in the opposite case B due to mass conservation. The ice thickening in parts of the

accumulation area of experiment A was more distinct than in experiment B. Therefore, the effect of the redistribution is more distinctive on the left side.

The results demonstrate that the two sides of the glacier of experiment A and B behave differently. In case A, modifications in geometry occur along the entire left side of the glacier. The increase in thickness in experiment A is so strongly pronounced that the ice of the left side even flows into the right side in the central area of the glacier (Fig. 20 A). The maximum gains were found at the tongue and in the accumulation zone. The continuous increase in mass in at the tongue experiment A is supplied by the steady input and the large mass conveyed from the accumulation area. The absence of snow accumulation on the right side showed no significant impact on the glacier flux.

In case B, changes mainly occurred at the terminus, the accumulation area hardly changed after a few years (Fig. 20 B). The upper parts did not show any apparent alterations except for mass gain of one to three meters. The tongue was losing mass after 100 years despite its advance in the first years. The feedback effect of the increased accumulation was much smaller in experiment B than in experiment A. It is difficult to assess, whether the two sides influenced each other in some way.

The different reactions of experiment A and B can be related to the flow velocity which is strongly correlated to the surface topography of the glacier, the distribution of the ice thickness, and the mass transport efficiency (Benn & Evans 2010). Even a small increase in ice thickness leads to a large increase in surface velocity due to higher shearing stresses and consequently more mass being conveyed from the accumulation to the ablation area. Certainly the reverse is also true. Even a small loss in thickness results in significant slowing down of the glacier (Hooke 2005). Indeed, increasing velocities are found at locations where the glacier gained mass and the thickness increased. In case of experiment A, the glacier became thicker over its right side, resulting in a velocity increase over the whole area. In case B, the tongue showed a slight increase in ice thickness resulting from the feedback effect from the increased snow accumulation. However, the accumulation area itself changed less. Therefore, the flow patterns differ much from those of the reference case. In experiment C the whole glacier decreased in ice mass and thus the velocity decreased over the entire area.

Further knowledge about the effect of the redistribution on advance or retreat of the glacier tongue is gained by considering the changes in the mass balance gradient, which explain the glacier flux in more detail. As mentioned in chapter 2.2, the mass balance gradients reflect the feedback effect of the increasing accumulation (Hooke 2005). Figure 26 shows the new mass

balance gradients of the different experiments. The elevation is plotted on the x-axis although it is the independent variable and the mass balance on the y-axis. The plot makes no statements about the horizontal distribution, as there is no third dimension included.

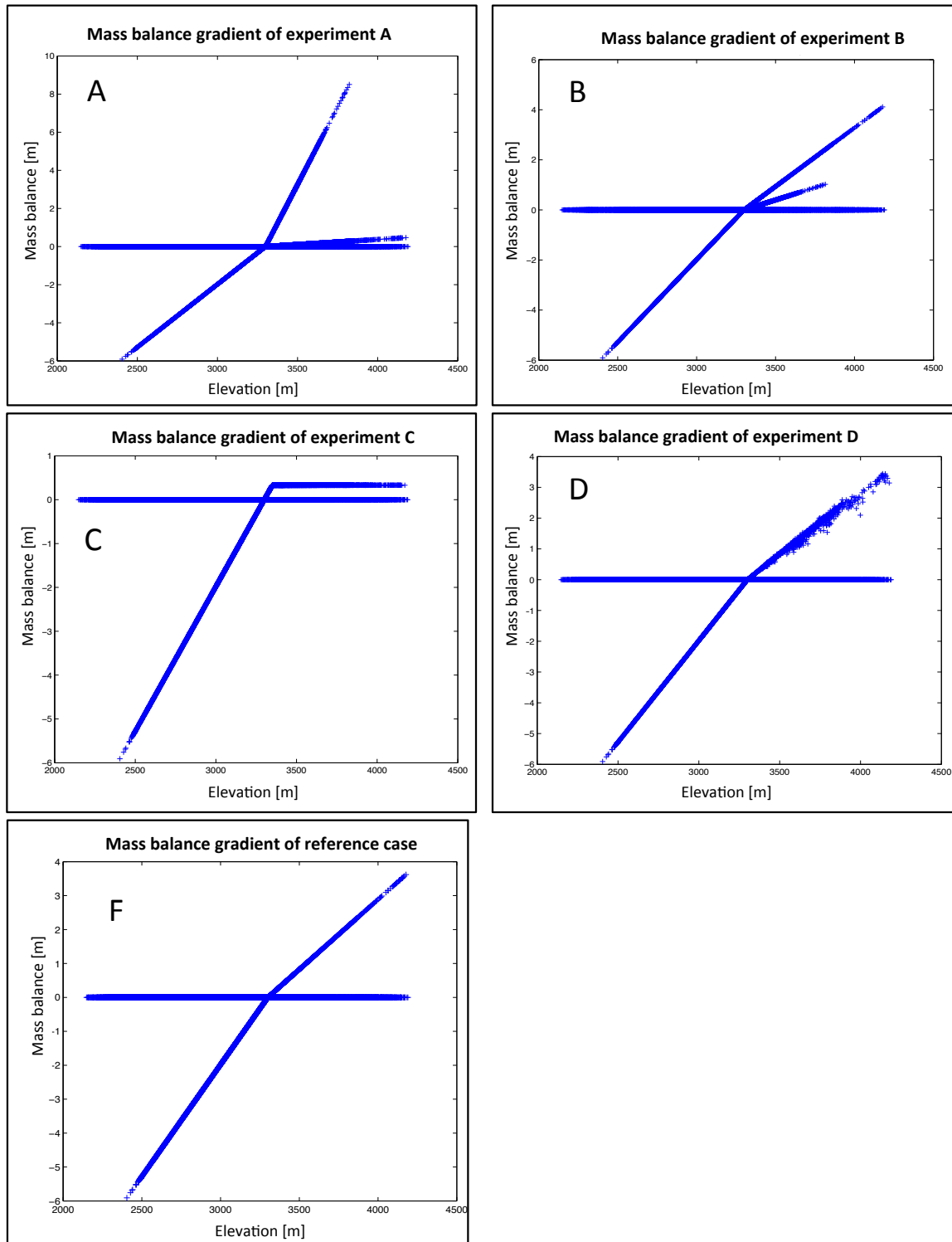


Fig. 26: Mass balance gradient with elevation A= shift to the left side, B= shift to the right side, C= cut of increasing accumulation at 3350 m.a.sl, D= shift according to curvature, F= reference case.

A glacier in equilibrium mostly exhibits a steeper gradient in the ablation area and a flatter one in the accumulation zone (Fig. 26 F). This ratio between the two gradients is typical for regions where precipitation feeds the accumulation area and loss of ice due to melt occurs in the ablation zone (Benn & Lehmkuhl 2000). If there is plenty of snow available in the accumulation area, only high mass fluxes can ensure the balance between accumulation and ablation (Hooke 2005).

The gain in ice mass in experiment A leads to a displacement of the mass balance gradients. The ablation gradient flattened while the one of the accumulation area steepened. The latter is now split into the two accumulation gradients, which represent the different amounts of snow on the left and the right side. The steeper one belongs to the left pattern, where the glacier significantly gained mass and the flat one to the right pattern (Fig. 26 A). Compared with the reference case, the steep accumulation gradient points out the greater increase of accumulation with elevation resulting from the increase in ice thickness on the left side. The ratio between the two gradients is large. For the evolution of the tongue, the smaller gradient on the right side can almost be neglected. The ablation gradient flattened compared to the one of the reference case. The increased ice mass in the accumulation area leads to higher flux and thus also to increased melting rates at the tongue of the glacier.

In contrast to case A, the distribution pattern in case B differed less from the one of the reference case. Consequently the impact of the redistribution was less pronounced than in case A. The balance ratio in case B (Fig. 26 B) is similar to the one of the reference case. The ratio between the two accumulation gradients is smaller. Thus, both sides influence the evolution of the glacier tongue. The ablation gradient in case B is steeper than in case A since less ice mass needs to be melted to balance out the ice flux from the accumulation area.

Experiment C clearly shows the cut of snow accumulation at 3350m.a.s.l (Fig. 26 C). The ablation gradient is slightly steeper due to the weakened ice flux.

As already mentioned, the flow velocity does not merely depend on the ice thickness but also on the surface topography of the glacier. The surface slope of the glacier likewise determines the shear stress at the glacier bed. According to Hook et al. (2005) a vertical column of ice is pushed by horizontal driving stresses, which depend on density, gravitation and ice thickness as well as the surface slope angle eq. (26). Thus, ice always flows in the direction of maximum surface slope. The slope of the glacier bed plays a minor role. If a glacier flows into a hollow, the ice is dammed, leading to an increase in thickness. Consequently, the surface slope gets flatter and velocity is reduced.

Glaciers are proportionally thinner on steeper slopes and thicker when the surface flattens. However, the bed surface cannot be fully ignored since surface slope is the sum of bed slope and the thickness gradient (Hooke 2005; Van der Veen 2013).

Taking a closer look at the surface topography of Findelen glacier, it is observable that the left part exhibits steeper slopes in the accumulation area, while the right part is generally flatter (Fig. 6 & A3). This observation matches the fact that the thick ice on the left side flows faster than the one on the right side (Fig. 21 A).

Towards the tongue, steep slopes on both sides characterize the terrain. In the central part of the glacier where the two main flow streams from the left and the right side confluence, the flow speed is lower, because the surface is relatively flat due to the topography. The ice is dammed there before overflowing the barrier and speeding up on the steeper slope.

Taking these factors into account the observed changes in the flow dynamics of the glacier and the varied mass flux are considered reasonable. To sum up, experiment A recorded a glacier advance. The snow shift to the left side resulted in an increase in thickness over the entire left side and the main flow stream changed from initially the right side to the left side with higher values in velocity. Since the surface slope is steeper on the left side, the glacier flows faster, which results in an increased ice flux from the accumulation area to the ablation zone. The acceleration of the flux at the tongue can further be explained by the narrowing of the valley (Cuffey & Paterson 2010).

In experiment C a larger amount of snow was lost. The mass flux has thus dwindled and the velocity of the flow stream slowed down. In this case it has to be remarked that the model shows an uncertainty since it is not fully mass conserving. This means that the mass loss is overestimated since snow accumulation is detracted from the model. Every year of run, more mass is missing as the surface is lower and the adapting mass balance decreases correspondingly. The glacier in experiment C has not yet reached a steady state after 150 years and accordingly will most likely retreat even more.

6.2 Time aspect

A further aspect to discuss is how the glacier evolves over time and how the ice fluxes of the different experiments influence the establishment of a new equilibrium state. Interpreting the glacier's development while it is not in an equilibrium state might lead to wrong conclusions. Experiment B exhibited a retreat after an early advance of the tongue in the first years. This change of the tongue development was not evident in the first 50 years. Another significant

feature of the reference case will be discussed in the following section about the impact of climate change.

It is difficult to estimate how long it takes for a glacier to react to changing environmental conditions as climate change impacts can be very complex and depend on the properties of the glacier. Alterations of glacier size generally indicate an indirect climate feedback. In our case study they are caused by a different snow accumulation distribution. A deficit or gain of input snow does not initiate an immediate retreat or advance of the glacier. It takes some time until the glacier reacts to a disturbance and adapts to the new conditions (Haeberli 1995). The response time can be derived from the flow velocities and the characteristic length of the glacier and appears to increase linearly with increasing ice thickness. Due to the greater ice volume, larger glaciers react slower to perturbations than do small glaciers. If a glacier is twice as long, its response time doubles. Furthermore, the response time depends on the mass balance gradient. A smaller balance gradient leads to a slower response time. To summarize, large balance gradients, steep slopes, and faster velocities result in faster response times (Bahr et al. 1998).

The interaction between the disturbance in the accumulation area in the form of redistribution and the achievement of a new steady state can easily be analysed based on the example of experiment A and B. In contrast to the theory of Bahr et al. (1998) we cannot compare different glacier lengths of the initial situation. In the present thesis the result of different glacier thicknesses on the response time is discussed in the two experiments A and B. Just analysing the profiles in Fig. 22 does not indicate which of the two experiments A and B reaches first the reference case. It can be seen that both glaciers reacted relatively rapidly to the disturbances in the accumulation area in the first years of run but the time where they reach a new equilibrium state is not observable. In order to obtain more detailed information, again the thickness changes at the tongue are analysed (Fig. 27) but this time without climate change. The red line shows the change in thickness of experiment B, the blue line the change of experiment A.

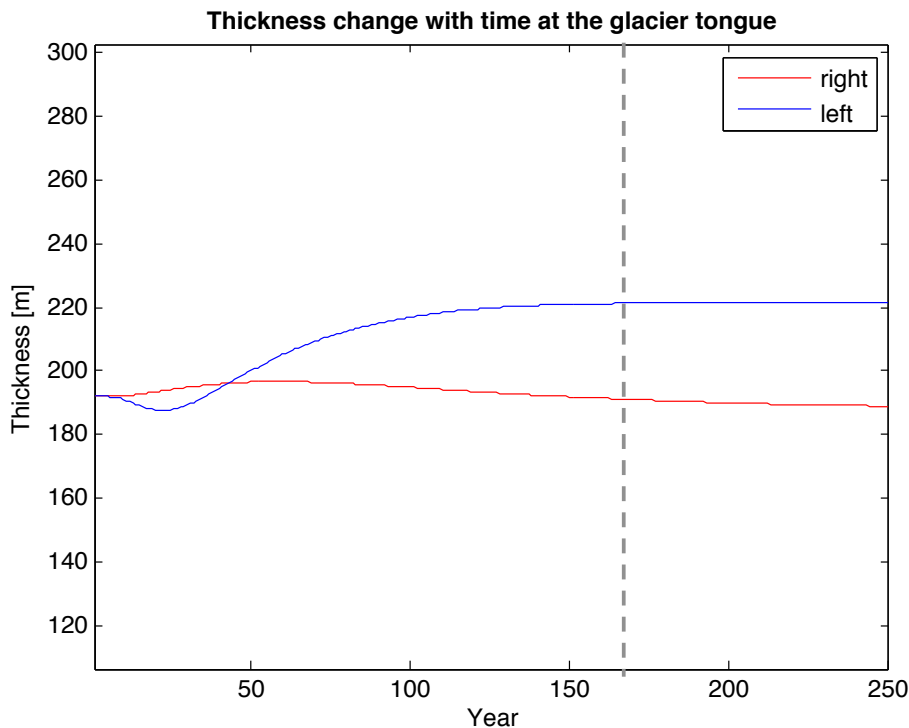


Fig. 27: Change in thickness at the tongue: red line = experiment B (right), blue line = experiment A (left).

The blue line levels off after approximately 160 years where the glacier reaches its steady state. The red line declines steadily since the glacier is constantly losing ice volume. In case of experiment A, the glacier gained mass in the accumulation area. The initial bend in the blue curve can be explained by the fact that it takes a few decades until the mass gain in the accumulation area is conveyed down to the tongue. The loss at this early stage might also be related to the ice mass loss of the right accumulation area (Fig. 20 A). However, as soon as the accumulated ice reaches the tongue after around 50 years, the curve rises sharply. After about 150 years, the thickness gain levels off and the glacier keeps its surface elevation, which indicates the new steady state.

The red line of experiment B on the other hand shows a steady decrease after an initial mass gain. Since the glacier in experiment B only got slightly thicker on the right side, but lost mass on the left side, the ice flux is much smaller and slower than in experiment A (Fig. 22 B). Annual mass changing rates are also smaller, therefore the decrease shown by the red line is weak but consistent.

Further we have to consider that the mass balance gradient also has an impact on the response time. For a small gradient it takes longer until the glacier responds and finds the new equilibrium (Oerlemans 2001). In this chapter we have seen that for experiment A the mass

balance gradient increased and got steeper in the accumulation area while it flattened in case B. This again explains why the response time for case A was shorter than in the other experiment.

6.3 Climate change

Climate change is reflected in the change of the equilibrium line altitude. If the temperature rises the ELA shifts up as well resulting in an indirect effect on the glacier flow dynamics and changes in length and extent (Haeberli 1995).

The results for the climate change experiment demonstrated that both experiments A and B responded equally to the increased altitude of the ELA (Fig. 25). Glacier thickness was lost in both experiments at almost the same ratio ($\Delta x \approx \Delta y$). The relative difference in thickness in the new steady state after 150 years at the initial temperature is the same as for the changed climatic conditions.

This leads to the conclusion that, under steady state conditions, the effect of the snow distribution in the accumulation area on glacier dynamics is not dependent on the specific temperature.

This evidence can be very useful for modelling the future evolution of glaciers. Even if the initial situation such as volume, length or flow velocity of the glacier is not fully known, the relative changes can be predicted. However, such an assumption can only be made under the condition that the initial glaciers were in a steady state, which is rather unlikely nowadays.

These findings do not only concern the modelling of future glacier development scenarios, but also the reconstruction of palaeoglacial ice flow. Such modelling of glacier dynamics is mostly based on insights from geomorphological mapping of palaeo-ice divides, flow trajectories, flow phasing, sedimentological evidences and subglacial bed form identification. Using these indicators, researchers try to reconstruct the glaciers' geometry, flow path, extent and how it developed under the climatic conditions of the time of interest. Since no data in form of direct measurements exists, the modelling is based on various assumptions of the boundary conditions. The reproduction of the glacier flow direction and its changes during the glacial cycles is only achievable with the help of geomorphological indications. Evans et al. (2009) derived the accumulation behaviour from present-day precipitation, wind direction and various correction factors. Yet, even if moisture patterns, temperature, and wind are reconstructed, the accumulation is still calculated linearly and without any heterogeneity (Evans et al. 2009). Concerning the conclusion of the climate change experiment a linear approach seems applicable as long as the pattern does not significantly change during the glacier evolution. This seems to be rather unlikely. The question arises whether the wind direction and amount of precipitation

would stay as well constant during the modelled period. Reconstruction of the temperature in the Quaternary based on ice core studies from Greenland have indicated that the climate was characterized by “several millennial-scale” phases of atmospheric warming and cooling (Brown et al. 2013). Time periods like the “Younger Dryas” (Fig. 28) were cold but very non-steady and the climate fluctuated strongly. This period was followed by a phase of more stable climate conditions with smaller amplitudes of fluctuation. If information about the past wind systems and a climate condition, as precipitation, was available, an assumption about the stability of the accumulation patterns would be possible. Rough changes in wind direction would indicate rather a change in the accumulation pattern.

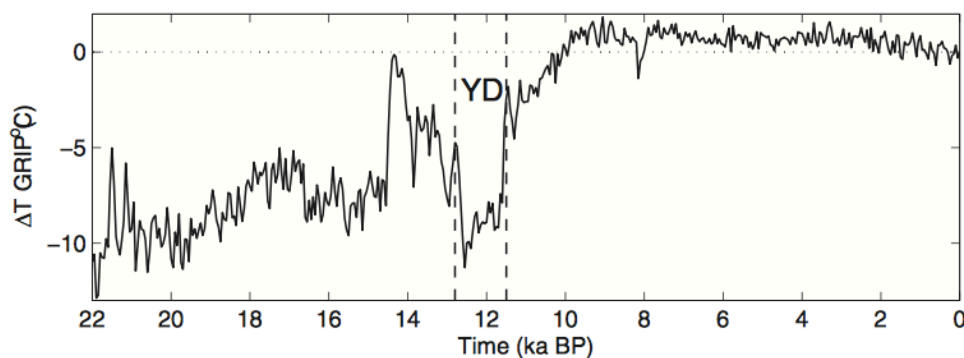


Fig. 28: The temperature anomaly in Greenland from 22 ka BP to present derived from ice core records (Brown et al. 2013).

6.4 Experiment curvature and wind

For the curvature experiment D it turned out that the changes in geometry and glacier dynamics are on a much smaller scale. The differences in thickness are smaller than in the other experiments and velocity does hardly differ from the reference case. The shift of snow is calculated within a 3x3 matrix with resolutions of 50 m. Snow is only transported between neighbouring pixels and not over longer distances; this could be the case with the influence of wind. Thus redistribution occurs very locally. In this experiment the weighting has a very strong influence on the results. Ridges and depressions are weighted based on the maximum and minimum elevation. If this value is set lower, much more snow is transported (eq. 20). The weighting factor f showed no significant influence. The model can further be improved by including wind shift.

The wind redistribution provides a new accumulation pattern, which shows some similarity to the snow depth measurements from the LIDAR survey of Sold et al. (2013). According to the

recognition of Sold et al. (2013) the heterogeneous snow accumulation is indeed related to wind shift. However, it must be noted that the snow depth results correspond to the winter accumulation of 2009/2010 while the results of this thesis are calculated for the summer and thus include ablation. Consequently, snow depth values cannot be compared directly but some trends concerning preferential areas of accumulation are observable. In both cases the wind came from the south.

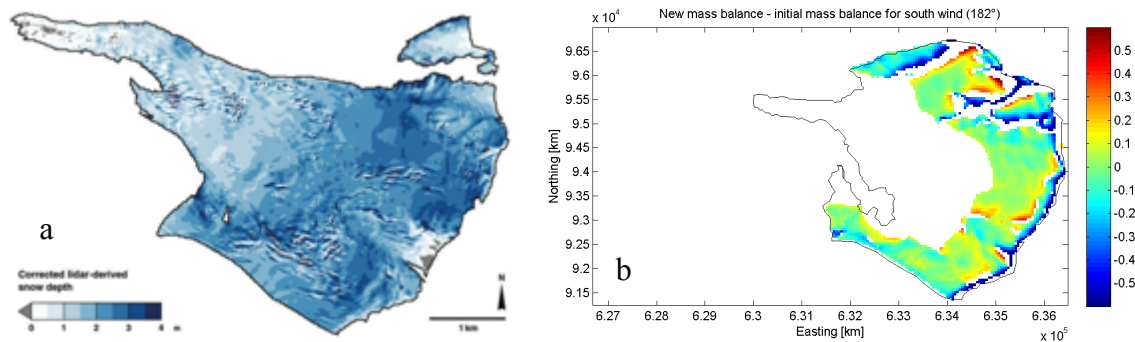


Fig. 29: left: snow depth derived from LIDAR - DEMs; right: difference in snow accumulation depth between wind shift and reference case (steady state) (south wind).

The best fit between the results of Sold et al. (2013) and the wind shift experiment was achieved with wind from the south direction (Fig. 29). The main snow accumulation areas are at the foot of steep rock walls as, for example below Adler glacier. Both plots show further accumulation in the hollow areas to the left and right side of Cima di Jazzi, while snow is eroded higher up the mountain. On the left side of the glacier the LIDAR plot shows further snow accumulation right under the zone with the crevasse where the terrain drops steeply. The same accumulation pattern is visible in the wind model in Fig. 29b. The zone with those crevasses is a location where wind is diverting along the curvature and thus snow is deposited. The shallower snow depth on most parts of the accumulation area of Adler glacier corresponds to the redistribution of the wind model, because snow is transported towards the wall. The wind model was also run for the other three wind directions but none of them showed such a good agreement (Fig. A6 & A7). In case of the easterly wind, similar accumulation patterns were achieved, again with increasing snow depth in concave areas and less snow on hills. Surprisingly, the left side of the glacier shows hardly any deposition along the north facing walls in front of Stockhorn (3532 m.a.s.l.). The wind speed of the easterly wind does not seem to be strong enough to blow the snow from the valley towards the steeper slopes.

A further aim of the wind model was to reconstruct similar patterns such as were observed during the ground survey measurements in April 2015, which pointed out the heterogeneity of snow accumulation distribution on Findelen glacier. These field measurements exhibited considerably more snow accumulation in the north facing slopes on the left side of the glacier than observed on the right side. On the left side of the glacier below Stockhorn the field measurement with probes at the location of this significant snow depth was exhausting since the probes almost disappeared in the snow and digging snow pits deeper than 4 meters in one day was inconceivable. However, the measurement with the ground survey GPR (800 MHz) was easier. The results indicated similar snow depth distribution as recorded from the probings (Fig. 30). However, the snow was quite fresh since there was heavy snowfall with easterly wind the weekend before the measurement. Those snowfalls certainly influenced the snow pattern.

It was not entirely possible to reconstruct this situation with the model. The output of the south-wind redistribution showed some more snow accumulation along the slopes on the left side of the glacier. In case of the easterly wind conditions, which correspond to the wind situation in April 2015, the snow accumulation is more regularly distributed over the accumulation area but no significant differences between the two glacier sides are observable.

Nonetheless it would be interesting to look deeper into the observed patterns on Findelen glacier and how they change within the winter season and over several decades. As mentioned the distribution pattern of Findelen glacier is well known but the focus of the measurements lie on the survey of the mass balance and the snow accumulation distribution over elevation rather than along similar elevation. Further investigations of the observed accumulation pattern of the winter mass balance measurements of April 2015 further would be of interest to see whether they impact the glacier flux in any way.

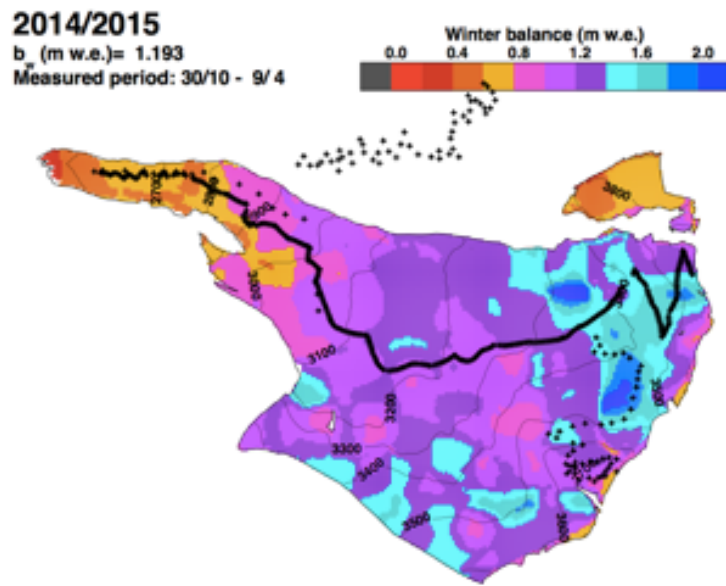


Fig. 30: Snow depth measurements from winter mass balance April 2015 (Findel-Wiki 2015).

6.5 Uncertainties

The following section deals with proposals for improvement of the model analysis, the uncertainty of some parameters and gives an outlook how the study could be continued.

6.5.1 Findelen glacier bed vs. U-valley

For a better analysis of the sensitivity of all the investigated parameters it would be useful to test all the experiments with a simplified geometry instead of using a real glacier bed. This could be done with the assumption of a perfectly U-shaped glacier bed. The redistribution experiments as well as the alteration of the ELA and its influence on the glacier dynamics could be tested independently of the influence of the topographic differences. The glacier surface should thus be modelled as a parabolic surface profile (Benn & Evans 2010). The reason for using the glacier bed of Findelen glacier is that the accumulation pattern of the glacier has been exhaustively investigated. The knowledge of the heterogeneity of the snow accumulation was the inspiration for the thesis.

Further, experiments A and B are strongly influenced by the size of the two areas. Since the left pattern leads to a significantly thicker ice layer than the right one, the influence of the topography on the ice flux cannot be tested independently. Therefore it would be appropriate to rerun both experiments again with two patterns of the same size.

6.5.2 Sun correction

One important parameter, which was omitted in the model, is the impact of solar radiation on ice melt. So far melt is only included due to mass conservation. The model provides a function, which allows including solar radiation by shifting up the ELA if the aspect was facing south. By shifting the ELA similar effects of snow melt are attained. This means that without the effect of the sun, the total glacier ice volume is slightly overestimated.

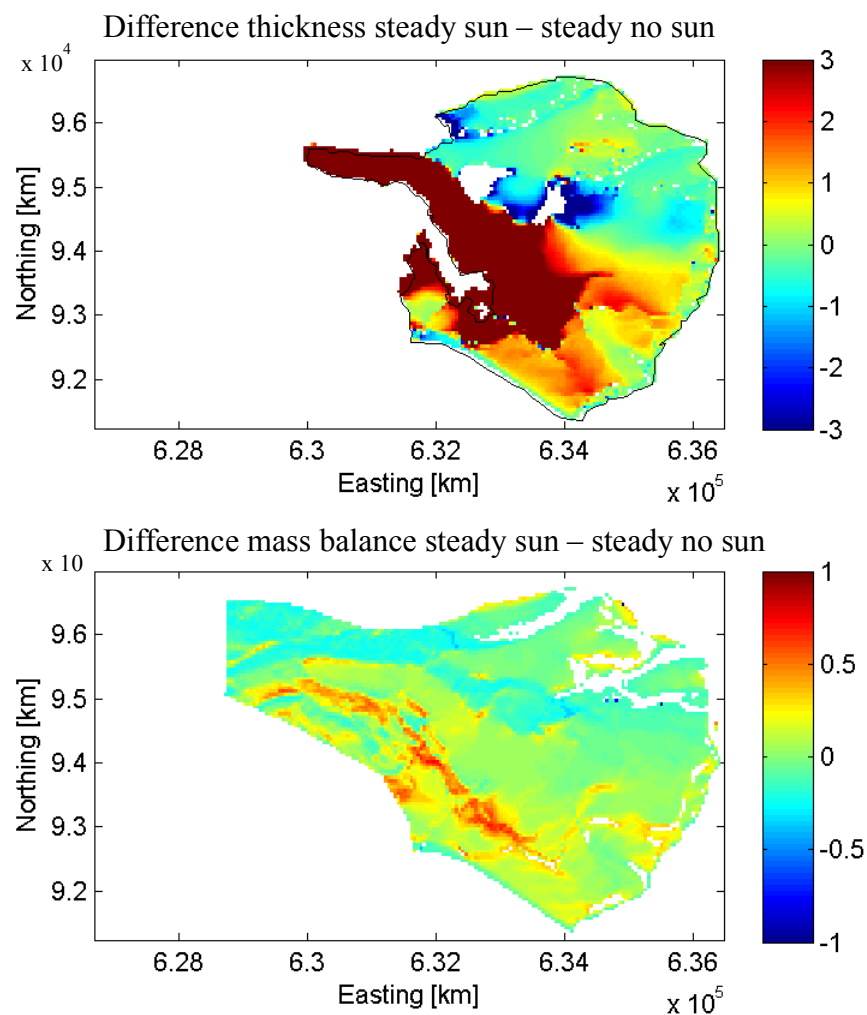


Fig. 31: Difference between reference case modelled with solar radiation (steady sun) and without solar radiation (steady no sun). Upper plot: difference in thickness; lower plot: difference in mass balance.

Fig. 31 shows the difference between the reference case, generated once with and once without sun correction. The south-facing walls on the right side are slightly blue which indicates the enhanced loss of ice due to the melt caused by solar radiation. North facing slopes on the other hand have some more snow since they are more protected from the sun. The lower plot with the difference in mass balance indicates the same insights. Snow accumulation loss and gain are in the range of -0.25 and 0.25m. The accumulation on the left side is larger than on the right side, where snow melt occurs. The tongue gained significantly mass due to the feedback from the accumulation area. Consequently, the omission of the solar radiation makes a difference in the results regarding the total mass and the accumulation pattern.

Instead of using the proposed sun correction method for this model, other options exist such as the degree-day model which would generate snow melt by including sun radiation (chapter 4.2). The albedo is another neglected parameter which impacts the melt. It controls the outgoing long wave radiation. Albedo depends on the consistency of the ice. It ranges from 0.1 for dirty ice up to 0.9 for fresh snow. This means that for the former, more short wave radiation is absorbed than for the latter, which increases the melt rate (Hock 2005).

Since the model for the thesis neither includes assumptions on the incoming solar radiation, nor on the metamorphosis of the ice and snow, the albedo was not further considered. As the intention of this thesis was to analyse the sensitivity and not the total differences in ice volume, the omission of the sun parameter is of modest relevance.

6.5.3 Boundary between ice and glacier bed

Basal sliding is also not considered directly in the model. This parameter makes up about 50% of the flow velocity of temperate glaciers (Kamb 1970). In addition, the sliding has an impact on annual fluctuations (Meier & Post 1969). For an appropriate modelling of basal motion, knowledge of spatial variation of basal and lateral drag under the ice is necessary, as well as the full stress in the glacier ice itself (Benn & Evans 2010). Today, the knowledge of modelling basal sliding is still at an early stage (Parizek & Alley 2004). Models for glacier-scale hydrology have been developed by Flowers (2002) in the last decade, which are able to involve the basal sliding of the glacier (Flowers 2002).

Further we assume a fixed geometry of the glacier bed. As we have already seen the dynamic of the glacier is very complex due to the interaction of different variables. The deformation of the glacier bed is a further key parameter. The glacier ice shapes the glacier bed, which in turn influences the surface geometry of the glacier which further determines the glacier flux. Whether deformation occurs depends on such factors as the coupling of the glacier with the bed, the temperateness of the ice, the hydrological conditions, and the properties of the underplaying rocks. For example a glacier coupled to its bed receives a speed up in velocity and thus a decrease in thickness or surface slope (Hart & Rose 2001). However, if high water pressure exists, the glacier might be decoupled from its bed and consequently flows faster at the expense of glacier bed deformation. Little friction resistances facilitate the deformation of sediments. The overlying ice mass applies shear stress on the water-saturated soft bed and deformation occurs. In case of a coupled situation, the movement of the glacier is mainly controlled by sediment

mechanical properties (Clark 1999). Over the whole time of the glacier evolution when the glacier advances, the bed topography changes due to the sub-glacial erosion. The dynamic of the glacier thus is influenced, too, since slopes are changed (Durand et al. 2007).

The sophisticated processes are not just occurring at the boundary of the ice and the rock but also at the ice and the atmosphere. Climate change enhances faster flow due to more sub-glacial discharge. This, in turn, enhances sediment deformation. Sub-glacial sediment transportation was not considered in the thesis even if it is one of the main glacial processes (Hindmarsh 1997).

6.5.4 Feedbacks

As discussed in chapter 4.4.1 it is important how long the model is run. If the glacier gets thicker in the accumulation area, the surface reaches a new level in the mass balance gradient curve which subsequently changes to maintain the balance. If the model is not run long enough, those feedbacks of ice thickness still exert influence on the whole dynamic processes and change the glaciers geometry. Depending on which year of the run is analysed, a wrong trend could be obtained as discussed in experiment B (chapter 6.2). For all experiments the models were run until the glacier almost or entirely reached the new steady state. However, to be absolutely sure that no feedbacks are remaining which influence the glacier dynamics, the glacier flow experiments should be run another 200 years in every case.

6.5.5 Constant meteorological conditions

Over the whole modelling period meteorological conditions are supposed to be constant (Brown et al. 2013). In case of experiment A, B, and C, the ELA remains constant during the whole model process, which indicates no change in temperature. For the wind experiment, we assume that the wind direction is not changing over the time of modelling. In reality, the weather conditions are anything but constant (IDAWB 2015). The effect of sun on glacier melt was already discussed in chapter 2.5. Considering the climate change, in chapter 2.6 it was pointed out that temperature is expected to increase in the future, which has an effect on the snow-rain line altitude and further on the amount of snow accumulation. Consequently, the ELA will also adapt to changing climate conditions. Certainly, the variability of precipitation is on a larger scale and probably does not affect the pattern of snow accumulation distribution on the small scale as investigated in this thesis (Oerlemans et al. 1998).

7 Conclusion

The aim of this thesis was to investigate the effect of redistribution of snow accumulation on the geometry and flow dynamics of a glacier based on a case study of Findelen glacier and five different experiments. The following results were achieved:

- The case of an extreme redistribution such as the shift towards the right and left side at a ratio of 1:10 significantly impacts the evolution of the glacier. The same is true for a scenario in which the snow accumulation has been truncated at a certain elevation.
- In the first experiment (A) the increase of glacier thickness was sufficient for a glacier advance over 150 years.
- In the case of experiment B the increase of glacier mass in the accumulation area was merely enough for a temporary advance in the first 50 years but afterwards less ice mass was conveyed to the glacier tongue and the increase in thickness was reversed.
- The most considerable retreat of the glacier tongue resulted in experiment C where less snow accumulation was available due to the cut.

The explanation for the different reactions of the glacier in these experiments is the following:

- The impact of the accumulation pattern on the flow dynamics and the glacier geometry is not only associated with the glacier's intrinsic properties but also with the local topography of the area, where the snow has been accumulated.
- The left side of the glacier exhibited steeper and hillier terrain than the right one. Since the glacier thickness increased significantly in experiment A the terrain enabled faster velocities and thus higher fluxes of ice mass compared to the right side.
- The slower conveyance in case of experiment B and the thinner glacier ice were not enough to provide a sufficient flux, which resulted in decreases of the ice mass in the tongue.

The accumulation pattern influenced the duration of the reaction time after a disturbance in the accumulation area and the point in time when the glacier reached a new equilibrium state. The higher ice mass flux in case A led to a faster achievement of the new steady state than in case B. It is therefore indispensable for the experiments to be run for time periods of sufficient length. As long as the glacier's is in a non-steady progress, remaining feedbacks still change the glaciers

geometry and wrong conclusions may be drawn unintentionally from the transient states in experiment B. The steady state is even more important if the evolution of the glacier with time is associated with a change in climatic conditions. The results indicated that the relative changes in glacier mass and geometry upon shifting up the ELA were the same in both experiments A and B. Therefore the following conclusion can be made:

- If a glacier is in a steady state and the accumulation pattern does not change during a period of new climate conditions such as increased temperature, the distribution of the snow accumulation has no significant impact on the relative reaction of the glacier in the two climatic scenarios.

The redistribution of snow between concave and convex topography indicated an impact on the glacier dynamic on a very small scale. However, even this small redistribution was enough to induce a slight advance of the glacier. The model was supposed to be improved by shifting more snow over a larger area with the help of wind. Unfortunately, the wind model experiment was not sufficiently well developed to be included into the flow model for the purpose of investigating the impact of wind on the glacier dynamic. However, the simulated effect of wind shift showed similar patterns as observed in field measurements. Wind coming from the south, which is mostly the case, leads to enhanced snow accumulation on the right side of the glacier along the rock walls below Adler glacier as well as in depressions while snow got eroded along ridges.

The take home message of the thesis is the following: A redistribution of the accumulation pattern does have an influence on the glacier geometry and flow dynamics. If the temperature increases due to a climate change, the pattern has no influence anymore as long as two conditions are fulfilled: (1) the accumulation pattern is supposed to stay constant during the phase of climate change and (2) the glacier must have been in a steady state before the temperature started to increase.

8 Appendix



Fig. A1: View on Findelen glacier, September 2014 (Photo: Ladina Glaus)



Fig. A2: left: Adler horn and terminus of Adler glacier, right: Findelen glacier, September 2014 (Photo: Ladina Glaus)

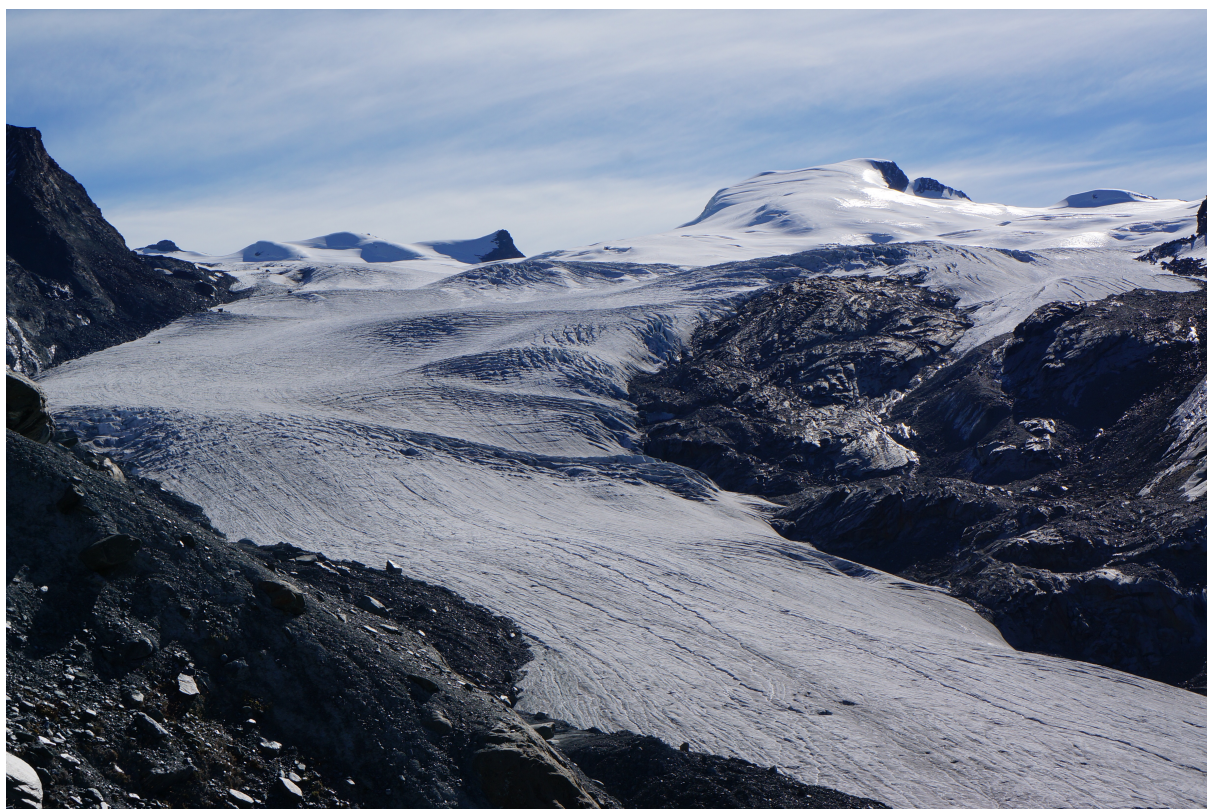


Fig. A3: View towards the accumulation area of Findelen glacier, September 2014 (Photo: Ladina Glaus)

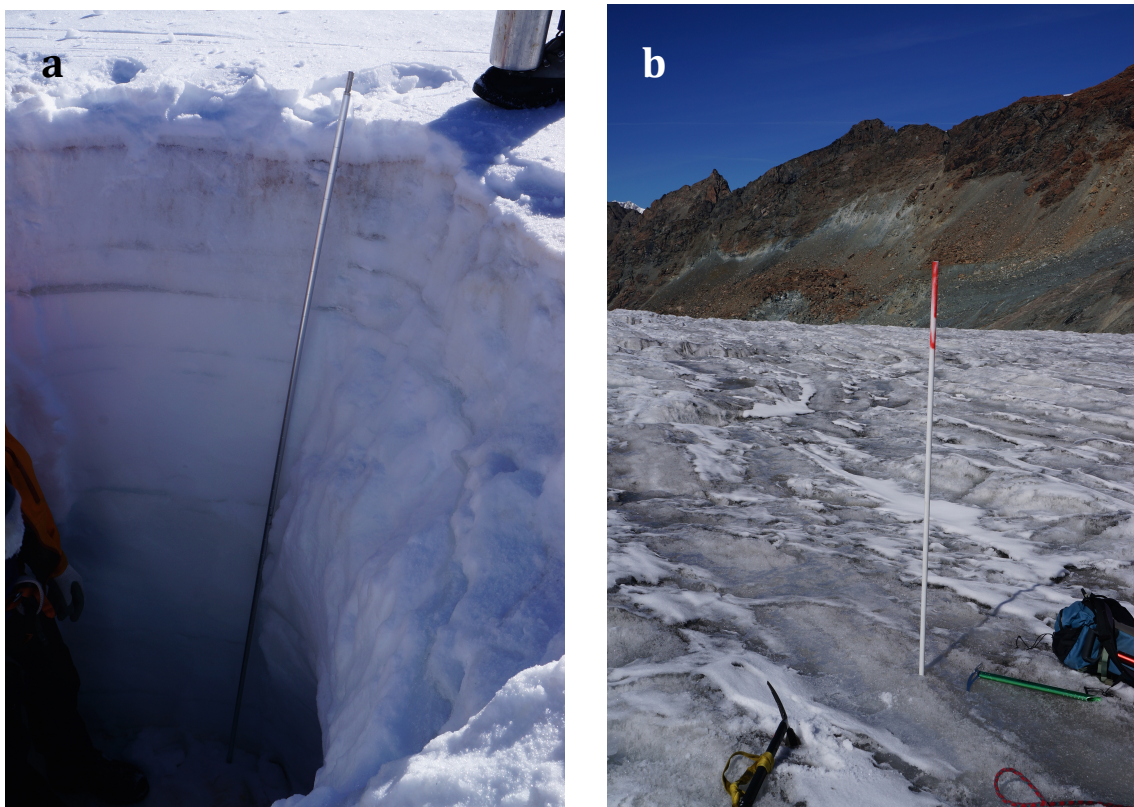


Fig. A4: left: snow pit, right: ablation stake, September 2014 (Photo: Ladina Glaus)



Fig. A5: Accumulation stake below Cima di Jazzi, September 2014 (Photo: Ladina Glaus)

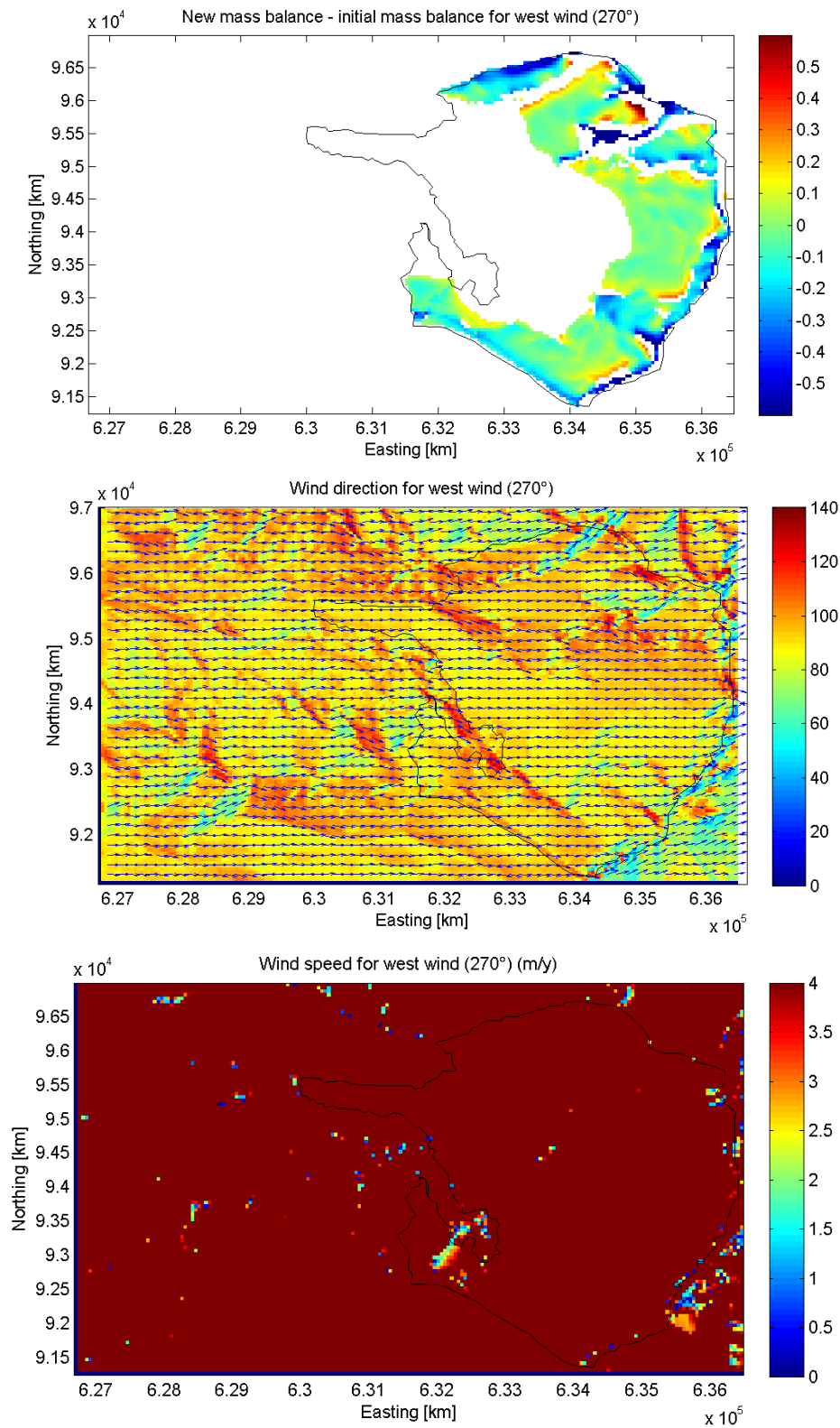


Fig. A6: West-wind experiment.

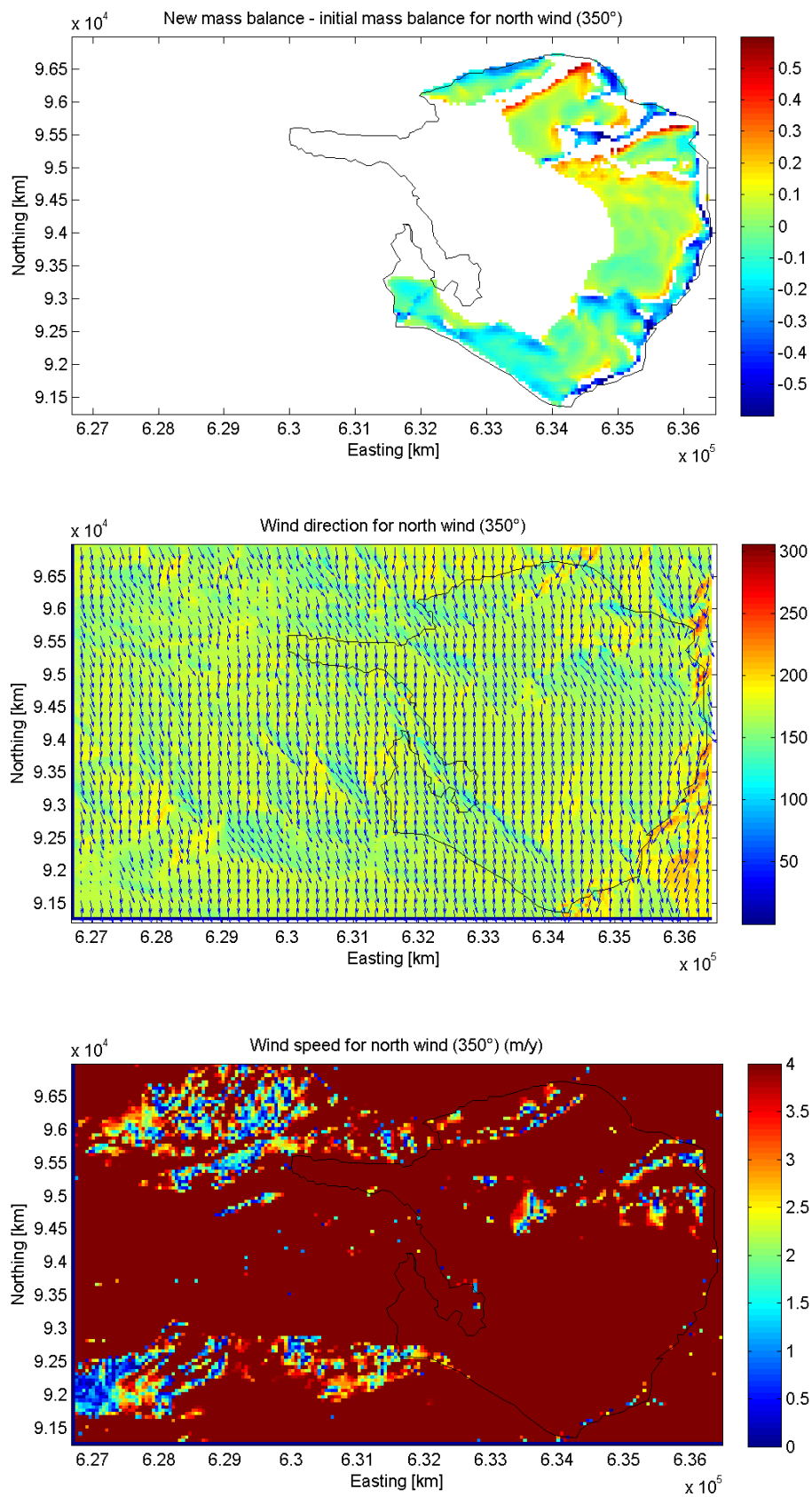


Fig. A7: North-wind experiment.

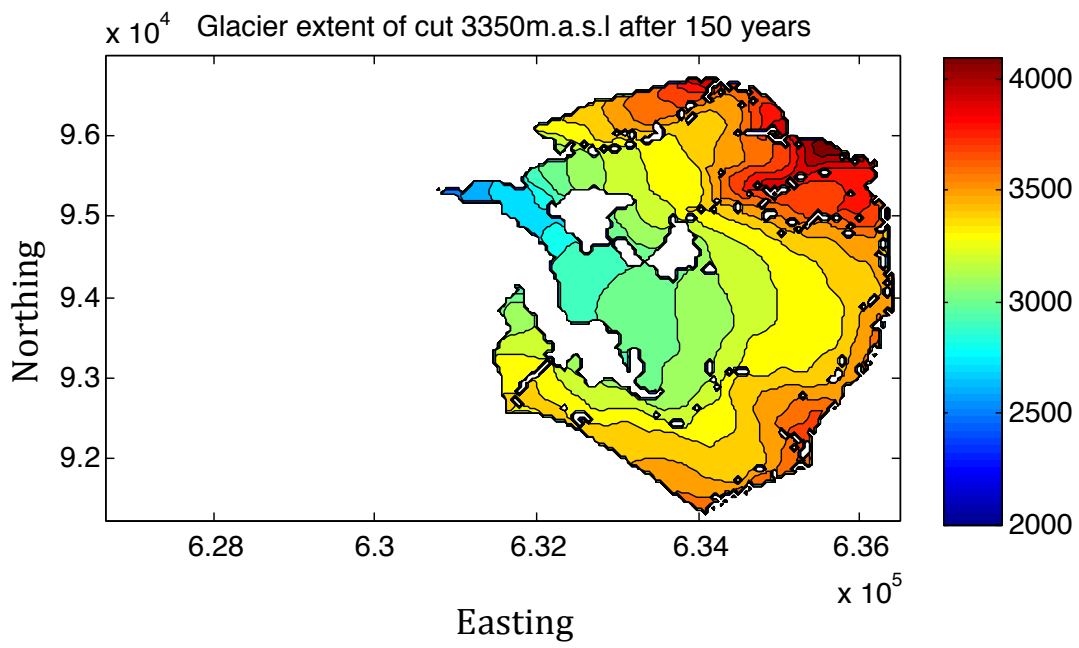


Fig. A8: Glacier extent of experiment C after 150 years of run. Tongue retreated significantly.

Acknowledgment

This thesis gave me the great opportunity for a deep comprehensive insight into scientific research work and modelling techniques. This challenge was feasible thanks to the support of several people.

First of all, I would like to thank my supervisor Andreas Vieli for his reliable and valuable support concerning the realization of the thesis. I very appreciate his motivation and his patience when I faced apparently unsurmountable obstacles. Further thanks go to the research group of the Findelen mass balance program, who enabled me practical fieldwork on Findelen glacier in September 2014 and April 2015. The visit of the glacier was great motivation for the thesis and an unforgettable experience. Thus, my thanks go to Andreas Vieli, Matthias Huss, Nadine Salzmann, Leo Sold, Daniel Farinotti, Gwendolyn Leysinger, Mathias Luethi and all the other people who were involved.

A special thank goes to Marius Wolfensberger, Christoph Rohner and Ross Purves for the technical support and advices regarding the modelling part.

Last but not least I'd like to thank everyone else for their support, advices and motivating words during this year: Nico Moelg, Beverly Strassmann, Simon Etter, Moriz Reisser, Seraina Glaus, Martin Glaus, Corin Meier, Daniela Müller, Lukas Gmünder and all my fellow students in G10.

References

- BAFU (Bundesamt für Umwelt). (2013). Klimaänderung in der Schweiz. <http://www.bafu.admin.ch/publikationen/publikation/01709/index.html?lang=de>. [Accessed: 2015-25-04]
- Bahr, D.B. et al., 1998. Response times of glaciers as a function of size and mass balance. *Journal of Geophysical Research*, 103(B5), pp.9777–9782.
- Barnett, T.P., Adam, J.C. & Lettenmaier, D.P., 2005. Potential impacts of a warming climate on water availability in snow-dominated regions. *Nature*, 438(7066), pp.303–309.
- Bauder Andreas, Steffen Simon, U.S., 2014. *The Swiss Glaciers 2007/08 and 2008/09. Glaciological Report (Glacier). No. 129/130*, Zürich, Switzerland.
- Benn, D. & Evans, D.J.A., 2010. *Glaciers and Glaciation, 2nd Edition*, London: Brithish library Cataloguing in Publication Data.
- Benn, D.I. & Lehmkuhl, F., 2000. Mass balance and equilibrium-line altitudes of glaciers in high-mountain environments. *Quaternary International*, 65-66, pp.15–29. Available at: <http://www.sciencedirect.com/science/article/pii/S1040618299000348> [Accessed May 31, 2015].
- Benn, D.I. & Lehmkuhl, F., 2000. Mass balance and equilibrium-line altitudes of glaciers in high-mountain environments. *Quaternary International*, 65-66, pp.15–29.
- Bloschl, G., Kirnbauer, R. & Gutknecht, D., 1991. Distributed snowmelt simulations in an alpine catchment I. Model evaluation on the basis of snow cover patterns. *Water Resources Research*, 27(12), pp.3171–3179.
- Brown, V.H. et al., 2013. The Younger Dryas in the English Lake District: reconciling geomorphological evidence with numerical model outputs. *Boreas*, p.n/a–n/a. Available at: <http://doi.wiley.com/10.1111/bor.12020> [Accessed September 16, 2015].
- Carey, M. et al., 2012. An integrated socio-environmental framework for glacier hazard management and climate change adaptation: Lessons from Lake 513, Cordillera Blanca, Peru. *Climatic Change*, 112(3-4), pp.733–767.
- Clark, P.U., 1999. Northern Hemisphere Ice-Sheet Influences on Global Climate Change. *Science*, 286(5442), pp.1104–1111.
- Cuffey, K.M. & Paterson, W.S.B., 2010. *The Physics of Glaciers, 4th Edition | Kurt Cuffey, W. S. B. Paterson | ISBN 9780123694614*, Academic Press, 2010. Available at: <http://store.elsevier.com/The-Physics-of-Glaciers/Kurt-Cuffey/isbn-9780123694614/> [Accessed July 20, 2015].
- Dadic, R. et al., 2010. Wind influence on snow depth distribution and accumulation over glaciers. *Journal of Geophysical Research: Earth Surface*, 115(1), pp.1–8.

- Durand, G. et al., 2007. Change in ice rheology during climate variations & implications for ice flow modelling and dating of the EPICA Dome C core. *Climate of the Past*, 3(1), pp.155–167.
- Evans, D.J.A. et al., 2009. The palaeoglaciology of the central sector of the British and Irish Ice Sheet: reconciling glacial geomorphology and preliminary ice sheet modelling. *Quaternary Science Reviews*, 28(7-8), pp.739–757. Available at: <http://www.sciencedirect.com/science/article/pii/S0277379109000195> [Accessed August 23, 2015].
- Farinotti, D. et al., 2011. Runoff evolution in the Swiss Alps: projections for selected high-alpine catchments based on ENSEMBLES scenarios. *Hydrological Processes*, 26, pp.1909–1924.
- Farinotti, D. et al., 2010. Snow accumulation distribution inferred from time-lapse photography and simple modelling. *Hydrological Processes*. Available at: <http://doi.wiley.com/10.1002/hyp.7629> [Accessed May 19, 2015].
- Findel-Wiki, Findel-Wiki. Available at: <https://findel.wiki.geo.uzh.ch/ProtokolleFeldarbeit> [Accessed September 28, 2015].
- Fischer, L. et al., 2006. Geology, glacier retreat and permafrost degradation as controlling factors of slope instabilities in a high-mountain rock wall: the Monte Rosa east face. *Natural Hazards and Earth System Science*, 6(5), pp.761–772.
- Fischer, U.H. & Clarke, G.K.C., 2001. Review of subglacial hydro-mechanical coupling: Trapridge Glacier, Yukon Territory, Canada. *Quaternary International*, 86, pp.29–43.
- Flowers, G.E., 2002. A multicomponent coupled model of glacier hydrology 1. Theory and synthetic examples. *Journal of Geophysical Research*, 107(B11), p.2287. Available at: <http://doi.wiley.com/10.1029/2001JB001122> [Accessed July 29, 2015].
- Fohn, P.M.B. & Meister, R., 1983. Distribution of snow drifts on ridge slopes: measurements and theoretical approximations. *Annals of Glaciology*, 4(Fohn 1980), pp.52–57.
- Gallee, H., Guyomarc'h, G. & Brun, E., 2001. Impact of snow drift on the antarctic ice sheet surface mass balance: Possible sensitivity to snow-surface properties. *Boundary-Layer Meteorology*, 99(1), pp.1–19.
- Gardner, A.S. & Sharp, M., 2009. Sensitivity of net mass-balance estimates to near-surface temperature lapse rates when employing the degree-day method to estimate glacier melt. *Annals of Glaciology*, 50(50), pp.80–86.
- Geo.admin, geo.admin.ch: das Geoportal des Bundes. Available at: <http://www.geo.admin.ch/> [Accessed September 28, 2015].
- Grünewald, T., Bühler, Y. & Lehning, M., 2014. Elevation dependency of mountain snow depth. *The Cryosphere*, 8(6), pp.2381–2394. Available at: <http://www.the-cryosphere.net/8/2381/2014/>.

References

- Haerberli, W., 1995. glacial fluctuation and climate change.pdf. *georg.Fis dinam. Quat*, 18, pp.191–199.
- Haerberli, W. et al., 2007. Integrated monitoring of mountain glaciers as key indicators of global climate change: the European Alps. *Annals of Glaciology*, 46, pp.150–160.
- Haerberli, W., Burn, C.R. & Sidle, R.C., 2002. Natural hazards in forests: glacier and permafrost effects as related to climate change. *Environmental changes and geomorphic hazards in forests*, pp.167–202.
- Haerberli, W., Cihlar, J. & Barry, R., 2000. Glacier monitoring within the Global Climate Observing System. *Annals of Geology*, 31, pp.241–246.
- Hart, J. & Rose, J., 2001. Approaches to the study of glacier bed deformation. *Quaternary International*, 86, pp.45–58.
- Haug, T. et al., 2009. Geodetic mass balance of the western Svartisen ice cap, Norway, in the periods 1968-1985 and 1985-2002. *Annals of Glaciology*, 50(50), pp.119–125.
- Hindmarsh, R., 1997. Deforming beds: Viscous and plastic scales of deformation. *Quaternary Science Reviews*, 16(9), pp.1039–1056.
- Hock, R., 2005. Glacier melt: a review of processes and their modelling. *Progress in Physical Geography*, 29(3), pp.362–391.
- Hock, R., 2003. Temperature index melt modelling in mountain areas. *Journal of Hydrology*, 282(1-4), pp.104–115.
- Hooke, R.L., 2005. *Principles of Glacier Mechanics*, Cambridge: Cambridge University Press. Available at: /ebook.jsf?bid=CBO9780511614231 [Accessed July 20, 2015].
- Huang, H.-C. & Cressie, N., 1996. Spatio-temporal prediction of snow water equivalent using the Kalman filter. *Computational Statistics & Data Analysis*, 22(2), pp.159–175.
- Hubbard, B. & Glasser, N., 2005. *Field Techniques in Glaciology and Glacial Geomorphology* L. C. of G. John Wiley and Sons, ed., University of Wales.
- Huss, M. et al., 2009. Determination of the seasonal mass balance of four Alpine glaciers since 1865. *Mitteilungen der Versuchsanstalt für Wasserbau, Hydrologie und Glaziologie an der Eidgenössischen Technischen Hochschule Zurich*, 113(213), pp.11–29.
- Huss, M. et al., 2013. Towards remote monitoring of sub-seasonal glacier mass balance. *Annals of Glaciology*, 54(63), pp.75–83.
- Huss, M. & Farinotti, D., 2012. Distributed ice thickness and volume of all glaciers around the globe. *Journal of Geophysical Research: Earth Surface*, 117(4), pp.1–10.
- IDAWEB, MeteoSchweiz IDAWEB. Available at: <https://gate.meteoswiss.ch/idaweb/login.do> [Accessed September 28, 2015].

-
- IPCC, 2001. *Climate Change 2001: The Scientific Basis*, Intergovernmental Panel on Climate Change. Cambridge, New York.
- IPCC, 2013. *Climate Change 2013. The Physical Science Basis*, Available at: http://www.climatechange2013.org/images/report/WG1AR5_SummaryVolume_FINAL.pdf [Accessed September 28, 2015].
- Joerg, P., Morsdorf, F. & Zemp, M., 2012. Uncertainty assessment of multi-temporal airborne laser scanning data: A case study on an Alpine glacier. *Remote Sensing of Environment*, 127, pp.118–129. Available at: <http://www.sciencedirect.com/science/article/pii/S0034425712003240>.
- Kamb, B., 1970. Sliding motion of glaciers: Theory and observation. *Reviews of Geophysics*, 8(4), p.673.
- Kuhn, M., 1985. Fluctuations of climate and mass balance: different responses of two adjacent glaciers. *Z Gletscherk Glazalgeol*, 21, p.409:416.
- Lehning, M. et al., 2008. Inhomogeneous precipitation distribution and snow transport in steep terrain. *Water Resources Research*, 44(7), pp.1–19.
- Leysinger Vieli, G.J.-M.C. & Gudmundsson, G.H., 2004. On estimating length fluctuations of glaciers caused by changes in climatic forcing. , 44(March), pp.0–14. Available at: <http://nora.nerc.ac.uk/12246/>.
- Li, L. & Pomeroy, J.W., 1997. Estimates of Threshold Wind Speeds for Snow Transport Using Meteorological Data. *Journal of Applied Meteorology*, 36(3), pp.205–213.
- Liston, G.E., 2004. Representing subgrid snow cover heterogeneities in regional and global models. *Journal of Climate*, 17(6), pp.1381–1397.
- Machguth, H. et al., 2006. Strong spatial variability of snow accumulation observed with helicopter-borne GPR on two adjacent Alpine glaciers. *Geophysical Research Letters*, 33(13), pp.1–5.
- Maisch, M., 2000. *Die Gletscher der Schweizer Alpen: Gletscherhochstand 1850, aktuelle Vergletscherung, Gletscherschwund-Szenarien [Projektschlussbericht im Rahmen des Nationalen Forschungsprogrammes]*, Zürich: vdf Hochsch.-Verl. an der ETH.
- Marchand, W.D. & Killingtveit, Å., 2005. Statistical probability distribution of snow depth at the model sub-grid cell spatial scale. *Hydrological Processes*, 19(2), pp.355–369.
- Meier, M.F. & Post, A., 1969. What are glacier surges? *Canadian Journal of Earth Sciences*, 6(4), pp.807–817. Available at: http://www.nrcresearchpress.com/doi/abs/10.1139/e69-081#.VbjHiiTrU_V [Accessed July 29, 2015].
- Mellor, M., 1965. *Blowing snow*, Hanover, N.H.
- Le Meur, E. et al., 2004. Glacier flow modelling: A comparison of the Shallow Ice Approximation and the full-Stokes solution. *Comptes Rendus Physique*, 5(7), pp.709–722.
-

References

- Le Meur, E. & Vincent, C., 2003. A two-dimensional shallow ice flow model of glacier de Saint Sorlin, France. *Journal of Glaciology*, 49, pp.527–538.
- Mölg, T., Cullen, N.J. & Kaser, G., 2009. Solar radiation, cloudiness and longwave radiation over low-latitude glaciers: Implications for mass-balance modelling. *Journal of Glaciology*, 55(190), pp.292–302.
- Oerlemans, J., 2001. *Glaciers and Climate Change* S. & Z. B. (Lisse), ed., Amsterdam: Swets & Zeitlinger BV, Lisse.
- Oerlemans, J. et al., 1998. Modelling the response of glaciers to climate warming. *Climate Dynamics*, 14(4), pp.267–274.
- Parizek, B.R. & Alley, R.B., 2004. Implications of increased Greenland surface melt under global-warming scenarios: ice-sheet simulations. *Quaternary Science Reviews*, 23(9-10), pp.1013–1027. Available at: <http://www.sciencedirect.com/science/article/pii/S0277379104000241> [Accessed July 29, 2015].
- Paterson, W.S. & Bud, W., 1982. Numerical recipes; the art of scientific computing (Fortran version). *Vetterling.*, (Cambridge, Cambridge University Press.).
- Paul, F. et al., 2007. Alpinewide Distributed Glacier Mass Balance Modeling. *Orlove VN - readcube.com*, pp.111–125. Available at: http://scholar.google.com/scholar?cluster=8223270520376690422&hl=en&as_sdt=0,22\nc:\Users\Alfonso\Documents\PhD\Review\Paul et al. - 2007 - Alpinewide Distributed Glacier Mass Balance Modeling.pdf.
- Pellicciotti, F. et al., 2005. An enhanced temperature-index glacier melt model including the shortwave radiation balance: Development and testing for Haut Glacier d’Arolla, Switzerland. *Journal of Glaciology*, 51(175), pp.573–587.
- Press, W.H. et al., 1993. *Numerical Recipes in C: The Art of Scientific Computing, Second edition*, Cambridge University Press. Available at: <http://www.nr.com>.
- Purves, R.S. et al., 1998. The development of a rule based spatial model of wind transported and deposition of snow. *Annals of Glaciology*, 26(Annals of Glaciology, 26), pp.197–202.
- Rasmussen, L.A. & Meier, M.F., 1982. Continuity Equation Model of the Predicted Drastic Retreat of Columbia Glacier, Alaska. *Geological Survey Professional Paper*, 1258-A(U.S. Geological Survey, Alexandria). Available at: <http://pubs.usgs.gov/pp/1258a/report.pdf>.
- Report, G., 2014. The Swiss Glaciers 2007/08 and 2008/2009. , (129/130), pp.27–31.
- Ryan, B.C., 1977. A Mathematical Model for Diagnosis and Prediction of Surface Winds in Mountainous Terrain. *Journal of Applied Meteorology*, 16(6), pp.571–584. Available at: [http://journals.ametsoc.org/doi/abs/10.1175/1520-0450\(1977\)016%3C0571%3AAMMFDA%3E2.0.CO%3B2](http://journals.ametsoc.org/doi/abs/10.1175/1520-0450(1977)016%3C0571%3AAMMFDA%3E2.0.CO%3B2) [Accessed September 28, 2015].

- Sold, L. et al., 2013. Methodological approaches to infer end-of-winter snow distribution on alpine glaciers. *Journal of Glaciology*, 59(218), pp.1047–1059.
- Solomatine, D.P. & Wagner, T., 2011. *Hydrological Modeling* B. V. Elsevier, ed., The Netherlands, University Park, PA, USA.
- Terminology, M., 2011. Glossary of Glacier Mass. *Organization*, 86, p.114. Available at: unesdoc.unesco.org/images/0019/001925/192525e.pdf.
- Van der Veen, C.J., 2013. *Fundamentals of Glacier Dynamics* Typor & Francic Group, ed., 6000 Broken South Parkway NY, Suite 300: CRC Press.
- Winstral, A. & Marks, D., 2014. Long-term snow distribution observations in a mountain catchment: Assessing variability, time stability, and the representativeness of an index site. *Water Resources Research*, 50(1), pp.293–305.
- Zemp, M. et al., 2006. Alpine glaciers to disappear within decades? *Geophysical Research Letters*, 33(13), pp.6–9.
- Zemp, M. & Haeberli, W., 2007. Glaciers and Ice Caps. *UNEP: Global Outlook for Ice and Snow*, pp.115–152.
- Zemp, M., Hoelzle, M. & Haeberli, W., 2007. Distributed modelling of the regional climatic equilibrium line altitude of glaciers in the European Alps. *Global and Planetary Change*, 56(1-2), pp.83–100.
- Zevenbergen, L.W. & Thorne, C.R., 1987. Quantitative analysis of land surface topography. *Earth surface processes and landforms*, 12, pp.47–56.

Personal Declaration

I hereby declare that submitted thesis is the result of my own, independent, work. All external sources are explicitly acknowledged in the thesis.

City, Date:

Signature:

Ladina Glaus
